INFORMATION TO USERS

This manuscript has been reproduced from the microfilm master. UMI films the text directly from the original or copy submitted. Thus, some thesis and dissertation copies are in typewriter face, while others may be from any type of computer printer.

The quality of this reproduction is dependent upon the quality of the copy submitted. Broken or indistinct print, colored or poor quality illustrations and photographs, print bleedthrough, substandard margins, and improper alignment can adversely affect reproduction.

In the unlikely event that the author did not send UMI a complete manuscript and there are missing pages, these will be noted. Also, if unauthorized copyright material had to be removed, a note will indicate the deletion.

Oversize materials (e.g., maps, drawings, charts) are reproduced by sectioning the original, beginning at the upper left-hand corner and continuing from left to right in equal sections with small overlaps. Each original is also photographed in one exposure and is included in reduced form at the back of the book.

Photographs included in the original manuscript have been reproduced xerographically in this copy. Higher quality 6" x 9" black and white photographic prints are available for any photographs or illustrations appearing in this copy for an additional charge. Contact UMI directly to order.

UMI

A Bell & Howell Information Company
300 North Zeeb Road, Ann Arbor MI 48106-1346 USA
313/761-4700 800/521-0600

Université d'Ottawa · University of Ottawa

Effect of Transverse Convex Surface Curvature on Fluid Flow and Heat Transfer in the Entrance Region of Concentric Annuli

by

© **Eugene Suk**

A thesis submitted to the school of Graduate Studies
and Research in partial fulfilment of
the requirements for the degree of

Master of Applied Science
in the
Department of Mechanical Engineering

The Ottawa-Carleton Institute for
Mechanical and Aeronautical Engineering

Department of Mechanical Engineering
University of Ottawa
Ottawa, Ontario
Canada

ABSTRACT

The effect of transverse convex surface curvature on turbulent boundary layer flow and heat transfer in the entrance region of concentric annulus is studied analytically. The analytical results are obtained through a turbulent model based on the variable von Kármán's constants, κ_i, proposed by Kim and Lee in 1995. A computer program is developed for the calculation of the desired hydrodynamic and thermal characteristics. The solutions are found for the case of the heat transfer where the inner core surface is uniformly heated and the outer insulated. It is assumed that the fluid flow is turbulent everywhere and the thermodynamic fluid properties are independent of temperature.

It is shown that both the friction factor and Nusselt number increase with the decreasing value of the inner core radius of the concentric annuli, r_i, while the hydrodynamic and thermodynamic entrance lengths decrease with the decreasing value of the inner core radius, r_i.

It is concluded that as in the fully developed turbulent flow, the effect of the transverse convex curvature in the developing region of concentric annuli seems significant.

ACKNOWLEDGEMENTS

The author wishes to express his sincere appreciation to Professor Yung Lee for the opportunity to work under his supervision and guidance. His help and patience with immeasurable love and his knowledge in this field helped bring this study to fruition.

The author expresses his sincere thanks to Professors W. Hallet, Chairman, R. Milane and S.C. Cheng for their kind advice and interest, and also to the technical staff, and secretaries in the Department of Mechanical Engineering, University of Ottawa, for their valuable help.

Special thanks go to the author's father and mother for their love, prayers and support. Also to Dr. Son, Mrs. Son, Daniel, Mark and John. The author is personally indebted to colleagues Dr. M.W. Kim, Mr. S.H. Rhi, Mr. B. Kim, Dr. H.C. Park, Dr. K.H. Choi and Mr. J.S. Huh for their advice.

The author sincerely appreciates his good friends, Caroline, Ji Young, Ji-Yun and Charlie who gave continuous encouragement and love which made it possible to carry on this work.

Thanks to the Lord for his great deliverance.

TABLE OF CONTENTS

LIST OF TABLES & FIGURES

NOMENCLATURE

A	surface area of the hot junction [m^2] or van Driest's damping constant
A^+	dimensionless van Driest's damping parameter
C or c	constant
c_p	specific heat at constant pressure [kJ/kg·°C]
D	substantial derivatives defined by Eq. (2.2)
De	equivalent diameter of annulus, 2 (r_o - r_i), [m]
f_j	friction factor, concentric annulus, (2 τ_j /$\rho \cdot u_b^2$)
F	force [N], function
G	mass flow rate of the fluid [kg/m^2]
h	convective heat transfer coefficient [W/m^2 °C]
k	thermal conductivity [W/m°C] or turbulent kinetic energy
k_t	eddy conductivity [W/m°C]
l	Prandtl's mixing length [m]
l^+	dimensionless Prandtl mixing length parameter, circular cylinder, ($l \cdot u_\tau$ /v)
L	length [m]
Nu	Nusselt number; circular cylinder (h·x / k), concentric annulus (h·De / k)
p	pressure [N/m^2]
Pr	Prandtl number, ($c_p \cdot \mu$/k)
Pr_t	turbulent Prandtl number, ($\varepsilon_M/\varepsilon_H$)

q	heat flux per unit area [W/m^2]
q'	heat generation per unit volume [J/m^3]
r	radial coordinate measured from cylinder axis [m]
r_j	radius of circular cylinder [m]
R_j	radius of concentric annuli [m]
R_j^+	dimensionless radius parameter, concentric annulus, $(R_j \cdot u_{\tau j}/\nu)$
Re	Reynolds number
Re_r	Reynolds number based on radius of the circular cylinder
t	time [sec]
T	temperature [°C]
T^+	dimensionless temperature parameter, $[(T_w - T) \cdot \rho \cdot c_p \cdot u_{\tau j} / q_i]$
u	velocity in x-direction [m/s]
u_j^+	dimensionless velocity parameter, $(u/u_{\tau j})$
$u_{\tau j}$	friction velocity, $(\tau_j / \rho)^{0.5}$ [m/s]
u_b	bulk velocity [m/s]
v	velocity in y-direction [m/s]
w	velocity in z-direction [m/s]
x, y, z	cartesian coordinates [m]
y	distance from the wall [m]
y_j^+	dimensionless distance parameter, $(y \cdot u_{\tau j}/\nu)$

Greek Symbols:

α	radius ratio of annulus, (r_i/r_o), thermal diffusivity $[m^2/s]$
δ_j	$\lvert R_j - r_j \rvert$
δ_j^+	$\delta_j(\tau_w/\rho)_j^{0.5}/\nu$
Δ_j	δ_j^+ / r_j^+
ε	eddy diffusivity $[m^2/s]$
ζ_j	normalized distance, (y_j^+ / δ_j^+)
θ	azimuthal coordinate
κ_j	von Karman's constant
μ	dynamic viscosity [kg/m·s]
μ_t	eddy viscosity [kg/m·s]
ν	kinematic viscosity $[m^2/s]$
ρ	density $[kg/m^3]$
τ	shear stress $[kg/m \cdot s^2]$.

Superscripts:

$^+$	quantity non-dimensionalized by means of ν, τ_w, and ρ on the same side, e.g., $r_i^+ = r_i(\tau_w/\rho)_i^{0.5}/\nu$
$^{++}$	quantity non-dimensionalized by means of ν, τ_w, and ρ on the other side, e.g., $r_i^{++} = r_i(\tau_w/\rho)_o^{0.5}/\nu$
$'$	fluctuating component or specific value
$\bar{}$	mean
*	normalized by the value of r = 1.0 m, e.g., r^* $(= r / r_{1.0\,m})$, f^* $(= f / f_{1.0\,mj})$

Subscripts:

b	bulk
d	fully developed
e	free stream
H	thermal
i	inner
i, j, k	inner or cartesian coordinate direction
j	designate number (i or o)
k	turbulent kinetic energy
l	laminar
m	corresponding to the maximum velocity point
M	momentum
l	laminar
o	outer
R_j	radius of circular cylinder or concentric annulus
t	turbulent
w	wall
x	local or developing

CHAPTER 1
INTRODUCTION

1.1 General Overview

Fluid flow in an annular cross section has been studied extensively because of its importance in a variety of engineering applications. Nuclear reactors and heat exchangers are examples of heat transfer systems. In nuclear reactors, fuel elements of cylindrical form are in cylindrical coolant channels. Design for such reactors require consideration of data concerning turbulent fluid flow and heat transfer in annuli.

Cases on fully developed turbulent flow have been the subject of many analytical and experimental studies. Research by Kim and Lee [1995], which consider the effect of the transverse convex surface curvature on turbulent flow, have further completed and provided accuracy to previous study on fluid flow and heat transfer phenomena. However, the theory of the effect of the transverse convex curvature surface has not yet been applied to the turbulent flow and heat transfer in the entrance regions of concentric annuli. Even though this effect is not yet available in published literature, this problem is important on a practical level because the design of many heat transfer systems require a detailed knowledge of flow and heat transfer characteristics.

For the analytical work in this study, modified versions of previously accepted turbulence models were combined with integral momentum and energy equations to predict friction factors and heat transfer rates in annular tube geometries. The turbulence models of van Driest [1956] and Reichardt [1943] were used for developing turbulent fluid flow and heat transfer in annuli. All the turbulence

models are adapted to reflect the variable von Kármán constant, κ_i, that is required for the effect of the transverse convex surface curvature which is introduced in this thesis.

The aim of this research is to apply the proposed variable von Kármán constant that can successfully describe the effect of the transverse convex surface curvature and to obtain an analytical prediction based on the model for developing turbulent fluid flow and heat transfer in entrance regions.

The work is subdivided into several parts. First, a survey of relevant works in published literature is carried out, outlining past theoretical analyses of developing turbulent flows and heat transfer on the geometries in question. This is followed by a mathematical development of analyses, showing the integration of momentum and energy equations with the adapted turbulence models based on variable von Kármán constants, κ_i. The governing equations of the systems are presented, their numerical solutions are then described, demonstrating the approximation of the governing equations. Finally, the analytical results are produced to evaluate the effects of the transverse convex surface curvatures.

Throughout the analysis, the fluid properties are considered constant to simulate an ideal situation. Conditions for the analysis are constant wall heat flux, radial symmetry and uniform free stream velocity at the entrance. Temperature distributions with the effects of natural convection and axial conduction are kept negligible.

1.2 Literature Survey

Until recently, the studies on the flow and heat transfer in circular and non-circular ducts have been concerned primarily with problems of many applications. The requirement for the understanding of fluid flow and heat transfer characteristics in a concentric annulus has been particularly important in industry. The fully developed flow for both laminar and turbulent cases have been the subject of many analytical and experimental studies due to their great simplicity and wide applications, but little work has been done on developing flow in ducts.

The problems of fully developed turbulent flow in a concentric annulus have been studied experimentally and analytically by many workers : Bailey [1950], Knudsen and Katz [1950], Rothfus et al. [1950, 1966], Mizushina [1951], Barrow [1955], Beck [1960], Reynold et al. [1963], Lee and Barrow [1964], Brighton and Hones [1964], Levy [1967], Quarmby [1967, 1968], Michiyoshi and Nakajima [1968], Wilson and Medwell [1968], Randhava [1969], Lawn and Elliott [1972] and Kim [1996]. Among these previously listed, the work of Kim [1996] is of particular significance to this study.

The importance of Kim's study [1996] is that the modified turbulent closure model is used to describe the effect of the transverse convex wall surface curvature for the first time. This effect is considered for the developing flow in this study. Before Kim [1996], previous researchers only considered the effect of radius ratio, α, Reynolds number, Re, and Prandtl number (for heat transfer), Pr, in studies of turbulent fluid flow and heat transfer in concentric annular ducts.

In contrast to the studies of fully developed turbulent flow, only a few studies of the flow of a fluid in the entrance region of a concentric annulus are found in the literature; These have been reported by Rothfus et al. [1955], Olson and Sparrow [1963], Okiishi and Seroby [1967], Sridhar

et al. [1970], and Park [1971].

Rothus et al. [1955] indicate entrance region behaviour which is quite different than that of turbulent flows in circular tubes and between parallel plates. Their results were based on the ratio of the local apparent shear stress to the fully developed value and used annuli of radius ratios, 1.78 and 2.97. The entrance lengths appear to be larger by a factor of ten than the typical circular tube entrance lengths and strongly affected by the Reynolds number. Since the circular tube and parallel plate channel are special cases of the annulus, it is not clear why the results from concentric annuli are so different.

To explore this apparent anomaly, Olson and Sparrow [1963] investigated the entrance region by measuring the wall static pressure for water flowing through annuli. They found that the length required to approach within 5% of the fully developed pressure gradient was about 15 to 20 hydraulic diameters which are in general accord with the entrance length results for tubes and parallel plates.

Okiishi and Serovy [1967] used two annular configurations using both square-edged and rounded entrances to study the flow in the inlet region. They were able to obtain the fully developed turbulent flow based on the local velocity profile approaching its limiting value only for the case of the square-edged entrance. For the case of the rounded entrance, the length of the apparatus was insufficient because their maximum available test length was 35 equivalent diameters.

On the other hand, Sridhar et al. [1970], reported that the entrance lengths, based on the core velocity reaching a constant value, for annuli with square-edged entrances were between 25 and 35 diameters. However, the entrance lengths for the bellmouth entrances were about 10 to 15 equivalent diameters more than those of the square-edged entrances. Apparently, there does not exist the same consistency and good agreement among the different investigations as there are for the

plain circular tube.

Park [1971] studied the problem from an integral view point, based on a modified model for the eddy diffusivity of momentum together with a new ratio of eddy diffusivities obtained from experiment. Comparisons were made between experiments and analytical computations conducted on the effects of various factors on the turbulent flow in the developing regions of concentric annuli. Air was used as the working fluid and four annuli having radius ratios (r_o / r_i) of 1.61, 2.31, 3.83 and 15.32 were used over a range of Reynold numbers between about 20,000 and 110,000. The hydrodynamic entrance lengths based on friction measurements were obtained for approximately 6 to 12 equivalent diameters, which agreed with his prediction. Velocity profiles in the inner region of a concentric annulus were significantly affected by the Reynolds number, radius ratio and entrance length.

The thermal entrance region has been defined, either as the distance required for the local heat transfer coefficient to approach that of the fully developed value or as the distance from the entrance to the cross section where the non-dimensionalized temperature profile becomes independent of the flow direction. Most of the thermal entry region solutions so far considered have been based on the assumption that the velocity profile is fully developed. Since the velocity profile of the fluid entering a heat transfer passage is already fully developed, it is often called a "purely thermal entrance region" to distinguish it from a simultaneously developing region. In a simultaneously developing region, the heat transfer occurs near the actual entrance of a tube or annulus where the velocity profile is not developed but rather developing. Often the design of a heat transfer sections (flow conditions) are such that the entire section is simultaneously developing, but with very long flow passages, the entry length is only a small fraction of the whole length and its influence is negligible. However, with

certain fluid and thermal boundary conditions, these entry effects might be very important and cognizance of them must be taken.

For the purely thermal entrance region problem in the entrance regions of concentric annuli, the only pertinent analytical studies to date are those of Kays and Leung [1963], Lee [1968], Quarmby and Anand [1970, 1970], and Chen and Yu [1970]. Results of experimental work are reported by Farman and Beckmann [1967], and Quarmby [1967].

In the study of simultaneously developing entrance region, there have been some studies, and because of the emphasis of this study, a brief review from the cases of laminar flow through a duct is made for completeness.

One of the earliest analytical studies on the combined entry-length problem of laminar flow and heat transfer in a circular tube appears to be that of Kays [1955]. He obtained a numerical solution for a Prandtl number of 0.71, employing Langhaar's velocity profiles [1942]. He reported the relationships between the mean and local Nusselt numbers for the three different boundary conditions.

Sparrow [1955] did research on the problem of laminar heat transfer in the entrance section of flat rectangular ducts. The flat ducts considered were two parallel planes with heat being transferred through each plane. The two dimensional energy equations for laminar heat transfer were solved by using a parabolic velocity profile given as,

$$\frac{u}{u_\delta} = 2\frac{y}{\delta} - \left(\frac{y}{\delta}\right)^2$$

where u_δ : velocity at the edge of the boundary layer,

δ : the thickness of the boundary layer,

and y : the distance from wall where velocity is u.

Nusselt numbers were reported for the range of Prandtl numbers from 0.01 to 50.

Solutions for circular tubes and annuli for laminar flow with constant heat flux and various Prandtl numbers were given by Heaton et al. [1964]. They linearized the energy equation by an approximation first introduced by Langhaar [1942] in connection with the hydrodynamic problem, and they were then able to obtain a generalized entry region temperature profile which could be used in the entry integral equation.

Deissler [1955] analytically investigated the effects of various factors on turbulent heat transfer and friction in the entrance regions of smooth passages. He used the integral heat transfer and momentum equation for calculating the thickness of the thermal and boundary layers. The influence of the Reynolds number, the Prandtl number, initial velocity distribution, wall-boundary conditions, and variable fluid properties were studied. His results indicate that fully developed heat transfer and friction are obtained in an entrance length approximately less than 10 diameters. The effect of initial velocity distribution on heat transfer in the entrance region was that the values of Nu_x/Nu_d for a uniform initial velocity distribution were higher than those for a fully developed velocity distribution.

Barrow [1968] and Roberts [1968] employed a rather different procedure for the turbulent heat transfer in the entry region of a pipe and a concentric annulus respectively. They used the concept of an "equivalent immersed body", but the analysis was based entirely on experimental correlations: (1) a correlation for the velocity of the potential core; (2) a local skin friction correlation ; (3) a modified Reynolds analogy factor ; and (4) a shape factor of the turbulent velocity profile. Since the boundary layer-potential stream model is no longer applicable near the fully developed core region,

the analysis does not permit the determination of Nu_d or entry length. They also conducted experimental investigations with air in the entry region of internally heated annuli using two radius ratios. The effects of boundary layer tripping wire size on the wall temperature distribution and local heat transfer coefficient were given in their studies.

The work of Wilson and Medwell [1970] relies upon the eddy viscosity distribution suggested by Levy [1967] for fully developed turbulent annular flow with a constant universal mixing constant identical to that used in circular tubes. This assumption disagreed with many analytical and experimental findings for developing flow; It even disagreed with results in the fully developed flow studies [Brighton et al., 1964, Levy, 1967, Barrow et al. 1965]. Levy [1967] himself did not use a universal mixing length constant for the inner region of concentric annuli.

The problem of developing turbulent flow and heat transfer in the simultaneously developing regions of concentric annuli were studied both analytically and experimentally by Park [1971]. The fully developed heat transfer was attained from both the analytical and experimental studies in entrance lengths of less than 40 equivalent diameters for the air flow. For very small Prandtl numbers, "pseudo thermal entrance lengths" were predicted. This showed that, even though the thermal boundary layer had extended itself across the flow duct, the generalized temperature profile continued to chafe until the flow was hydrodynamically fully developed. The Nusselt numbers for the heated inner wall were always greater than those for the heated outer wall.

It is apparent, from this review of published literature of studies on turbulent flow and heat transfer in the developing region of concentric annuli in which velocity and temperature profiles are developing simultaneously, that the effect of the transverse convex wall surface curvature has not been considered.

CHAPTER 2
ANALYTICAL STUDY

2.1 Basic Equations

Employing a cylindrical coordinate system as axial direction x along the wall, radial and azimuthal direction r and θ to the wall, u, v, and w are corresponding velocities to the coordinates, respectively. Considering the case of incompressible fluid flow, the Navier-Stokes equations for the cylindrical coordinate is expressed in the following forms:

$$\rho\left(\frac{\partial u}{\partial t}+u\frac{\partial u}{\partial x}+v\frac{\partial u}{\partial r}+\frac{w}{r}\frac{\partial u}{\partial \theta}\right)=F_x-\frac{\partial p}{\partial x}+\mu\nabla^2 u \qquad (2.1.a)$$

$$\rho\left(\frac{\partial v}{\partial t}+u\frac{\partial v}{\partial x}+v\frac{\partial v}{\partial r}+\frac{w}{r}\frac{\partial v}{\partial \theta}-\frac{w^2}{r}\right)=F_r-\frac{\partial p}{\partial r}-\mu\left(\frac{v}{r^2}+\frac{2}{r^2}\frac{\partial w}{\partial \theta}\right)+\mu\nabla^2 v \qquad (2.1.b)$$

$$\rho\left(\frac{\partial w}{\partial t}+u\frac{\partial w}{\partial x}+v\frac{\partial w}{\partial r}+\frac{w}{r}\frac{\partial w}{\partial \theta}+\frac{vw}{r}\right)=F_\theta-\frac{1}{r}\frac{\partial p}{\partial r}-\mu\left(\frac{w}{r^2}+\frac{2}{r^2}\frac{\partial v}{\partial \theta}\right)+\mu\nabla^2 w \qquad (2.1.c)$$

For the constant-property flow (density ρ, specific heat c_p, and thermal conductivity k), the corresponding energy equation has the following forms:

$$\rho c_p\frac{DT}{Dt}=k\nabla^2 T+v\frac{Dp}{Dt}+q'+\mu\left(\frac{\partial u}{\partial r}\right)^2 \qquad (2.2)$$

$$where \qquad \nabla^2=\frac{1}{r}\frac{\partial}{\partial r}\left(r\frac{\partial}{\partial r}\right)+\frac{1}{r^2}\frac{\partial^2}{\partial q}+\frac{\partial^2}{\partial x^2}$$

D = the substantial derivatives

q' = specific heat generation

The continuity equation for incompressible steady flow is:

$$\frac{\partial u}{\partial x}+\frac{\partial v}{\partial r}+\frac{1}{r}\frac{\partial w}{\partial \varphi}+\frac{v}{r}=0 \tag{2.3}$$

In turbulent flow, Reynolds [Hinze, 1975] modified the momentum equation by introducing mean fluctuation values of flow quantities in place of instantaneous values. The velocity components are given as the sum of the mean component and fluctuating component in the same direction. Therefore, the transformation of Navier-Stokes equations due to Reynolds modifications is obtained by introducing:

$$u=\overline{u}+u',\quad v=\overline{v}+v',\quad w=\overline{w}+w',\quad \&\quad p=\overline{p}+p'$$

The Navier-Stokes equations in cylindrical coordinates have the following forms for incompressible steady flow in straight uniform cross section, neglecting the body force, as:

$$\rho\left(\frac{\partial \overline{u}}{\partial t}+\overline{u}\frac{\partial \overline{u}}{\partial x}+\overline{v}\frac{\partial \overline{u}}{\partial r}+\frac{\overline{w}}{r}\frac{\partial \overline{u}}{\partial \theta}\right)=-\frac{\partial \overline{p}}{\partial x}+\mu\nabla^2\overline{u} -\left[\frac{\partial}{\partial x}\left(\rho\overline{u'^2}\right)+\frac{1}{r}\frac{\partial}{\partial r}\left(r\rho\overline{u'v'}\right)+\frac{1}{r}\frac{\partial}{\partial \theta}\left(\rho\overline{u'w'}\right)\right] \tag{2.4.a}$$

$$\rho\left(\frac{\partial \overline{v}}{\partial t}+\overline{u}\frac{\partial \overline{v}}{\partial x}+\overline{v}\frac{\partial \overline{v}}{\partial r}+\frac{\overline{w}}{r}\frac{\partial \overline{v}}{\partial \theta}-\frac{\overline{w}^2}{r}\right)=-\frac{\partial \overline{p}}{\partial r}+\mu\left(\nabla^2\overline{v}-\frac{\overline{v}}{r^2}-\frac{2}{r^2}\frac{\partial \overline{w}}{\partial \theta}\right) -\left[\frac{\partial}{\partial x}\left(\rho\overline{u'v'}\right)+\frac{1}{r}\frac{\partial}{\partial r}\left(\rho\overline{v'^2}\right)+\frac{1}{r}\frac{\partial}{\partial \theta}\left(\rho\overline{v'w'}\right)-\frac{\rho\overline{w'^2}}{r}\right] \tag{2.4.b}$$

$$\rho\left(\frac{\partial \overline{w}}{\partial t}+\overline{u}\frac{\partial \overline{w}}{\partial x}+\overline{v}\frac{\partial \overline{w}}{\partial r}+\frac{\overline{w}}{r}\frac{\partial \overline{w}}{\partial \varphi}+\frac{\overline{v}\,\overline{w}}{r}\right)=-\frac{1}{r}\frac{\partial \overline{p}}{\partial \theta}+\mu\left(\nabla^2\overline{w}+\frac{2}{r^2}\frac{\partial \overline{w}}{\partial \theta}-\frac{\overline{w}}{r^2}\right) -\left[\frac{\partial}{\partial x}\left(\rho\overline{u'w'}\right)+\frac{\partial}{\partial r}\left(\rho\overline{v'w'}\right)+\frac{1}{r}\frac{\partial}{\partial \theta}\left(\rho\overline{w'^2}\right)-\frac{2\left(\rho\overline{v'w'}\right)}{r}\right] \tag{2.4.c}$$

The corresponding energy equation for heat transfer in turbulent flow is:

$$\frac{\partial \overline{T}}{\partial t}+\overline{u}\frac{\partial \overline{T}}{\partial x}+\overline{v}\frac{\partial \overline{T}}{\partial r}+\frac{\overline{w}}{r}\frac{\partial \overline{T}}{\partial \theta}=\alpha\nabla^2\overline{T}-\left[\frac{\partial}{\partial x}\left(\overline{u'T'}\right)+\frac{1}{r}\frac{\partial}{\partial r}\left(r\overline{v'T'}\right)+\frac{1}{r}\frac{\partial}{\partial \theta}\left(\overline{w'T'}\right)\right] \qquad (2.5)$$

All of the derivatives with respect to time, t, and the body force are neglected under the condition of developing, steady, incompressible, constant cross-sectional duct flow. The three normal stresses $-\rho\overline{u'^2}$, $-\rho\overline{v'^2}$, and $-\rho\overline{w'^2}$ and three shear stresses $-\rho\overline{u'v'}$, $-\rho\overline{v'w'}$, and $-\rho\overline{u'w'}$, in Eq. (2.4), are known as Reynolds stresses or eddy stresses.

For non-circular cross section geometry [White, 1968] the shear stresses are nearly constant along the phase sides, dropping off sharply to zero in the corners of the cross section in the turbulent flow through the same cross-section. This is because of the phenomenon of turbulent secondary flow, in which there are non-zero mean velocities v and w in the plane of the cross-section. In a circular cross section, if there is no secondary flow, Eq. (2.4.a) is sufficient for determining the axial velocity distribution. In most situations, the axial thermal conduction and eddy diffusion are either zero or negligibly small, and the terms $\frac{\partial^2\overline{T}}{\partial x^2}-\frac{\partial}{\partial x}\left(\overline{u'T'}\right)$ can be ignored. The terms $\frac{\partial^2\overline{u}}{\partial x^2}$ and $\frac{\partial \overline{u'^2}}{\partial x}$ can also be ignored with the boundary layer approximation. The v and w are zero in axisymmetric and two dimensional flows.

Therefore, for axisymmetric and two-dimensional flow such as in a pipe or in a concentric annulus, the appropriate equation of momentum is:

$$\overline{u}\frac{\partial \overline{u}}{\partial x}+\overline{v}\frac{\partial \overline{u}}{\partial r}+\frac{1}{\rho}\frac{\partial \overline{p}}{\partial x}=\frac{\nu}{r}\frac{\partial}{\partial r}\left(\frac{\partial \overline{u}}{\partial r}\right)-\frac{1}{r}\frac{\partial}{\partial r}\left(r\overline{u'v'}\right) \qquad (2.6)$$

The corresponding equation of energy is:

$$\overline{u}\frac{\partial \overline{T}}{\partial x}+\overline{v}\frac{\partial \overline{T}}{\partial r}=\frac{k}{r}\frac{\partial}{\partial r}\left(r\frac{\partial \overline{T}}{\partial r}\right)-\frac{1}{r}\frac{\partial}{\partial r}\left(r\overline{v'T'}\right) \tag{2.7}$$

In Eq. (2.6) and (2.7), the last terms $-\overline{u'v'}$ and $-\overline{v'T'}$ are often expressed as $\varepsilon_M\cdot\left(\partial\overline{u}/\partial r\right)$ and $\varepsilon_H\cdot\left(\partial\overline{T}/\partial r\right)$, respectively. Unlike the molecular counter-part (ν and k), the eddy diffusivity is not a fluid property because it is a function of position and flow condition. The first researcher to work on this problem was J. Boussinesq [Schlichting, 1979]. In a similar way with the coefficient of viscosity in Stokes's Law for laminar flow:

$$\tau_l=\mu\frac{\partial u}{\partial r}=\rho\nu\frac{\partial u}{\partial r}$$

Boussinesq introduced a mixing coefficient [Schlichting, 1979], A_τ, which is known as eddy diffusivity, for the Reynolds stress in turbulent flow by putting:

$$\tau_t=-\rho\,\overline{u'v'}=A_\tau\frac{d\overline{u}}{dr}=\rho\varepsilon_\tau\frac{d\overline{u}}{dr} \tag{2.8}$$

where ε_τ is kinematic eddy diffusivity. Prandtl [1928] hypothesized that the behavior of the apparent shear stress was similar to the laminar stress, and proposed the identity for the momentum equation:

$$-\overline{u'v'}=\varepsilon_M\left(\frac{\partial\overline{u}}{\partial r}\right) \tag{2.9}$$

and for the energy equation:

$$-\overline{v'T'}=\varepsilon_H\left(\frac{\partial\overline{T}}{\partial r}\right) \tag{2.10}$$

With Eq. (2.9), Eq. (2.6) becomes:

$$\bar{u}\frac{\partial \bar{u}}{\partial x}+\bar{v}\frac{\partial \bar{u}}{\partial r}+\frac{1}{\rho}\frac{\partial \bar{p}}{\partial x}=\frac{1}{r}\frac{\partial}{\partial r}\left[r\left(\nu+\varepsilon_M\right)\frac{\partial \bar{u}}{\partial r}\right] \tag{2.11}$$

and with Eq. (2.10), Eq. (2.7) becomes:

$$\bar{u}\frac{\partial \bar{T}}{\partial x}+\bar{v}\frac{\partial \bar{T}}{\partial r}=\frac{1}{r}\frac{\partial}{\partial r}\left[r\left(\alpha+\varepsilon_H\right)\frac{\partial \bar{T}}{\partial r}\right] \tag{2.12}$$

The corresponding equations in the rectangular coordinates are:

$$\bar{u}\frac{\partial \bar{u}}{\partial x}+\bar{v}\frac{\partial \bar{u}}{\partial y}+\frac{1}{\rho}\frac{\partial \bar{p}}{\partial x}=\frac{\partial}{\partial y}\left[\left(\nu+\varepsilon_M\right)\frac{\partial \bar{T}}{\partial y}\right] \tag{2.13}$$

and

$$\bar{u}\frac{\partial \bar{T}}{\partial x}+\bar{v}\frac{\partial \bar{T}}{\partial y}=\frac{\partial}{\partial y}\left[\left(\alpha+\varepsilon_H\right)\frac{\partial \bar{T}}{\partial y}\right] \tag{2.14}$$

2.2 Governing Equations of Momentum and Energy : Developing Turbulent Fluid in a Concentric Annulus

For a concentric annular flow channel in which the hydrodynamic and thermal boundary layers are developing simultaneously in the entrance region, we may need the solutions of the basic equations in the developing region to find the velocity and temperature distributions. However, even though the equations, Eq. (2.6) and Eq. (2.7), can be greatly simplified, it is still extremely difficult to solve because of non-linearities involved in the equations.

The problem will be studied from an integral view point based on a modified model of Reichardt's expression for the eddy diffusivity of momentum with the concept of a turbulent Prandtl number. The distribution of the shear stress, τ, and heat flux, q, will be derived from the equations of momentum and energy, and boundary conditions will be considered for the heat transfer solutions. (i.e., one wall has a constant heat flux while the other is insulated.)

The force balance action on the annular fluid element for the entrance region described in Figure 2.1 yields:

$$\left[p-\left(p+\frac{\partial p}{\partial x}dx\right)\right]2\pi r\,dr \;+\; \left(\tau+\frac{\partial \tau}{\partial r}dr\right)2\pi(r+dr)dx - 2\pi r\tau\,dx = \left[-\frac{\partial p}{\partial x}+\frac{1}{r}\frac{\partial}{\partial r}(\tau\cdot r)\right]2\pi r\,dr\,dx \tag{2.15}$$

The time rate change of momentum in the cylindrical volume is:

$$\rho\frac{d}{dt}\left\{\left[\left(u+\frac{\partial u}{\partial x}dx\right)-u\right]+\left[\left(u+\frac{\partial u}{\partial r}dr\right)-u\right]\right\}2\pi r\,dr\,dx = \rho\left(u\frac{\partial u}{\partial x}+v\frac{\partial u}{\partial r}\right)2\pi r\,dr\,dx \tag{2.16}$$

To employ the momentum theorem, in which the time rate change of momentum is equal to the external forces, take the right hand side terms from Eqs (2.15) and (2.16):

$$-\frac{\partial p}{\partial x} + \frac{1}{r}\frac{\partial}{\partial r}(\tau \cdot r) = \rho\left(u\frac{\partial u}{\partial x} + v\frac{\partial u}{\partial r}\right) \tag{2.17}$$

and rearrange Eq. (2.17) to obtain:

$$\left(u\frac{\partial u}{\partial x} + v\frac{\partial u}{\partial r}\right) + \frac{1}{\rho}\frac{\partial p}{\partial x} = \frac{1}{\rho r}\frac{\partial}{\partial r}(\tau \cdot r) \tag{2.18}$$

The energy balance of a cylindrical fluid element in the developing region described in Figure 2.2, then, gives:

$$\begin{aligned} -2\pi r\,dr\rho\,uc_P\frac{\partial T}{\partial x}dx - 2\pi r\,dr\rho\,v\,dx\frac{\partial T}{\partial r}dr = \\ 2\pi(r+dr)\,dx\left(q + \frac{\partial q}{\partial r}dr\right) - 2\pi r\,dx\,q \end{aligned} \tag{2.19}$$

Rearrange Eq. (2.19) to obtain:

$$u\frac{\partial T}{\partial x} + v\frac{\partial T}{\partial r} = -\frac{1}{\rho c_P r}\frac{\partial}{\partial r}(q \cdot r) \tag{2.20}$$

Eqs. (2.18) and (2.20) in combination with Eqs. (2.8) and (2.9) yield:

$$\frac{\tau}{\rho} = (\nu + \varepsilon_M)\frac{\partial u}{\partial r} \tag{2.21}$$

and,

$$-\frac{q}{c_P\rho} = (\alpha + \varepsilon_H)\frac{\partial T}{\partial r} \tag{2.22}$$

The velocity and temperature distributions, u and T, for a given wall heat flux and fluid flow may

be determined from Eqs. (2.21) and (2.22) if ε_M and ε_H are both known. To obtain the velocity profiles in the developing regions of concentric annular ducts, a model of modified eddy diffusivity for momentum is proposed. The proposed model is based on the model of Reichardt for a circular tube, but taking into account the radius ratio of the two ducts as well as the similarity of the function for ε_M in the direction of flow. A turbulent Prandtl number will be given as a unit value in this study. There are several empirical correlations obtained from experimental studies for the calculation of the thermal eddy diffusivity, ε_H, but the choice of a particular correlation is not crucial in the analysis.

2.3 Variable von Kármán Constants, κ_i : A New Modified Model

The u(x, y) and v(x, y) are the mean velocities in the direction of rectangular coordinates x and y in a steady, two-dimensional, turbulent shear flow. In experiments of turbulent shear flows, "the law of the wall" describes the mean velocity in the region near the surface, viscous sublayer, as, $\frac{u}{u_\tau} = f\left(\frac{y u_\tau}{\nu}\right)$. The universal law established the form in the special case of two-dimensional mean flow of an incompressible fluid as:

$$\frac{u}{u_\tau} = \frac{1}{\kappa}\ln\left(\frac{y u_\tau}{\nu}\right) + c \tag{2.23}$$

where κ, the von Kármán constant, and c are constants to be determined experimentally. Prandtl's mixing length theory [Holman, 1995 and Schlichting, 1968] can be employed to obtain Eq. (2.23).

In the research of Yu [1958] and Rao [1967], variations in the value of the von Kármán constant, κ, have been observed in the turbulent boundary layer, and it was found that the von Kármán constant, κ, varied with the Reynolds number based on the radius of the circular cylinder, Re_{r_i}. Rao and Keshavan [1972] suggested that as the Reynolds number becomes larger, the von Kármán constant, κ, has a tendency to reach a value of approximately 0.4.

In previous literature [Coles, 1956, Willmarth et al., 1970, Kim et al., 1990, Lee et al., 1993] of turbulent boundary layer flow on a cylindrical body, near the wall surface, the velocity gradient, $(\partial u/\partial y)$, becomes steeper and the value of the von Kármán constant, κ, increases as the radius becomes smaller. This implies that the turbulent eddies are strongly affected by the change in the value of the transverse convex wall curvature, i.e, the cylinder radius r_i.

To characterize the effect of transverse convex surface curvature, it is proposed in the research of Kim et al. [1995] that the von Kármán constant, κ_i, not be a fixed value and it may take the

following form:

$$\kappa_i = \kappa_o \cdot F(r_i) \tag{2.26}$$

$F(r_i)$ was approximated in the following form as a hyperbolic tangent function of the radius of a cylindrical body, r_i, with the experimental data given by Willmarth et al. [1970], and by Kim and Lee [1990]:

$$F(r_i) = 1 + 1.5 \cdot \tanh\left(0.0064 / r_i^{0.72} \right) \tag{2.27}$$

Even though the Eq. (2.27) is adequate, it is still in a dimensional form. To transform Eqs. (2.26) and (2.27) to dimensionless form, Eq. (2.27) is normalized by $r_i = 1.0$ m as:

$$\kappa_i = \kappa_o \cdot F\left(r_i / r_{ref} \right) \tag{2.28}$$

where $\kappa_o = 0.4$ and $r_{ref} = 1.0$ m:

$$F(r^*) = 1 + 1.5 \cdot \tanh\left(0.0064 / r^{*0.72} \right) \tag{2.29}$$

where $r^* = r_i / r_{ref}$.

Kim et al. [1995] assumed that measurements of values of y^+ ($= y \cdot u_\tau / \nu$) less than 100 approximately would be unreliable as a result of large fluctuations in velocity, wall interference, poor probe sensitivity at low velocities, probe position error, or uncertainty in static pressure. The function, $F(r_i)$, together with the experimental results of Willmarth et al. [1970] and Kim and Lee [1990, 1993] are shown in Figure 2.3 and are summarized in Table 2.1.

Figure 2.3 shows that the value of κ_i increases with the decreasing value of the cylinder radius, r_i, or r_i^* suggesting that the length scale distribution of the turbulent eddies, which is a function of wall shear stress is strongly affected by the change in the value of r_i (i.e., the transverse convex surface curvature) while over a flat plate with $dp/dx < 0$, the range of the von Kármán constant, κ,

is fixed at 0.4 to 0.41. Therefore, by the slope in the logarithmic region of non-dimensionalized velocity profiles, physically known as von Kármán constant as shown in Eq. (2.23), you might be able to find out the involved physical mechanism.

Eq. (2.28) and Eq. (2.29) form the basis of this analytical study, and all of the analytic results will be explained in terms of the modified von Kármán constant, κ_i.

2.4 Problem Definition and Assumptions

The selected model of the equations for the study of the velocity and temperature profiles in the entrance region for a concentric annulus has a series of assumptions, and this analysis for the fluid flow and heat transfer is subjected to the following conditions:

(1) The annulus is concentric, the inner core is uniformly heated with constant heat flux while the outer wall is insulated.

(2) The flow is steady and turbulent at all points along the flow channels (within the boundary layer).

(3) The thermodynamic properties (density, viscosity, specific heat, etc.) of the fluid are constant. The turbulent Prandtl number Pr_t is 1.0.

(4) The velocity and temperature profiles are uniform across the entrance section, and the hydrodynamic boundary layer and thermal boundary layer thicknesses are zero at the entrance section.

(5) The turbulent velocity and thermal boundary layers develop along a cylinder whose axis is parallel to the free stream fluid flow.

(6) The flow fields can be divided into two regions such as the sublayer and the fully turbulent region.

(7) At the radius where the local mean velocity is a maximum, the shear stress is also zero.

(8) The flow in the region outside the inner and outer boundary is a potential flow.

The assumption that the point where the radius of maximum velocity coincides with the point where of zero shear stress is not necessarily true [Kjellström et al.,1966 and Lee, 1964]. On the other

hand, it is not possible to theoretically calculate the radius of zero shear stress or the shear stress at the radius of maximum velocity. However, the radius of zero shear will very likely be a radius not too different from the radius of the maximum velocity for a smooth concentric annulus.

2.5 Analysis : Adiabatic Turbulent Flow in the Developing Regions through a Concentric Annulus

A modified form of Reichardt's expression for eddy diffusivity of momentum will be applied to the entire developing turbulent regions of a concentric annulus. Then, we shall proceed to solutions for the turbulent velocity distributions in the entrance regions with the momentum and energy equations which were derived in the previous section. The momentum integral equation for the developing turbulent boundary layer will be developed in a general manner, so that the hydrodynamic entrance length can be deduced from it. The local friction factors will be also obtained from the usual definitions.

2.5.1 Eddy Diffusivity for Momentum, ε_M

For the calculation of velocity distributions in turbulent boundary layers, the information to evaluate the term $\overline{u'v'}$ which is defined as an apparent turbulent shear stress, is required. This is frequently referred to as the turbulent *closure* problem, and it is usually solved using a turbulence model based either on an algebraic equation or differential equation, for $\overline{u'v'}$. For many practical applications, it is close enough to state the relationship with the mean velocity profile as:

$$-\rho\overline{u'v'} = \rho\varepsilon_M\frac{\partial\overline{u}}{\partial y} \tag{2.30}$$

where as a proportionality factor, ε_M, is defined as the eddy diffusivity for momentum. However, there are still some problems in evaluating ε_M. The eddy diffusivity models for momentum in this study are originally from van Driest [1956] and Reichardt [1943] for sublayer regions and fully turbulent regions, respectively. Those models were modified for the flow channel geometry in this study with the variable von Kármán constant, κ_i, proposed by Kim et al [1995]. It is assumed that

the von Kármán constant, κ_i, for the inner core of transverse convex surface curvature, is a function of the radius of an inner core in a concentric annulus, r_i, or r^*, which was discussed in Section 2.3.

For the fully developed regions outside the sublayer, Reichardt [1943] proposed the following expression for ε_M based on experimental data for the turbulent core in a smooth pipe:

$$\frac{\varepsilon_M}{\nu} = \frac{\kappa R^+}{6}\left[1-\left(\frac{r}{R}\right)^2\right]\left[1+2\left(\frac{r}{R}\right)^2\right] \tag{2.31}$$

where κ is assumed to be a constant and equals to 0.4.

Assuming that the expression of Eq. (2.31) would be applicable in a modified form, Levy [1967] and Roberts [1967] both derived expressions for the velocity profiles in the turbulent flow through the fully developed region of a concentric annulus, and their expressions were seen to be valid for all the regions of a concentric annulus, provided appropriate values were given to the constant κ_i for the inner wall regions.

In this study, it is further postulated that Reichardt's expression [1943] for the eddy diffusivity for momentum can be applied to the entire developing turbulent flow regions on both sides of the concentric annulus with proper modification for the regions outside the sublayer, $\left(y_{js}^+ \le y_j^+ \le \delta_j^+\right)$, as:

$$\left(\frac{\varepsilon_M}{\nu}\right)_j = \frac{\kappa_j \delta_j}{6}\left[1-\left(1-\frac{y_j^+}{\delta_j^+}\right)^2\right]\left[1+2\left(1-\frac{y_j^+}{\delta_j^+}\right)^2\right] \tag{2.32}$$

where j refers to region i (inner) or o (outer) and further reduced to for $\left(\zeta_{js} \le \zeta_j \le 1\right)$ as:

$$\left(\frac{\varepsilon_M}{\nu}\right)_j = \frac{\kappa_j \delta_j}{6}\zeta_j\left(2-\zeta_j\right)\left(3-4\zeta_j+2\zeta_j^2\right) \tag{2.33}$$

where $\zeta_{js} = y_{js}^{+}/\delta_{j}^{+}$.

For regions close to each wall, the concept of a sublayer [Kays and Crawford, 1993] is used. This idea demands the sublayer model for which the eddy diffusivity retains a small magnitude throughout the sublayer and goes to zero only at the wall itself. The van Driest hypothesis [Kays and Crawford, 1993] is a turbulent model that provides for an eddy diffusivity that is only zero at y = 0, and allows a continuous calculation through the sublayer and into the fully turbulent region without discontinuities. With this, the Prandtl mixing length [Kays and Crawford, 1993] is used all the way to the wall instead of putting it to zero at an assumed effective outer edge of the sublayer. Rather, by introducing a damping function into the mixing length equation, the sublayer is simulated as:

$$l = \kappa\, y\left(1 - e^{-y^{+}/A^{+}}\right) \tag{2.34}$$

where A^{+} is the damping constant which is an effective sublayer thickness determined empirically. Eq. (2.34) can be substituted into the following equation for the proper form in terms of eddy diffusivity for momentum:

$$\frac{\varepsilon_M}{\nu} = \frac{l^2}{\nu}\frac{du}{dy} = l^{+2}\frac{du^{+}}{dy^{+}} \tag{2.35}$$

Rearranging Eq. (2.35) with the proposed variable von Kármán constant, κ_i, the modified eddy diffusivity distributions, $\left(\frac{\varepsilon_M}{\nu}\right)_j$, for regions close to each wall, $\left(0 \le y_j^{+} \le y_{js}^{+}\right)$, becomes:

$$\left(\frac{\varepsilon_M}{\nu}\right)_j = \kappa_j^2\, y_j^{+2}\left[1 - \exp\left(-\frac{y_j^{+}}{A_j^{+}}\right)\right]^2\left|\frac{\partial u_j^{+}}{\partial y_j^{+}}\right| \tag{2.36}$$

Eq. (2.36) maybe be further expressed for $\left(0 \le \zeta_j \le \zeta_{js}\right)$ as (see Appendix 3),

$$\left(\frac{\varepsilon_M}{\nu}\right)_j = \frac{1}{2}\left[-1 + \left\{1 + 4\left(\kappa_j \delta_j^+\right)^2 \zeta_j^2 \left[1 - \exp\left(-\frac{\delta_j^+ \zeta_j}{A_j^+}\right)\right]^2 \left(\frac{\tau}{\tau_R}\right)_j\right\}^{0.5}\right] \tag{2.37}$$

2.5.2 Velocity distribution

From Section 2.2, the basic governing equation for the transport of momentum may be rewritten for our study as:

$$\frac{\tau_j}{\rho} = \left(\nu + \varepsilon_M\right)\frac{\partial u_j}{\partial y_j} \tag{2.38}$$

in dimensionless form of Eq. (2.38):

$$\frac{\partial u_j^+}{\partial \zeta_j^+} = \delta_j^+\left[\frac{\left(\tau/\tau_R\right)_j}{1 + \left(\varepsilon_M/\nu\right)_j}\right] \tag{2.39}$$

for ($0 \le \zeta_j \le 1$), where from a force balance the shear stress distribution is:

$$\left(\frac{\tau}{\tau_w}\right)_j = \frac{\left(1 - \zeta_j\right)\left\{1 \pm \left[\Delta_j \zeta_j / \left(2 + \Delta_j\right)\right]\right\}}{\left(1 \pm \Delta_j \zeta_j\right)} \tag{2.40}$$

With the eddy diffusivities, $\left(\frac{\varepsilon_M}{\nu}\right)_j$, which is established for the entire developing fluid flow regions in the last section 2.5.1, the velocity profiles within the developing boundary layers can be derived.

2.5.3 Friction Factor

The local friction factor based on the local shear stress at the wall, excluding momentum changes due to a developing velocity profile may be defined by:

$$f_j = \frac{\tau_{w_j}}{\frac{1}{2}\rho\, u_b^2} \tag{2.41}$$

The local friction factor for the outer wall can be stated in dimensionless parameters which have been derived in the preceding section as:

$$f_{ox} = \frac{2}{\left(u_{bo}^{+\,2}\right)_x} \tag{2.42}$$

Since it is assumed that the pressure gradient is constant, the force balance on the developing layers yields the following equation:

$$\frac{dp}{dx}\cdot\left[\left(r_o^2 - R_o^2\right) + \left(R_i^2 - r_i^2\right)\right] = 2\,\bar{\tau}\left(r_i + r_o\right) \tag{2.43}$$

also for the outer boundary layer:

$$\frac{dp}{dx}\cdot\left(r_o^2 - R_o^2\right) = 2\,\tau_{w_o}\, r_o \tag{2.44}$$

Then from Eq. (2.43) with Eq. (2.44), we have, (see Appendix 4):

$$f_x = \frac{r_o\left(2r_o\delta_o - \delta_o^2 + 2r_i\delta_i + \delta_i^2\right)}{\left(2r_o\delta_o - \delta_o^2\right)\left(r_i + r_o\right)}\cdot f_{ox} \tag{2.45}$$

or, in dimensionless quantity, the average local friction factor f_x is:

$$f_x = \frac{r_o^{+}\left(2r_o^{+}\delta_o^{+} - \delta_o^{+2} + 2r_i^{++}\delta_i^{++} + \delta_i^{++2}\right)}{\left(2r_o^{+}\delta_o^{+} - \delta_o^{+2}\right)\left(r_i^{++} + r_o^{+}\right)}\cdot f_{ox} \tag{2.46}$$

where the superscript ++ indicates that the parameters of the inner region are made dimensionless using the local shear velocity of the outer region for the parameter conformity. For example, r_i^{++}

is defined as:

$$r_i^{++} = \frac{r_i u_{\tau_o}}{\nu} = \frac{r_i u_{\tau_i}}{\nu}\frac{u_{\tau_o}}{u_{\tau_i}} = r_i^{+}\sqrt{\frac{\tau_{w_o}}{\tau_{w_i}}}$$

where shear stress ratio are coming from force balance on an annular fluid element between r_i and δ_i and between δ_o and r_o with the assumption that the pressure is constant in the radial direction (see Appendix 1), as:

$$\left(\frac{\tau_{w_i}}{\tau_{w_o}}\right)_x = \frac{r_o}{r_i}\frac{\left(2r_i\delta_i + \delta_i^2\right)}{\left(2r_o\delta_o - \delta_o^2\right)} \tag{2.47}$$

and

$$\left(\frac{\tau_{w_i}}{\tau_{w_o}}\right)_d = \frac{r_o}{r_i}\frac{\left(r_m^2 - r_i^2\right)}{\left(r_o^2 - r_m^2\right)} \tag{2.48}$$

Therefore, the average local friction factor, f_x, can be calculated from the velocity profile given from previous section (2.5.1 & 2.5.2).

Bulk velocity is defined as:

$$u_b = \frac{\int_{dA} u\, dA}{\int_{dA} dA} \tag{2.49}$$

which can be written in the dimensionless form for the entrance region as:

$$\left(u_{bo}^{+}\right)_x = \frac{2}{r_o^{+2}\left(1-\alpha^2\right)}\left(\int_0^{\delta_i^{++}} u_i^{++} r^{++} dy_i^{++} + \frac{1}{2}u_{\delta o}^{+}\left(R_o^{+2} - R_i^{++2}\right) + \int_0^{\delta_o^{+}} u_o^{+} r^{+} dy_o^{+}\right) \tag{2.50}$$

It is more simplified in Appendix 4, Eq. (A4.3), for the convenience of computation.

The Reynolds number is defined as:

$$\mathrm{Re} = \frac{\rho\, u_b De}{\mu} = \frac{u_b De}{\nu} \tag{2.51}$$

where $De = 2\,(r_o - r_i)$ and rewritten as:

$$\mathrm{Re} = \frac{4}{r_o(1+\alpha)\nu} \int_{r_i}^{r_o} u\, r\, dr \tag{2.52}$$

and in dimensionless parameters, as:

$$\mathrm{Re} = 2\, r_o^+ \left(u_{bo}^+\right)(1-\alpha) \qquad or \qquad 2\, r_i^+ \left(u_{bi}^+\right)\left(\alpha^{-1}-1\right) \tag{2.53}$$

Eq. (2.49) and Eq. (2.53) give the relation between Re and δ_j^+ or $u_{\delta_j}^+$ for a given value of r_j^+.

2.5.4 Hydrodynamic Entrance Length

The hydrodynamic entrance length is referred to the length of the entire developing boundary region distance from the entrance to the meeting point of the two boundary layers where it is assumed that the fully developed region begins. Analytically, it can be obtained from applying the momentum integral equation for the developing hydrodynamic boundary layer in a concentric annulus. Since the force acting on the fluid in a space is equal to the rate of flow of momentum out of the space, the momentum equation for the flow boundary layers can be written as:

$$\begin{aligned} dF_x = &-\left\{ \left[\int_0^{\delta_j} \rho\, u_j^2\, 2\pi r\, dy_j \right]_2 - \left[\int_0^{\delta_j} \rho\, u_j^2\, 2\pi r\, dy_j \right]_1 \right\} \\ &+ \left\{ \left[\int_0^{\delta_j} \rho\, u_j\, 2\pi r\, dy_j \right]_2 - \left[\int_0^{\delta_j} \rho\, u_j\, 2\pi r\, dy_j \right]_1 \right\} \cdot u_{\delta_j} \end{aligned} \tag{2.54.a}$$

where 1 and 2 refer to the planes indicated. Rearrangement gives:

$$\tau_{w_j} r_j \, dx \; - \; \frac{1}{2}\left(R_j^2 - r_j^2 \right) dp \; = \; u_{\delta_j} \cdot d\left[\int_0^{\delta_j} \rho \, u_j \, r \, dy_j \right] \; - \; d\left[\int_0^{\delta_j} \rho \, u_j^2 \, r \, dy_j \right] \qquad (2.54.b)$$

There is no shear force at δ_j from the definition of the boundary layer.

From the items of the physical model in Section 2.4, we have:

(1) the flow outside of the boundary layer is frictionless, i.e., $dp = -\rho \, u_{\delta_j} \, du_{\delta_j}$

(2) the boundary layer thickness is taken as zero at x = 0, and

(3) the flow is turbulent everywhere, $x \geq 0$.

Integration of Eq. (2.54) with assumption (1) above between x = 0 and x = x with some rearrangement gives:

$$x_j = \int_{u_e}^{u_{\delta_j}} \frac{\rho \left(R_j^2 - r_j^2 \right)}{2 \, \tau_{w_j} r_j} u_{\delta_j} \, du_{\delta_j} \; - \; \int_0^A \frac{1}{\tau_{w_j} r_j} dA \; + \; \int_0^B \frac{u_{\delta_j}}{\tau_{w_j} r_j} dB \qquad (2.55)$$

where A and B are:

$$A = \int_0^{\delta_j} \rho \, u_j^2 \, r \, dy_j \qquad and, \qquad B = \int_0^{\delta_j} \rho \, u_j \, r \, dy_j$$

Eq. (2.55) can be made more general by stating it in terms of dimensionless parameters, as:

$$\left(\frac{x}{De} \right)_{M,j} = \int_{u_e^+}^{u_{\delta_j}^+} \frac{R_j^{+2} - r_j^{+2}}{2 \, r_j^+ \, De_j^+} u_{\delta_j}^+ \, du_{\delta_j}^+ \; - \; \int_0^{A^+} \frac{1}{r_j^+ \, De_j^+} dA^+ \; + \; \int_0^{B^+} \frac{u_{\delta_j}^+}{r_j^+ \, De_j^+} dB^+ \qquad (2.56)$$

where A^+ and B^+ are:

$$A^+ = \int_0^{\delta_j^+} u_j^{+2}\, r^+\, dy_j^+$$

$$B^+ = \int_0^{\delta_j^+} u_j^+\, r^+\, dy_j^+$$

$$\text{and,} \qquad De_j^+ = 2\, r_i^+\left(\alpha^{-1} - 1\right) \quad or \quad 2\, r_o^+\left(1 - \alpha\right)$$

From Eq. (2.52), the Reynolds number can be rewritten in terms of dimensionless parameters:

$$\mathrm{Re} = \left(u_e^+\right)_j \left(De^+\right)_j \tag{2.57}$$

By substituting Eq. (2.57) into Eq. (2.56), and some rearranging, we obtain:

$$\left(\frac{x}{De}\right)_{M,j} = \int_{\frac{\mathrm{Re}}{2}}^{E^+} \left[\frac{2\cdot\left(R_j^{+2} - r_j^{+2}\right)}{r_j^+\left(De_j^+\right)^3} E^+ - \frac{2}{r_j^+\left(De_j^+\right)^2} \int_0^{\delta_j^+} u_j^+\, r^+ dy_j^+ \right] dE^+ + \int_0^{D^+} \frac{1}{r_j^+\, De_j^+} dD^+ \tag{2.58}$$

where

$$D^+ = \int_0^{\delta_j^+} \left(u_{\delta_j}^+ - u_j^+\right) u_j^+ r^+ dy_j^+$$

$$\text{and,} \qquad E^+ = \frac{1}{2}\, u_{\delta_j}^+\, De_j^+$$

One can compute $(x/De)_x$ for the given δ_j^+ and Re from Eq. (2.58). The value of Re for a given r_i^+ and δ_j^+ will be obtained in the next section.

2.6 Analysis : Diabatic Turbulent Flow in the Developing Regions through a Concentric Annulus

In Section 2.5, the turbulent flow velocity profiles in the entrance regions of a concentric annulus were developed from a eddy diffusivity of momentum. In this section, we shall consider the problems of the combined hydrodynamic and thermal boundary layer development in the entrance regions where both the fluid velocity and temperature profiles are uniform. Employing the turbulent Prandtl number for unit value, the temperature distribution in these regions will be developed. The ratio of eddy diffusivities for momentum and heat will be discussed in some detail. The energy integral equation will be then applied and the relation between boundary layer thickness and entrance length will be obtained in a similar manner as considered in Section 2.5.4. Finally, the local Nusselt numbers will be obtained for the various Reynolds numbers, Prandtl numbers and radius ratios.

2.6.1 Eddy diffusivity for Heat

As was the case of the eddy diffusivity for momentum, the calculation for the turbulent boundary layer heat transfer requires information on $\overline{v'T'}$ in the energy equation. $\overline{v'T'}$ is an apparent turbulent heat flux in the direction normal to the main flow and by introducing the eddy diffusivity for heat, ε_H, as a proportional factor, the following equation can be defined:

$$c_p\rho \cdot \overline{v'T'} = c_p\rho \cdot \varepsilon_H \frac{\partial \overline{T}}{\partial y}$$

which was shown in the section 2.1.

Similarly, the ratio of the eddy diffusivity for momentum and heat, $\varepsilon_M / \varepsilon_H$, which is called the turbulent Prandtl number, Pr_t, can be defined as:

$$Pr_t = \frac{\mu_t c}{k_t} = \frac{\varepsilon_M}{\varepsilon_H} \tag{2.59}$$

where μ_t and k_t are eddy viscosity and eddy conductivity, respectively. Knowing ε_M at every point, the thermal boundary layer can be solved with the appropriate information on Pr_t. The turbulent Prandtl number, Pr_t, plays an important role in the analytical studies to predict heat transfer coefficients in turbulent convective heat transfer [Knudsen et al., 1958]. To simplify the mathematical manipulation, many of these analytical results are based on the assumption that this ratio is equal to unity. The simple assumption, $Pr_t = 1$, is equivalent to Reynolds analogy [Kays and Crawford, 1993]. According to the experimental works reported in references [Lee et al., 1964, Page et al., 1952, Sleicher et al., 1957, Mizushina et al., 1970 , Park, 1971, Kays and Crawford, 1993], it appears that the Pr_t is not equal to unity, but varies with the distance from the wall and has a complicated relationship with other variables such as y^+, Pr, Re, α, etc.

In the supporting investigation performed for the unity value of turbulent Prandtl number [Schlichting, 1979], H. Ludwieg [1956] found that the ratio , $\varepsilon_H/\varepsilon_M = 1/Pr_t$, varies from about unity at the wall to about 1.5 in the centre of a pipe and is independent of the Mach number. Similar results were reported by Johnson [1959] who made measurements in a boundary layer on a heated wall. According to these, the ratio $\varepsilon_H / \varepsilon_M$ increases from about unity at the wall to approximately 2 at the edge of the boundary layer. Fage and Falkner, and also Reichardt [Schlichting, 1979] reported the measurement of 2, the former in the wake behind a circular cylinder, and the latter in a free jet, both in an incompressible fluid flow. According to the preceding measurements, the ratio, $\varepsilon_H / \varepsilon_M$, is smaller in a boundary layer than in a free stream, due to the influence of the wall on the boundary layer. Therefore, it seems plausible that the ratio, $\varepsilon_H / \varepsilon_M$, has a value of unity at the wall

(according to Ludwieg, the value is 1.08 at $Pr_t = 0.9$) and increases to a value of 2 ($Pr_t = 0.5$) away from the wall. In practice, frequently, a constant value of $\varepsilon_H / \varepsilon_M = 1$ ($Pr_t = 1$) or of 1.3 (Reichardt, giving $Pr_t = 0.77$) is assumed. In this study the value of unity for the turbulent Prandtl number is used and this is because of the following facts.

From the real experimental works [Kays and Crawford, 1993], it is at least clear that the Pr_t, the ratio of the eddy diffusivity for momentum and heat, $\varepsilon_M / \varepsilon_H$, is,

(1) smaller than unity for air

(2) greater than unity for liquid metal.

However, it must be pointed that the available experimental evidence is not sufficiently consistent to arrive at any concrete conclusion.

Some workers such as Leung and his associates [1962] in their analysis on heat transfer with turbulent flow in concentric annuli with constant and variable heat flux used the theoretical treatment of Jenkins [1951]. Jenkins considered the heat conduction to or from an element of an eddy during its transverse to the main flow direction. From this consideration, a correlation for Pr_t was obtained. However, Leung et al. [1962] used a multiplying factor of 1.2 to fit the expression better to their experimental data.

In his study of the thermal entrance problems of concentric annuli, Lee [1968] divided the annular passage into two regions and allowed the variation of $\varepsilon_H/\varepsilon_M$ based on his previous experimental measurements. Park [1971] formulated an empirical correlation of the turbulent Prandtl number, $\varepsilon_H/\varepsilon_M$, as a function of y^+ and radius ratio, α from the results of his experimental work as:

$$\sigma\left(y_j^+\right) = \frac{\varepsilon_H}{\varepsilon_M}\left(y_j^+\right) = 0.968\ \alpha^{-0.045}\ y_j^{+0.031} \tag{2.60}$$

In his analysis, Eq. (2.60) is used for the case of Prandtl numbers bigger than 0.5 because the experimental results were obtained using air as the working fluid.

The axial variation of the ratio of the eddy diffusivity for momentum and heat, $\varepsilon_H/\varepsilon_M$, in the thermal entrance region of circular duct seems to be negligible according to the experimental work of Abberch and Churchill [1960], but the work of Hanratty [1961] indicates that at smaller values of axial distance x, the values of the eddy diffusivity for heat near the centre of the pipe are seen to decrease for air. However, for the axisymmetric case as in the study of Park [1971], this difference in the eddy diffusivity obtained by the two workers from their experiments seems to be of little importance, since the heat flux is already small in the outer region and their studies show also little effect on the variation with (x/De). Therefore, it is assumed in this study that the Pr_t variation in the entrance region of the concentric annulus is independent of the length, x.

It appears that the problem of the turbulent Prandtl number is still subject to further studies, both experimentally and analytically. The effects of turbulence structure, fluid properties and wall characteristics on eddy motion must be taken into consideration.

2.6.2 Temperature Distribution

Temperature distribution can be derived from the energy equation, given by Eq. (2.22), if the functions for heat flux and eddy diffusivity for heat are known. Eq. (2.22) in non-dimensional parameters are (see Appendix 2):

$$\frac{\partial T_j^+}{\partial \zeta_j} = \pm \Pr \cdot \delta_j^+ \left[\frac{q_j/q_{w_i}}{1 + \left(\Pr/\Pr_t\right)\cdot\left(\varepsilon_M/\nu\right)_j} \right] \qquad \left(0 \le \zeta_j \le 1\right) \tag{2.61}$$

where

$$T_j^+ = \frac{\left(T_{w_i} - T_j\right) c \ \tau_{w_j}}{q_{w_i}\left(\tau_{w_j}/\rho\right)^{0.5}}$$

and +ve for j = i and -ve for j = o.

The heat flux distribution may be obtained from an energy balance with the boundary condition of uniform heat flux from the inner core only, (see Appendix 1):

$$q_i/q_{w_i} = \frac{1 - \alpha^2\left(1 + \Delta_i\zeta_i\right)^2}{\left(1 - \alpha^2\right)\left(1 + \Delta_i\zeta_i\right)} \qquad \left(0 \le \zeta_i \le 1\right) \tag{2.62.a}$$

and

$$q_o/q_{w_i} = \frac{\alpha\left(2 - \Delta_o\zeta_o\right)\Delta_o\zeta_o}{\left(1 - \alpha^2\right)\left(1 - \Delta_o\zeta_o\right)} \qquad \left(0 \le \zeta_o \le 1\right) \tag{2.62.b}$$

In Eqs. (2.62), q_{w_i} refers to the uniform heat flux at the inner core tube surface, and the initial conditions for Eq. (2.60) are,

$$T_i^+ = 0 \ \text{ at } \zeta_i = 0 \text{ and } \ T_o^+ = T_{om}^+ \ \text{ at } \zeta_o = 1$$

Eqs. (2.4) and (2.8) for the eddy diffusivity for momentum and Eq. (2.61) for heat flux can be put together into Eq. (2.60) to obtain the temperature distributions of either the inner or outer region.

2.6.3 Nusselt-Number

The local heat transfer coefficient and Nusselt number are defined in the usual way, respectively as:

$$h_{x,j} = \left(q_{w_i}\right)_{x,j} \Big/ \left(T_{w_i} - T_b\right)_{x,j} \tag{2.63.a}$$

and

$$Nu_{x,j} = \frac{h_{x,j} \cdot 2\left(r_o - r_i\right)}{k} \tag{2.63.b}$$

In dimensionless form, Eq. (2.63.b) becomes (see Appendix 4):

$$Nu_{x,j} = 2\left[\frac{1-\alpha}{\alpha}\right]\frac{r_i^+ \cdot \mathrm{Pr}}{\left(T_b^+\right)_{x,j}} \tag{2.64}$$

Eq. (2.64) can be determined using the appropriate δ_{ij}^+ and by finding the local bulk temperature, $\left(T_b^+\right)_{x,j}$, of the fluid flow at any given value of $(x/De)_x$.

The bulk temperature, $\left(T_b\right)_{x,j}$, is defined as:

$$\left(T_b\right)_{x,j} = \left(\frac{\int_{dA} T\,u\,dA}{\int_{dA} u\,dA}\right)_{x,j} = \left(\frac{\int_{r_i}^{r_o} r\,u\,T\,dr}{\int_{r_i}^{r_o} r\,u\,dr}\right)_{x,j} \tag{2.65}$$

and, in terms of dimensionless parameters, as:

$$\left(T_b^+\right)_{x,j} = \left(\frac{\int_{r_i^+}^{r_o^+} T^+u^+r^+dr^+}{\int_{r_i^+}^{r_o^+} u^+r^+dr^+}\right)_{x,j} \tag{2.66}$$

For the boundary condition that is used in this analysis, the dimensionless local bulk temperature is (see Appendix 4):

$$\left(T_b^+\right)_{x,i} = \frac{2}{r_i^{+2}\left(\alpha^{-2}-1\right)u_{bi}^+}\left[\int_0^{\delta_i^+} T_i^+u_i^+r^+dy_i^+ + \frac{1}{2}T_{\delta_{ii}}^+\,u_{\delta_i}^+\left(R_o^{++2} - R_i^{+2}\right) + T_{\delta_{ii}}^+\int_0^{\delta_o^{++}} u_o^{++}r^+dy_o^{++}\right] \qquad for \quad \delta_i^+ = \delta_t^+ \tag{2.67.a}$$

$$\left(T_b^+\right)_{x,i} = \frac{2}{r_i^+\left(\alpha^{-2}-1\right)u_{bi}^+}\left[\int_0^{\delta_i^+} T_i^+ u_i^+ r^+ dy_i^+ + \int_{\delta_i^+}^{\delta_{ti}^+} T_i^+ r^+ dy_i^+ + \frac{1}{2}u_{\delta_i}^+ T_{\delta_{ti}}^+\left(R_o^{++2} - r_{\delta_{ti}}^{+\,2}\right) + T_{\delta_{ti}}^+ \int_0^{\delta_o^{++}} u_o^{++} r^+ dy_o^{++}\right] \qquad for \quad \delta_i^+ < \delta_{ti}^+ \tag{2.67.b}$$

$$\left(T_b^+\right)_{x,i} = \frac{2}{r_i^+\left(\alpha^{-2}-1\right)u_{bi}^+}\left[\int_0^{\delta_{ti}^+} T_i^+ u_i^+ r^+ dy_i^+ + T_{\delta_{ti}}^+ \int_{\delta_{ti}^+}^{\delta_i^+} u_i^+ r^+ dy_i^+ + \frac{1}{2}u_{\delta_i}^+ T_{\delta_{ti}}^+\left(R_o^{++2} - R_i^{+2}\right) + T_{\delta_{ti}}^+ \int_0^{\delta_o^{++}} u_o^{++} r^+ dy_o^{++}\right] \qquad for \quad \delta_i^+ > \delta_{ti}^+ \tag{2.67.c}$$

Appendix 4 caontains more simplified equation for the purpose of easier computation.

2.6.4 Thermal Entrance Length

The energy integral equation for the thermal boundary layer with only the inner wall being heated can be written from an idealized model, which is described in Figure 2.2. The outer wall is insulated and the axial conduction is neglected in this equation:

$$2\pi\, r_j q_j dx + c_p T_{\delta_{tj}}\left[\left(\int_0^{\delta_{tj}} \rho\, u\, 2\pi r\, dy\right)_2 - \left(\int_0^{\delta_{tj}} \rho\, u\, 2\pi r\, dy\right)_1\right] + \left(\int_0^{\delta_{tj}} c_p T\, \rho\, u 2\pi r\, dy\right)_1 = \left(\int_0^{\delta_{tj}} c_p T\, \rho\, u 2\pi r\, dy\right)_2 \tag{2.68}$$

where the subscripts on the parentheses refer to planes 1 and 2 in the diagram.

Rearrange Eq. (2.68) to obtain:

$$2\pi r_j q_j dx = d\left(\int_0^{\delta_{tj}} c_p T \rho\, u 2\pi r\, dy\right) - 2\pi\, c_p T_{\delta_{tj}} d\left(\int_0^{\delta_{tj}} \rho\, u\, r\, dy\right) \tag{2.69}$$

The physical models used here, as described in Section 2.4, are:

(9) $\delta_i = \delta_{ij} = 0$ at $x = 0$,

(10) $dq_{w,j}/dx = 0$, and

(3) the flow is turbulent everywhere, $x \geq 0$.

An integration of Eq. (2.69), with these assumptions is given as:

$$\left(\frac{x}{De}\right)_{x,T,j} = \frac{1}{De\, r_j q_j} \int_0^{\delta_{ij}} \left(T - T_{\delta_{ij}}\right) c_p \rho\, ur\, dy \tag{2.70}$$

Eq. (2.70) can be now transformed into dimensionless forms utilizing various non-dimensional parameters as:

$$\left(\frac{x}{De}\right)_{x,T,i} = \frac{1}{2\, r_i^{+2}\left(\alpha^{-1} - 1\right)} \left[\int_0^{\delta_{ti}^+} \left(T_{\delta_{ti}}^+ - T_i^+\right) u_i^+ \left(y_i^+ + r_i^+\right) dy_i^+\right] \qquad for\ \ \delta_i^+ \geq \delta_{ti}^+ \tag{2.71.a}$$

and

$$\left(\frac{x}{De}\right)_{x,T,i} = \frac{1}{2\, r_i^{+2}\left(\alpha^{-1} - 1\right)} \left[\int_0^{\delta_i^+} \left(T_{\delta_{ti}}^+ - T_i^+\right) u_i^+ \left(y_i^+ + r_i^+\right) dy_i^+ + u_{\delta_i}^+ \int_{\delta_i^+}^{\delta_{ti}^+} \left(T_{\delta_{ti}}^+ - T_i^+\right)\left(y_i^+ + r_i^+\right) dy_i^+\right]$$

$$for\ \ \delta_i^+ < \delta_{ti}^+ \tag{2.71.b}$$

Eqs. (2.71.a) and (2.71.b) give the relation between $(x/De)_{x,T,j}$ and δ_{ij}^+ for concentric annuli with the specified boundary conditions in this study. The required values for δ_j^+ and δ_{tj}^+ will be given in the calculation procedures.

CHAPTER 3
COMPUTATION

3.1 General Overview

The calculations of this study involves solving ordinary differential equations (ODE) of the form,

$$\frac{dy}{dx} = f(x, y)$$

The general methods that are used to solve this kind of problem are called "one-step methods" and all one-step methods can be expressed in the general form that is shown below, with variations in the matter in which the slope is estimated.

New value = old value + slope × step size

According to this equation, the slope estimate is used to extrapolate from an old value to a new value over a distance h. This formula can be applied step-by-step to compute into the next step and hence, trace out the trajectory of the solution. The simplest approach is to use the differential equation to estimate the slope in the form of the first derivative at the previous point. In other words, the slope at the beginning of the interval is taken as an approximation of the average slope over the whole interval. This approach is called "Euler's method" [Chapra and Canale, 1990] and it is extremely simple to program on a personal computer.

The numerical solution of ordinary differential equations (ODEs) involves two types of errors: round-off error and truncation error [Chapra and Canale, 1990]. Round-off error is due to the fact that a computer can only represent quantities with a finite number of digits. Truncation

error is the discrepancy introduced by the fact that the numerical method employs an approximation to represent exact mathematical operations and quantities. It consists of two parts: The first is local truncation errors that result from an application of this method at each step. The second is a propagate truncation error that result from the approximations produced during the previous steps. The sum of the two is the total or global truncation error.

As it is known with Euler's method, the source of errors come from the fact that the derivative at the beginning of the interval is assumed to apply across the entire interval. Decreasing the step size may reduce these errors. However, to attain much better accuracy for the same computational effort we need to employ other one-step methods. For the calculations of this study the Runge-Kutta (RK) methods are used. Among the higher-order techniques of the RK methods, the Butcher's Fifth-Order RK method [1964] is used.

To solve the governing differential equations for developing turbulent flow in a smooth concentric annulus, a set of grids with uniform spacing is first generated within the physical domain. Grid points are designed to have the same boundaries of the physical domain for consideration of boundary conditions.

To obtain the velocity profiles, u_j^+, Eq. (2.10) is used as the basic form and once a certain velocity profile is identified at a specific condition, other information such as friction factors, temperature profiles, Nusselt numbers, and entrance lengths for momentum and heat transfer can then be produced. The thermal boundary layer in this study develops simultaneously with the velocity boundary layer. Since the thicknesses are not identical, the Prandtl number should be given before beginning the calculations. This parameter represents the ratio of momentum transfer in the flow to that of heat transfer. Therefore, it may represent relative velocity and

thermal boundary layer thickness. Then δ and δ_t, which are denoted as velocity and thermal boundary layer thicknesses, respectively, have the following relations:

$$\text{for} \quad Pr < 1 \quad ; \quad \delta < \delta_t$$

$$Pr = 1 \quad ; \quad \delta = \delta_t$$

$$\text{and} \quad \text{for} \quad Pr > 1 \quad ; \quad \delta > \delta_t$$

This concept is used when we assume a thermal boundary thickness in the calculation.

The integration that we perform in this study for such values as the bulk velocity and bulk temperature, etc., is numerically calculated using Simson's 1/3 rule [Chapra and Canale, 1990]. While there are higher-order formulas of Simson's rules, we have used it in this study because of its simplicity and accuracy.

3.2 Calculation Procedure

The point of maximum velocity is obtained from the velocity profiles in the fully developed region, which is assumed to be the same line as the meeting point of the two boundary layers (inner and outer) of a concentric annulus. The details of the velocity and temperature profiles in the developing region are given as follows:

1. The values of α, r_i, r_i^+ and Pr are prescribed. κ_i is calculated from Eqs. (2.26) and (2.27) with the inner radius, r_i. The r_i^+ value will be selected for the Reynolds number, Re.

2. Assume a value of r_m and obtain the value of $(\tau_{w_i}/\tau_{w_o})_d$ from Eq. (2.47). δ_{mi}^+ r_o^+ and δ_{mo}^+ are then decided as follows:

$$\delta_{mi}^+ = r_i^+\left(\frac{r_m}{r_i} - 1\right), \quad r_o^+ = \frac{r_i^+}{\alpha\cdot(\tau_{w_i}/\tau_{w_o})_d}$$

and $$\delta_{mo}^+ = r_o^+\left(1 - \frac{r_m}{r_o}\right)$$

3. The velocity profile for the fully developed region is obtained from integration of Eq. (2.38) with Eqs. (2.31), (2.32) and (2.39).

4. From the continuity of velocities at the location of maximum velocity ($r = r_m$, or $\zeta_i = \zeta_o = 1$), the relationship between u_{im}^+ and u_{om}^+ is used as the matching condition, shown below. If this equality works, the process will go on to the next step; if it does not, return to step (2) and reassume the value of r_m.

$$u_{om}^+ = (\tau_{w_i}/\tau_{w_o})_d^{0.5}\cdot u_{im}^+$$

5. Prescribe the value of δ^* for boundary layer thickness in the developing region. By some simple manipulations of the known parameters, $(\tau_{w_i}/\tau_{w_o})_x$ can be calculated from Eq. (2.46). Here, it is assumed that the thickness ratio of the developing boundary layers equals that of the fully developed.

6. Obtain the velocity profile for the developing region from Eq. (2.38) with Eqs. (2.31), (2.32) and (2.39). The flow in the region outside the boundary layer is uniform.

7. The results from step (6) are substituted into Eq. (2.49) for bulk velocity, u_{bo}^+, then f_x will be calculated from Eqs. (2.41) and (2.45), Re from Eq. (2.51), and $(x/De)_M$ from Eq. (2.57).

Once the developing turbulent flow velocity profiles are obtained in a concentric annulus, one can move to the heat transfer calculations. Here, we will obtain T_j^+, $(x/De)_{x,Tj}$, and $Nu_{x,j}$ for the simultaneously developing thermal boundary layer in a concentric annulus and these next calculation procedures are followed:

8. Since the momentum boundary layer thickness, δ_i, is known at a given $(x/De)_{x,M,i}$ from previous calculation, we now assume a certain value for δ_{ti}, the thermal boundary layer thickness.

9. Temperature distributions are computed from Eq. (2.60) with Eqs. (2.61.a) and (2.61.b) for the heat flux distributions and Eqs. (2.4) and (2.8) for the eddy diffusivity of momentum. Pr_t is assumed to be unit.

10. The Nusselt number, $Nu_{x,j}$, is computed from Eq. (2.63) with bulk temperature from Eq. (2.65) and the given value of Pr.

11. Thermal entrance length $(x/De)_{x,T,i}$ is then calculated with the assumed value of δ_{ti} from Eq. (2.70) and the values of $(x/De)_{x,T,i}$ are compared to that of $(x/De)_{x,M,i}$

12. Repeat steps (8) to (11) until the condition $(x/De)_{x,M,i} \approx (x/De)_{x,T,i}$ is met.

13. For the prescribed values of step (1) above, Re, $\left(T_b^+\right)_{x,j}$ and $Nu_{x,j}$ are computed from the appropriate equations with the known values of δ_i^+ and δ_{ti}^+ obtained from step (8).

3.3 Results of Computation

The governing differential equations have been solved by numerical procedure with the boundary conditions appropriate to developing turbulent flows in concentric annuli. To solve the equations, the following input parameters and fixed parameters are provided:

- **Input Parameters**

  r_i^* : 0.005, 0.01, 0.02, 0.05, 0.1, 0.2, 0.5 and 1.0

  α : 0.2, 0.5 and 0.8

  Re : $10^4 \sim 10^6$

  Pr : 0.7, 1.0 and 10

  Pr_t : fixed at one

- **Fixed Parameters**

  $\kappa_o = 0.4$ (von Kármán's constant for outer region)

The "variable mixing length" constant κ_i used in this study for the inner region of the developing turbulent flow in the concentric annuli is presented in Table 2.1 and plotted in Figure 2.3.

The predicted velocity distributions for three different van Driest Damping Parameters (effective thickness), A_i^+, at a given r_i^* of 0.001 is shown in Figure 2.4. *Two-layer model* was given from the Prandtl mixing-length model for the sublayer and fully turbulent region, and it is compared to the van Driest Model for velocity distributions [Lee, 1964]. Figure 2.5 and Figure 2.6 are for r_i^* of 0.1 and 1.0, respectively. The variations of effective thickness, A_i^+, for

different values of r_i^* were shown in Figure 2.7 to demonstrate the effect of Transverse Convex Curvature.

The relationship between r_i^+ and Reynolds number is shown in Figure 2.8 for a given value of $\delta^* = 0.5$. It is also drawn for the fully developed region, $\delta^* = 1.0$, in Figure 2.9. α is fixed at 0.5 and r_i^* is given as 0.005, 0.01, 0.02, 0.05, 0.1, and 1.0 over the range of 10,000 to 100,000 of the Reynolds number for both cases.

The predicted velocity distributions in the developing region of $\delta^* = 0.5$ for two different inner core radii, r_i^*, of 0.005 and 0.01 at a given Reynolds number, Re = 20,000, with a fixed α of 0.5 are plotted in Figure 2.10 and for the fully developed region, $\delta^* = 1.0$, in Figure 2.11, respectively.

The friction factors, f, calculated from Eq. (2.17) for the fully developed turbulent flow in a concentric annulus at radii of the inner cores, $r_i^* = 1.0$ and $\alpha = 0.999$ are plotted in Figure 2.12. They are plotted with two empirical correlation for fully developed turbulent flow between parallel plates of Reynolds number ranging between 10,000 and 100,000 [Kays & Crawford, 1993]. In Figure 2.13 to Figure 2.18, f^* ($= f / f_{1.0m}$) are plotted as a function of Re. Each figure is fixed at one of three radius ratios, α (= 0.2, 0.5, 0.7), for the developing or fully developed region. The calculation was carried out for the values of inner core radius, r_i^*, at 0.005, 0.01, 0.02, 0.05, and 0.1. Figure 2.19 is the friction factor distribution in the entrance distance at a fixed radius ratio, α (= 0.5), for several r_i^* to illustrate the effect of Transverse Convex Curvature.

The lengths of the entrance region of momentum for the various values of the Reynolds number for different r_i^* divided by the length of $r_i^* = 1.0$ at fixed α (= 0.2) are shown in Figure 2.20. Figure 2.21 and Figure 2.22 are similar plots for fixed radius ratio, α, at 0.5 and 0.8, respectively.

The predicted temperature distributions for two different radii of the inner cores with a fixed radius ratio of $\alpha = 0.5$ are plotted in Figure 2.23 for the developing region and Figure 2.24 for the fully developed region. Both are for a fixed Reynolds number (Re = 20,000) and Prandtl number (Pr = 0.7).

Figure 2.25 to Figure 2.27 show the predicted Nusselt numbers for the radii of the inner core at r_i^* =1.0 with a fixed radius ratio of $\alpha = 0.999$ to compare with the case of parallel plates [Kays & Crawford, 1993]. They are given in different Prandtl numbers (Pr = 0.7, 1.0, 10.0) over the range of Reynolds numbers between 10,000 and 100,000. The Nusselt numbers of several cases of the inner core radius with a fixed radius ratio of $\alpha = 0.5$, Reynolds number of Re = 20,000 and Prandtl number of Pr = 0.7 are shown in Figure 2.28. Figure 2.29 and Figure 2.30 are graphs for the cases of Pr = 1.0 and Pr = 10.0, respectively. The thermal lengths of the entrance region for the various values of the Reynolds number for different r_i^* divided by the length of $r_i^* = 1.0$ at fixed α (= 0.5) are shown in Figure 2.31 and Figure 3.32 for Pr = 0.7 and Pr = 10.0, respectively.

CHAPTER 4
DISCUSSION OF RESULTS

4.1 General Overview

The results from the analytical studies described in Chapter 2 enable us to evaluate the various characteristics of turbulent flow and heat transfer in the developing region for a concentric annulus with smooth surfaces. The analytical results were obtained through a mathematical model for turbulence based on a variable von Kármán constant, κ_i, proposed in the previous studies [Kim and Lee, 1995]. In this study, the effect of transverse convex curvature on fluid flow characteristics with regard to the velocity profile, friction factor, temperature profile, Nusselt number, and entrance length were predicted and investigated with numerical methods for the entrance region of developing turbulent flow. In the analysis it is assumed that heat is generated uniformly at the inner core.

The numerical procedure given in Chapter 3 was conducted on the effects of the inner radius, r_i^*, with the annuli having different values for the radii of the inner cores, r_i^*. The values are between 0 and 1.0 ; radii larger than 1.0 maintain the von Kármán constant, κ_i, at 0.4. The radius ratio, α, was fixed as a constant to demonstrate the effect of Transverse Convex Curvature (T.C.C.) with the Reynolds number ranging from 20,000 to 100,000. Three different Prandtl numbers (0.7, 1.0, and 10.0) were also used to view the T.C.C effect on heat transfer. Due to the lack of results that have been produced on the developing entrance region for turbulent flow in concentric annuli, the results from this study are compared to the special cases from previous studies such as flow in parallel plates.

4.2 Adiabatic Turbulent Flow in Developing Regions

In determining effective sublayer thickness, A^+, it was usually assumed that there is a fixed value of A^+, i.e. 26. The law of the wall is for the fully developed region in the two-layer model shown as follows:

$$u^+ = y^+ \qquad \text{for} \qquad 0 \le y^+ \le A^+$$

$$u^+ = (1/\kappa)\ln y^+ + 5.5 \qquad \text{for} \qquad A^+ \le y^+ \qquad [\textit{Law of wall}]$$

The van Driest hypothesis is a sublayer scheme that provides for an eddy diffusivity that is only 0 at y = 0. It is advantageous in that it allows continuous calculation through the sublayer and into the fully turbulent region with no discontinuities. With this scheme, the concept of the Prandtl mixing length was used all the way to the wall instead of truncating it to zero at an assumed effective outer edge of the sublayer, but the Damping function was introduced for simulating the sublayer in the mixing-length equation. A^+ was used as Damping parameter in the equation.

In this study, the value of A^+ for the inner core, A_i^+, seems to change with the changing inner core radius, r_i^*, as with the von Kármán constant for the inner core, κ_i. The model from van Driest for velocity distribution [Lee, 1964] is shown as:

$$u_i^+ = \int_0^{y_i^+} \frac{2}{1+\left\{1+4\kappa_i^2 y_i^{+2}\left[1-\exp\left(-y_i^+/A_i^+\right)\right]^2\right\}^{0.5}}\, dy_i^+ \qquad for \qquad 0 \le y_i^+$$

The comparison was made to the two-layer model as shown in Figure 2.4 to Figure 2.6 and the appropriate A_i^+ was given to each inner core radius, r_i^*. In Figure 2.7, the results were gathered on the A^+ vs. r_i^* graph to show A_i^+ approaching the fixed value of approximately 27.5.

4.2.1 Velocity Distribution

Velocity profiles were obtained for developing and fully developed turbulent flow in concentric annular tubes for a Reynolds number of approximately 20,000 with a fixed radius ratio, α (about 0.5), having two different radii of inner cores, $r_i^* = 0.005$ and 0.01, respectively in Figure 2.10 and Figure 2.11.

Most of the velocity profiles are plotted as dimensionless velocity, u_j^+, in order to plot all curves on the same basis. Since the shear stresses on the walls of both tubes are constant for the fully developed turbulent flows in concentric annular ducts, the friction velocities, u_{τ_j}, for the inner and outer region of the flow field can be determined. The conventional dimensionless parameters, u_i^+, u_o^+, y_i^+, and y_o^+ can be obtained from these friction velocities.

In Figure 2.10, the predicted velocity distribution of the developing turbulent flow ($\delta^* = 0.5$) for two different radii of the inner cores, r_i^*, at a given Reynolds number are shown where α is kept at 0.5. It shows that the velocity profiles in the outer region deviate very little with changes in the inner core radius, r_i^*, however, the velocity fields in the inner region deviate to some degree. For fully developed turbulent flow ($\delta^* = 1.0$) for the same Reynolds number, theoretical velocity distributions for the same two different radii of the inner cores are also given in Figure 2.11. This illustrates that the velocity fields in the inner region also deviate with changes of the inner core radius, r_i^*.

Throughout the evaluation of predicted velocity distribution, it is evident that the velocity profile deviates with a changing inner core radius, r_i, for the developing turbulent flow in a circular annulus but in the outer region there is hardly any deviation. The transverse convex

surface curvature, therefore, is also one of factors which affects the characteristics of turbulent fluid flow in addition to the radius ratio, α, and the Reynolds number, Re.

4.2.2 Friction Factors

Since there is no comparative data from previous studies on developing turbulent flow in entrance region of a concentric annulus, the results for fully developed turbulent flow are used for comparisons. Figure 2.12 shows the friction factors, f, calculated from Eq. (2.17) for fully developed turbulent flow with the inner core radius, $r_i^* = 1.0$, and a fixed radius ratio of α = 0.999. By giving the radius ratio, α, as 0.999 and the inner core radius, r_i^*, as 1.0, the geometry of the concentric annulus is regarded as parallel plates, therefore, the experimental results for fully developed turbulent flow in the parallel plates is given for the comparison. The calculation is in a good agreement with the experimental data of Reynolds number, Re > 20,000.

Figure 2.13 illustrates friction factors vs. Reynolds numbers for developing turbulent flow at a fixed radius ratio, $\alpha = 0.2$. The values from calculations made for several r_i^* are normalised by the case of an inner core radius, $r_i^* = 1.0$, which are indicated as f^*. It shows that the normalised friction factor, f^*, increases with a decreasing value of the inner core radius, r_i^*. This implies that as r_i^* decreases, the shear stress at the inner wall increases for a given Reynolds number at a fixed value of α. This is due to the fact that as the inner core radius, r_i^*, decreases, κ_i increases and the velocity gradient, $(\partial u/\partial y)$, near the wall surface for the inner region becomes flatter, which means the wall shear stress of the inner core, τ_{W_i}, increases. Figure 2.14 shows the same trend for fully developed turbulent flow with fixed α, which Kim [1996] proved experimentally.

Figure 2.15 and Figure 2.16 show the effect of transverse convex curvature at the radius ratio, $\alpha = 0.5$ on the friction factor calculated for different values of inner core radii r_i^*. Figure 2.17 and Figure 2.18 show the same for $\alpha = 0.7$.

In Figure 2.19, friction factors, f, are plotted over the entrance length for different radii of inner cores at fixed radius ratios, α. It also shows that the friction coefficient, f, increases with a decreasing value of the inner core radius, r_i^*.

4.2.3 Hydrodynamic Entrance Length

Generally, the entrance length is defined in terms of the length of the flow channel required for a certain quantity to approach its limiting value. Different quantities have been used for the definition of hydrodynamic entrance length by different investigators. In this analysis, the velocity profile approaches its limiting value for the entrance length, which was also used as the definition by Park [1971]. The lengths defined by different quantities are not necessarily the same and also these local values in the flow direction tend asymptotically to their limiting values because the influence of the viscosity in the boundary layer decreases asymptotically outward through the tube [Schlichting, 1979]. Therefore, the definition of fully developed flow is different according to the definition that is used. For example, Olson and Sparrow [1963], whose definition of the entrance length is based on the local pressure gradient or local wall shear stress, took a value within 5% of its limiting value to be a fully developed flow. While Lana and Christiansen [1967], who used the same definition of entrance length as in this analysis, assumed that a value within 1% of the limiting to be fully developed flow.

The results of this analysis on the hydrodynamic entrance length for developing turbulent flow in concentric annuli are shown in Figures 2.20 to 2.22. Entrance lengths for momentum, $(x/De)_M$, for several inner core radii at a fixed radius ratio ($\alpha = 0.2, 0.5, 0.8$) were calculated for

Reynolds numbers ranging from 10,000 to 100,000. The calculations were normalised by the results of inner radius, $r_i^* = 1.0$, and indicated as $(x/De)_M^*$. As seen in the figures, the normalized entrance length, $(x/De)_M^*$, decreases with a decreasing value of the inner core radius, $r_i^* = 1.0$.

It can be concluded that this analysis, from the integral view point, using a velocity profile based on a modified Reichardt's eddy diffusivity for momentum, satisfactorily demonstrates the *effect of transverse convex curvature* on developing turbulent flow in concentric annuli.

4.3 Diabatic Turbulent Flow in Developing Regions

4.3.1 Temperature Distribution

In Figure 2.23, the effect of the transverse convex surface curvature obtained in this analysis on temperature distribution is shown for different radii of the inner cores with the fixed values of $\alpha = 0.5$, Pr = 0.7 and Re = 20,000 for the developing turbulent flow ($\delta^* = 0.5$) in concentric annuli. The figure illustrates that, as the inner core radius, r_i^*, becomes smaller, the value of the bulk temperature, T_b^+, becomes smaller and it is evident from Eq. (2.65) that at given fixed values of α, Pr and Re, the turbulent heat transfer becomes more vigorous with a decreasing value of r_i^*. The abscissa of the curve in the figure is chosen to be a non-dimensional distance, $(r - r_i)/(r_o - r_i)$, in order to plot all curves on the same basis, because annuli of different inner core radii, r_i^*, are considered.

Figure 2.24 shows the predicted temperature distributions for different radii of the inner cores with the fixed values of $\alpha = 0.5$, Pr = 0.7 and Re = 20,000 for fully developed turbulent flow ($\delta^* = 1.0, \delta_{th}^* = 1.0$) in concentric annuli. It is obvious in the figure that the effect of the transverse convex surface curvature is produced with different radii of inner cores. This tendency confirms the research of [Kim, 1996].

It is important for any turbulent heat transfer analysis to consider the ratio, $\varepsilon_H/\varepsilon_M$, links between momentum and heat transfer. According to the experimental study of Mizushina et al. [1970], the effect of Prandtl numbers could not be detected for values ranging from 6 to 40. It is extremely difficult to develop an accurate correlation of $\varepsilon_H/\varepsilon_M$ from experimental studies due to the inherent difficulties associated with it. However, it is concluded from the experimental results together with those of Mizushina et al. [1970] and others [Lee et al., 1964, Page et al.,

1952, Sleicher et al., 1957] that the ratio, $\varepsilon_H/\varepsilon_M$, is affected slightly by Prandtl numbers (for Pr>0.5) and is greater than unity in the range of Reynolds numbers and radius ratios investigated.

The experimental results on the ratio, $\varepsilon_H/\varepsilon_M$, by Park [1971] in the entrance region of the annuli also indicated that the axial variation of the ratio is negligibly small. This is in accord with the findings of Abberch and Churchill [1960] in their work on the thermal entrance region of circular ducts.

For these reasons, Park [1971] decided to use Eq.(2.59) in his analysis of turbulent heat transfer with Prandtl numbers greater than 0.5 in the entrance region of concentric annuli and a correlation for the ratio, $\varepsilon_H/\varepsilon_M$, proposed by Dwyer [1966] for very low Prandtl number flow which is given as:

$$\sigma\left(y_j^+\right) = 1.0 - \frac{0.2/\mathrm{Pr} - 2.0}{\left(\varepsilon_M/\nu\right)^{0.9}}$$

Since the ratio has only a very minor effect in the final result, the ratio, Pr_t $(=\varepsilon_M/\varepsilon_H)$, is given as unit in this analysis, as discussed in Section 2.6.1.

4.3.2 Nusselt Number

As was for the case of the friction factor, since no previous results on the heat transfer for developing turbulent flow are available, the comparison between the results of fully developed turbulent flow and the results of this study is made. Figures 2.25, 2.26 and 2.27 are plotted for this purpose with different Prandtl numbers, Pr, of 0.7, 1.0 and 10.0 respectively.

The resent analysis uses an input of $\alpha = 0.999$ and $r_i^* = 1.0$ to closely simulate parallel plates geometry. The Nusselt numbers from this input for fully developed turbulent flow is comparable to those reported by Kays and Leung [Kays & Crawford, 1993] with $\mathrm{Pr} \geq 0.7$ and $\mathrm{Pr}_t = 0.9$.

The Nusselt numbers of this analysis for fully developed heat transfer are plotted against Reynolds numbers over the results of Kays and Leung [Kays & Crawford, 1993] in the figures which show a reasonable agreement between two.

For Figures 2.28 to 2.30, the analytical results showing the effect of transverse convex surface curvature on developing heat transfer coefficients in terms of the Nusselt number in concentric annuli are plotted on the Nusselt number vs. Entrance distance graphs. The predicted Nusselt numbers are calculated from Eq. (2.63) for concentric annuli having different inner core radii with a fixed radius ratio of $\alpha = 0.5$, and a Prandtl number of Pr = 0.7, 1.0, and 10.0 at a Reynolds number, Re = 20,000. It shows that the effect of the transverse convex surface curvature is similar to the case of the friction factor. That is, the smaller the radius of the inner core, the higher the heat transfer rate. This is because the smaller the value of the inner core radius, r_i^*, the smaller the bulk temperature, T_b^+, at fixed values of α, Pr and Re due to the increase of the production term of turbulent heat convection, $-c_p \rho \overline{v'T'}(\partial T/\partial y)$, resulting in greater heat transfer near the wall surface. Therefore, the Nusselt number for developing turbulent flow in concentric annuli with a smaller inner core diameter is always greater than that of the annulus with a larger inner core radius.

4.3.3 Thermal Entrance Length

For the simultaneously developing region in a tube, it is essential to know the momentum boundary layer thickness as well as the thermal boundary layer thickness at a given value of (x/De) and Prandtl number, Pr. For example, as it was discussed in the Section 3.1, at Pr = 1, the boundary layers should have the same thickness if the turbulent Prandtl number, Pr_t, is also unity and the heating boundary condition is symmetric.

In a typical development for momentum and thermal boundary layers, the effect of the Prandtl number on the thermal boundary layer thickness is considerable. According to the research of Park [1971], for the range of $Pr < 0.7$, the effect of Pr on the thermal boundary layer thickness is significant where the inner core wall is heated uniformly and the outer wall is insulated, while for Prandtl numbers, $0.7 \sim 30.0$, the effect is rather small.

The thermal entrance length in simultaneously developing flow is defined in this study in terms of the length of tube needed from the entrance to a cross section in the flow direction where both the generalized velocity and temperature profiles are invariant in the axial direction, when the fluid properties are assumed to be constant. This definition can be stated as:

$$\frac{\partial}{\partial x}\left(\frac{T_w - T}{T_w - T_b}\right) = 0$$

For the case of constant heat flux, as in this study, the above differentiation equation combined with the definition of the heat transfer coefficient, h, Eq. (2.62.a), yields the following expression:

$$\frac{\partial T}{\partial x} = \frac{dT_w}{dx} = \frac{dT_b}{dx}$$

According to the research of Lee [1968], for the purely thermal entrance case where the velocity profile is already fully developed at the entrance, the thermal entrance length is usually defined as the distance from the entrance to the cross section where the temperature profile has no straight-line portion perpendicular to the fluid flow axis. This thermal entrance length of the purely thermal entrance case is denoted here as $(x/De)_{d,T,p}$ which is called "the pseudo thermal entrance length". For a fluid with Prandtl numbers above a certain value, $(x/De)_{d,T,p}$ can be made the same value as $(x/De)_{d,T}$ for simultaneously developing flow. However, it is not actually

exactly the same because the temperature profile continues to change until the flow is fully developed hydrodynamically. However, the comparison of the non-dimensional temperature profiles at $(x/De)_{d,T}$ made in the research of Park [1971], show that the effect of developing flow is very small.

The results of the analysis on the thermal entrance length for developing turbulent flow in concentric annuli are shown in Figures 2.31 and 2.32. The thermal entrance lengths, $(x/De)_T$, for several inner core radii at a fixed radius ratio ($\alpha = 0.5$) and Prandtl numbers ($Pr = 0.7$, 10.0) were calculated over the range of Reynolds numbers between 10,000 and 100,000. All of them were normalized by the results of a inner radius, $r_i^* = 1.0$, and indicated as $(x/De)_T^*$ to show the differences between them. From the figures, the normalized entrance length, $(x/De)_T^*$, decreases with a decreasing value of the inner core radius, $r_i^* = 1.0$, which is the *effect of transverse convex curvature* of developing turbulent flow in concentric annuli.

CHAPTER 5
CONCLUSION

This study analytically investigated the effect of transverse convex surface curvature on developing turbulent fluid flow and heat transfer in concentric annuli with smooth surfaces.

The effects of transverse convex surface curvature on fluid flow and heat transfer, i.e., velocity distribution, friction factor, eddy diffusivity distribution, temperature distribution, and heat transfer coefficient, have been studied. The analytical results were obtained through a mathematical model for turbulence based on the variable von Kármán constant, κ_i, proposed in previous research [Kim et al., 1995].

The computer program for this present study employs an interactive process to match the velocity and temperature profiles force and energy balances and calculates the desired momentum and thermal characteristics. It is assumed that thermodynamic fluid properties in the analysis were independent of temperature.

The following conclusions are reached :

(1) Transverse convex curvature significantly effects velocity distribution and temperature distribution of developing turbulent flow in concentric annuli.

(2) Both the friction factor and Nusselt number increase with a decreasing inner core radius value while the entrance length for momentum and heat transfer decreases.

(3) Tendencies shown in the developing turbulent flow are consistent with that of fully developed turbulent flow.

(4) The effect of transverse convex curvature in the developing region is also a significant factor as in fully developed turbulent flow.

APPENDIX 1

Distribution of Shear Stress and Radial Heat Flux in Concentric Annular Flow

A.1.1 Shear Stress Distribution

The schematic geometry of a concentric annulus with smooth surfaces is shown in Figure A1.1 below.

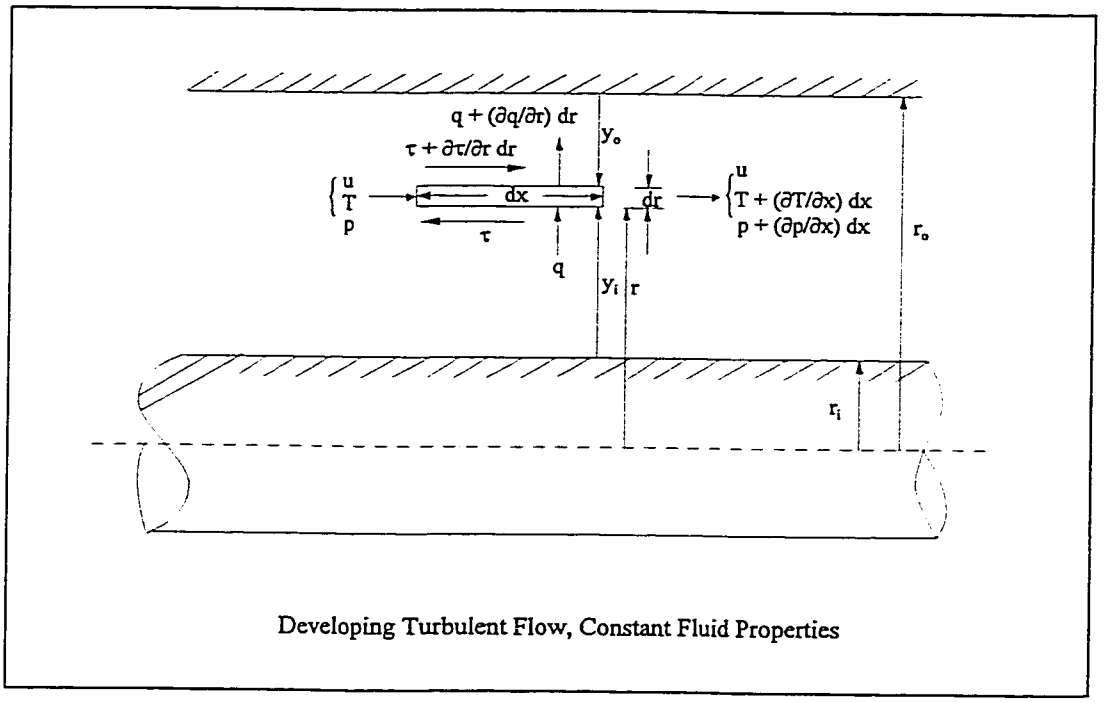

Figure A1.1 Shear Stress and Heat Flux Distribution in Annular Flow

The distribution of shear stress, τ_i, is derived using the momentum equation. Referring to Figure A1.1, a force balance for cylindrical fluid element in the inner region is:

$$-\tau_i(2\pi r)dx + \left(\tau_i + \frac{\partial \tau_i}{\partial r}\right)2\pi(r+dr)dx + p(2\pi r)dr - \left(p + \frac{\partial p}{\partial x}dx\right)2\pi r\,dr = 0 \qquad \text{(A1.1)}$$

Simplify Eq. (A1.1) as:

$$\frac{\partial}{\partial r}(\tau_i \cdot r) = \frac{\partial p}{\partial x}\, r \qquad \text{(A1.2)}$$

and integrate Eq. (A1.2) as:

$$(\tau_i \cdot r) = \frac{\partial p}{\partial x}\int_{r_i}^{r} r\,dr \qquad r_i \le r \le r_m \qquad \text{(A1.3)}$$

which is:

$$\tau_i \cdot r = \frac{\partial p}{\partial x}\frac{1}{2}\left(r^2 - r_i^2\right) + C \qquad \text{(A1.4)}$$

with the boundary condition ; $\tau_i = 0$ at $r = r_i + \delta_i$:

$$C = -\frac{\partial p}{\partial x}\cdot\frac{1}{2}\left[(r_i + \delta_i)^2 - r_i^2\right] \qquad \text{(A1.5)}$$

Substitution of Eq. (A1.5) into (A1.4) to yield:

$$\tau_i = \frac{1}{2r}\frac{\partial p}{\partial x}\left[r^2 - (r_i + \delta_i)^2\right] \qquad \text{(A1.6)}$$

at inner core wall (subscript w), $r = r_i$:

$$\tau_{w_i} = \frac{1}{2r_i}\frac{\partial p}{\partial x}\left[r_i^2 - (r_i + \delta_i)^2\right] \qquad \text{(A1.7)}$$

Divide Eq. (A1.6) by Eq. (A1.7) and with $r = r_i + y_i$ to obtain:

$$\left(\frac{\tau}{\tau_w}\right)_i = \frac{r_i}{r_i + y_i} \frac{(y_i - \delta_i)(2r_i + y_i + \delta_i)}{(2r_i + \delta_i)(-\delta_i)} \tag{A1.8}$$

Rearrange Eq. (A1.8) with $\zeta_i = y_i / \delta_i$ and $\Delta_i = \delta_i / r_i$:

$$\left(\frac{\tau}{\tau_w}\right)_i = \frac{(1-\zeta_i)\left[1 + \Delta_i \zeta_i / (2 + \Delta_i)\right]}{1 + \Delta_i \zeta_i} \tag{A1.9}$$

In the same way for the outer region:

$$\left(\frac{\tau}{\tau_w}\right)_o = \frac{(1-\zeta_o)\left[1 - \Delta_o \zeta_o / (2 + \Delta_o)\right]}{1 - \Delta_o \zeta_o} \tag{A1.10}$$

Therefore, we have Eq. (2.40), +ve for j = i and −ve for j = o.

$$\left(\frac{\tau}{\tau_w}\right)_j = \frac{(1-\zeta_j)\left[1 \pm \Delta_j \zeta_j / (2 + \Delta_j)\right]}{1 \pm \Delta_j \zeta_j} \tag{2.40}$$

To obtain the ratio of the shear stress, integration of Eq. (A1.1) for the outer region:

$$(\tau_o \cdot r) = \frac{\partial p}{\partial x} \int_r^{r_o} r \, dr \qquad r_m \le r \le r_o \tag{A1.11}$$

and boundary condition, $\tau_o = 0$ at $r = r_m$ gives:

$$\tau_o = \frac{1}{2r} \frac{\partial p}{\partial x} \left(r_m^2 - r^2 \right) \tag{A1.12}$$

At the outer wall, $r = r_o$, Eq. (A1.12) gives the shear stress as:

$$\tau_{w_o} = \frac{1}{2r_o} \frac{\partial p}{\partial x} \left(r_m^2 - r_o^2 \right) \tag{A1.13}$$

and inner wall, $r = r_i$, from Eq.(A1.7):

$$\tau_{w_i} = \frac{1}{2r_i}\frac{\partial p}{\partial x}\left(r_i^2 - r_m^2\right)$$

Divide Eq. (A1.7) by Eq. (A1.12) to obtain the ratio of the shear stress, Eq. (2.48):

$$\left(\frac{\tau_{w_i}}{\tau_{w_o}}\right)_d = \frac{r_o}{r_i}\left(\frac{r_i^2 - r_m^2}{r_m^2 - r_o^2}\right) \tag{2.48}$$

and for developing flow, with over $r_m = r_i + \delta_i$ and under $r_m = r_o - \delta_o$:

$$\left(\frac{\tau_{w_i}}{\tau_{w_o}}\right)_x = \frac{r_o}{r_i}\left(\frac{2r_i\delta_i + \delta_i^2}{2r_o\delta_o - \delta_o^2}\right) \tag{2.47}$$

A.1.2 Radial Heat Flux Distribution

In a concentric annulus, the heating condition considered is such that the core surface is heated and the outer surface is insulated. The heat analysis can be carried out by calculating the heat balance. The control volume for the heat balance is also expressed in Figure A1.1.

Consider a small cylindrical control volume as indicated in Figure. A1.1. If the axial thermal diffusion is negligible, according to the steady flow energy equation, the net heat transfer equals the enthalpy change in the present case as:

$$\rho c_p u T 2\pi r\,dr + q 2\pi r\,dx = \rho c_p u\left(T + \frac{\partial T}{\partial x}dx\right)2\pi r\,dx + \left(q + \frac{\partial q}{\partial r}dr\right)2\pi(r + dr)dx \tag{A1.14}$$

(i) Inner region

Simplify Eq. (A1.14) to obtain:

$$-\frac{\partial}{\partial r}(q_i \cdot r) = \rho c_p r u_i \frac{\partial T_i}{\partial x} \tag{A1.15}$$

Integration of Eq. (A1.15):

$$q_i \cdot r = -\rho c_p \frac{\partial T_i}{\partial x} \int_{r_i}^{r} r\, u_i(r)\, dr \tag{A1.16}$$

Assume, $u_i(r) = u_{ib}$, which is bulk motion:

$$q_i \cdot r = -\rho c_p \frac{\partial T_i}{\partial x} u_{ib} \frac{1}{2}\left(r^2 - r_i^2\right) + C \tag{A1.17}$$

with the boundary condition $q_i = 0$ at $r = r_o$:

$$C = \rho c_p \frac{\partial T_i}{\partial x} u_{ib} \frac{1}{2}\left(r_o^2 - r_i^2\right) \tag{A1.18}$$

Substitution of Eq. (A1.18) into Eq. (A1.17) yields:

$$q_i \cdot r = -\rho c_p \frac{\partial T_i}{\partial x} \cdot \frac{1}{2}\left(r^2 - r_o^2\right) u_{ib} \tag{A1.19}$$

For inner core wall ; $r = r_i$:

$$q_{w_i} \cdot r_i = -\rho c_p \frac{\partial T_i}{\partial x} \cdot \frac{1}{2}\left(r_i^2 - r_o^2\right) u_{ib} \tag{A1.20}$$

Divide Eq. (A1.19) by Eq. (A1.20) to obtain:

$$\frac{q_i}{q_{w_i}} = \frac{r_i}{r} \cdot \frac{\left(r^2 - r_o^2\right)}{\left(r_i^2 - r_o^2\right)} \tag{A1.21}$$

Rearrange Eq. (A1.21) with $r = r_i + y_i$, $\zeta_i = y_i / \delta_i$ and $\Delta_i = \delta_i / r_i$ to obtain Eq. (2.26.a).

$$\frac{q_i}{q_{w_i}} = \frac{1-\alpha^2\cdot\left(1+\Delta_i\zeta_i\right)^2}{\left(1-\alpha^2\right)\left(1+\Delta_i\zeta_i\right)} \tag{2.26.a}$$

(ii) Outer region

Simplify Eq. (A1.14) and integrate to obtain:

$$q_o \cdot r = -\rho c_p \frac{\partial T_o}{\partial x}\int_r^{r_o} r\, u_o(r)\, dr \tag{A1.22}$$

Assumption of $u_o(r) = u_{ob}$, which is bulk motion:

$$q_o \cdot r = -\rho c_p \frac{\partial T_o}{\partial x} u_{ob} \frac{1}{2}\left(r_o^2 - r^2\right) + C \tag{A1.23}$$

with the boundary condition, $q_o = 0$ at $r = r_o$, C is 0.

In the same way as the inner region:

$$\frac{q_o}{q_{w_i}} = \frac{r_i}{r}\frac{\left(r_o^2 - r^2\right)}{\left(r_o^2 - r_i^2\right)} \tag{A1.24}$$

and with $r = r_o - y_o$, $\zeta_o = y_o / \delta_o$ and $\Delta_o = \delta_o / r_o$ to obtain Eq. (2.62.b):

$$\frac{q_o}{q_{w_i}} = \frac{\alpha\left(2-\Delta_o\zeta_o\right)\left(\Delta_o\zeta_o\right)}{\left(1-\alpha^2\right)\left(1-\Delta_o\zeta_o\right)} \tag{2.62.b}$$

APPENDIX 2

Non-Dimensionalized Forms of the Velocity and Temperature Equation for Concentric Annular Geometry

A.2.1 Velocity Profile

The axial velocity of fluid, u(r), can be derived from the definition of total shear stress as:

$$\frac{\tau_j}{\rho} = \left(\nu + \varepsilon_M\right)_j \frac{\partial u_j}{\partial y_j} \tag{A2.1}$$

to non-dimensionalize the velocity gradient:

$$\frac{\partial u_j}{\partial y_j} = \frac{\partial u_j^+}{\partial y_j^+}\left(\frac{u_\tau^2}{\nu}\right)_j \tag{A2.2}$$

from

$$\partial u_j = u_{\tau_j}\,\partial u_j^+$$

$$\partial y_j = \left(\nu/u_\tau\right)_j \partial y_j^+$$

and

$$\partial y_j^+ = \delta_j^+\,\partial \zeta_j^+$$

With friction velocity:

$$u_\tau = \sqrt{\frac{\tau_w}{\rho}} \tag{A2.3}$$

Eq. (A2.1) can be transformed into dimensionless form as:

$$\frac{\partial u_j^+}{\partial \zeta_j} = \delta_j^+ \frac{\left(\tau/\tau_w\right)_j}{\left(1+\varepsilon_M/\nu\right)_j} \tag{A2.4}$$

A.2.2 Temperature Profile

The equation of a temperature profile across a flow cross-section can be derived from the basic heat transport equation:

$$-\frac{q_j}{c\rho} = \left(\alpha + \varepsilon_H\right)_j \frac{\partial T_j}{\partial r_j} \tag{A2.5}$$

(ii) Inner region

From the definition of T_i^+, ∂T_i^+ is available as:

$$\partial T_i = -\frac{q_{w_i} u_{\tau_i}}{c\tau_{w_i}} \partial T_i^+$$

from

$$T_i^+ = \frac{\left(T_{w_i} - T_i\right) c\, \tau_{w_i}}{q_{w_i} u_{\tau_i}}$$

From $r = r_i + y_i$, ∂ r is given as:

$$\partial r = \frac{1}{u_{\tau_i}} \delta_i^+ \, \partial \zeta_i \, \nu$$

the dimensionless form of Eq. (A2.5) in the inner region is:

$$\frac{\partial T_i^+}{\partial \zeta_i} = \mathrm{Pr} \cdot \delta_i^+ \frac{\left(q/q_w\right)_i}{\left(1 + \mathrm{Pr}/\mathrm{Pr}_t \cdot \varepsilon_M/\nu\right)_i} \tag{A2.6}$$

(iii) Outer region

In the same way as the inner region:

$$\frac{\partial T_o^+}{\partial \zeta_o} = -\mathrm{Pr}\cdot\delta_o^+ \frac{\left(q_o/q_{w_i}\right)}{\left(1 + \mathrm{Pr}/\mathrm{Pr}_t \cdot \varepsilon_M/\nu\right)_o} \tag{A2.7}$$

therefore, we can obtain:

$$\frac{\partial T_j^+}{\partial \zeta_j} = \pm\mathrm{Pr}\cdot\delta_j^+ \frac{\left(q_j/q_{w_i}\right)}{\left(1 + \mathrm{Pr}/\mathrm{Pr}_t \cdot \varepsilon_M/\nu\right)_j} \tag{2.61}$$

APPENDIX 3
Non-Dimensionalized Forms of the Turbulence Model for Concentric Annular Geometry

To solve the closure problems that arise in turbulence fluctuation terms, the eddy viscosity term, ε_M/ν, requires mathematical modelling because it cannot be determined analytically. The term will exhibit different behaviours, depending on the state of the boundary layers. Usually, the boundary layer can be regarded as consisting of two layers. The first one, the viscous sublayer, is confined to a region of flow near a solid boundary. Beyond of the viscous sublayer lays the fully turbulent regions. Therefore, both regions require the turbulence models, respectively.

A.3.1 Viscous Sublayer

From Eqs. (2.36) and (2.39):

$$\left(\frac{\varepsilon_M}{\nu}\right)_j = \kappa_j y_j^+ \left[1-\exp\left(-\frac{y_j^+}{A_j^+}\right)\right]^2 \left|\frac{\partial u_j^+}{\partial y_j^+}\right| \tag{2.36}$$

$$\frac{\partial u_j^+}{\partial \zeta_j^+} = \delta_j^+ \left[\frac{(\tau/\tau_R)_j}{1+(\varepsilon_M/\nu)_j}\right] \tag{2.39}$$

Substitution of Eq. (2.39) into Eq. (2.36) gives:

$$\left(\frac{\varepsilon_M}{\nu}\right)^2_j + \left(\frac{\varepsilon_M}{\nu}\right)_j = \left(\kappa_j y_j^+\right)^2 \left[1-\exp\left(-\frac{y_j^+}{A_j^+}\right)\right]^2 \left(\frac{\tau}{\tau_w}\right)_j \tag{A3.1}$$

Eq. (A3.1) is a form of an incomplete square polynomial of ε_M/ν ($= X$):

$$X^2 + X - A = 0$$

and its solutions:

$$X = \frac{-1 \pm \sqrt{1 + 4 \cdot A}}{2}$$

The positive root of the polynomial is:

$$\left(\frac{\varepsilon_M}{\nu}\right)_j = \frac{1}{2}\left[-1 + \left\{1 + 4\cdot\left(\kappa_j \delta_j^+ \zeta_j\right)^2\left[1 - \exp\left(1 - \frac{\delta_j^+ \zeta_j}{A_j}\right)\right]\left(\frac{\tau}{\tau_w}\right)_j\right\}^{0.5}\right] \tag{2.37}$$

With the variable von Kármán constant, κ_i, proposed in Kim's research [1996], the expression of $(\varepsilon_M/\nu)_j$ becomes:

(i) For the viscous sublayer of an inner region:

$$\left(\frac{\varepsilon_M}{\nu}\right)_i = \frac{1}{2}\left[-1 + \left\{1 + 0.64\cdot\left[F(r_i^*)\delta_i^+ \zeta_i\right]^2\left[1 - \exp\left(1 - \frac{\delta_i^+ \zeta_i}{A_i}\right)\right]\left(\frac{\tau}{\tau_w}\right)_i\right\}^{0.5}\right] \tag{A3.2}$$

(ii) For the viscous sublayer of an outer region:

$$\left(\frac{\varepsilon_M}{\nu}\right)_o = \frac{1}{2}\left[-1 + \left\{1 + 0.64\cdot\left(\delta_o^+ \zeta_o\right)^2\left[1 - \exp\left(1 - \frac{\delta_o^+ \zeta_o}{A_o}\right)\right]\left(\frac{\tau}{\tau_w}\right)_o\right\}^{0.5}\right] \tag{A3.3}$$

A.3.2 Fully Turbulent Regions

Since the velocity profiles outside the viscous sublayers should differ from the law of the wall, the logarithmic law of the wall cannot be used. In fully turbulent regions, the empirical model originally proposed by Reichardt [1943] is used in a modified form, Eq. (2.32), as:

$$\left(\frac{\varepsilon_M}{\nu}\right)_j = \frac{1}{6}\kappa_j \delta_j^+ \left[1-\left(1-\frac{y_j^+}{\delta_j^+}\right)^2\right]\left[1+2\cdot\left(1-\frac{y_j^+}{\delta_j^+}\right)^2\right] \tag{2.32}$$

and non-dimensionalized as follows:

$$\left(\frac{\varepsilon_M}{\nu}\right)_j = \frac{1}{6}\kappa_j \delta_j^+ \left[\zeta_j\left(2-\zeta_j\right)\left(3-4\cdot\zeta_j+2\cdot\zeta_j^2\right)\right] \tag{2.33}$$

(i) For the fully turbulent layer of an inner region:

$$\left(\frac{\varepsilon_M}{\nu}\right)_i = \frac{1}{15} f\left(r_i^*\right) \delta_i^+ \left[\zeta_i\left(2-\zeta_i\right)\left(3-4\cdot\zeta_i+2\cdot\zeta_i^2\right)\right] \tag{A3.4}$$

where the variable von Kármán constant, κ_i, proposed in this study was applied.

(ii) For the fully turbulent layer of an outer region:

$$\left(\frac{\varepsilon_M}{\nu}\right)_o = \frac{1}{6}\kappa_o \delta_o^+ \left[\zeta_o\left(2-\zeta_o\right)\left(3-4\cdot\zeta_o+2\cdot\zeta_o^2\right)\right] \tag{A3.5}$$

where κ_o is a constant, 0.4, in this study.

APPENDIX 4
Non-Dimensionalized Forms of Other Fluid Parameters for Concentric Annular Geometry

A.4.1 Bulk Velocity

The bulk velocity of the fluid across the concentric annulus cross-section is defined as:

$$u_b = \frac{\int_{dA} u\,dA}{\int_{dA} dA} = \frac{\int_{r_i}^{R_i} u_i r\,dr + \int_{R_i}^{r_m} u_i r\,dr + \int_{r_m}^{R_o} u_o r\,dr + \int_{R_o}^{r_o} u_o r\,dr}{\frac{1}{2}\cdot\left(r_o^2 - r_i^2\right)} \tag{A4.1}$$

and simplify the equation above to have:

$$u_b = \frac{2}{r_o^2\cdot\left(1-\alpha^2\right)}\left[\int_{r_i}^{R_i} u_i r\,dr + u_{\delta i}\frac{1}{2}\left(r_m^2 - R_i^2\right) + u_{\delta o}\frac{1}{2}\left(R_o^2 - r_m^2\right) + \int_{R_o}^{r_o} u_o r\,dr\right]$$

non-dimensionalize the equation:

$$u_b = \frac{2\,u_{\tau_o}}{r_o^+\cdot\left(1-\alpha^2\right)}\left[\delta_i^+\int_0^1 u_i^+(1+\Delta_i\zeta_i)\,d\zeta_i + \delta_o^+\int_0^1 u_o^+(1-\Delta_o\zeta_o)\,d\zeta_o\right] + \frac{u_{\tau_o}u_{\delta o}^+}{r_o^{+2}\cdot\left(1-\alpha^2\right)}\left(R_o^{+2} - R_i^{+2}\cdot\frac{\tau_{w_o}}{\tau_{w_i}}\right) \tag{A4.2}$$

Eq. (A4.2) can be rearranged in dimensionless parameters as:

$$u_{bo}^{+} = \frac{u_b}{u_{\tau_o}} = \frac{2}{r_o^{+}\cdot\left(1-\alpha^2\right)}\left[\delta_i^{+}\int_0^1 u_i^{+}(1+\Delta_i\zeta_i)\,d\zeta_i + \delta_o^{+}\int_0^1 u_o^{+}(1-\Delta_o\zeta_o)\,d\zeta_o\right] + \frac{u_{\delta o}^{+}}{r_o^{+2}\cdot\left(1-\alpha^2\right)}\left(R_o^{+2} - R_i^{+2}\cdot\frac{\tau_{w_o}}{\tau_{w_i}}\right) \tag{A4.3}$$

A.4.2 Friction Factor

If the flow is fully developed in a concentric annulus, the integration of Eq.(2.18) gives:

$$\tau_{w_i} = \frac{r_m^2 - r_i^2}{2r_i}\left(-\frac{dp}{dx}\right) \tag{A4.4}$$

and

$$\tau_{w_o} = \frac{r_o^2 - r_m^2}{2r_o}\left(-\frac{dp}{dx}\right) \tag{A4.5}$$

Therefore, the wall shear stress is a function of the pressure gradient and the radius of maximum velocity only. However, for the developing boundary layer in an annulus, the local wall shear stress is dependent not only on the local pressure gradient, but also on the changes in momentum flux.

The momentum integral equation for the developing region is:

$$-d\left(\int_{r_i}^{r_{\delta_i}} 2\pi r\rho u^2 dr + \int_{r_{\delta_o}}^{r_o} 2\pi r\rho u^2 dr\right) + u_{\delta_i}\, d\left(\int_{r_i}^{r_{\delta_i}} 2\pi r\rho u\, dr + \int_{r_{\delta_o}}^{r_o} 2\pi r\rho u dr\right) = 2\bar{\tau}\pi\left(r_o + r_i\right)dx + \frac{1}{2}dp\left(r_o^2 - r_i^2\right)\pi \tag{A4.6}$$

Rearrange Eq. (A4.6) to obtain:

$$\bar{\tau} = \frac{u_{\delta_i}}{(r_o + r_i)} \cdot \frac{d\left(\int_{r_i}^{\delta_i} \rho\, u\, r\, dr + \int_{\delta_o}^{r_o} \rho\, u\, r\, dr \right)}{dx} - \frac{1}{(r_o + r_i)} \cdot \frac{d\left(\int_{r_i}^{\delta_i} \rho\, u^2\, r\, dr + \int_{\delta_o}^{r_o} \rho\, u^2\, r\, dr \right)}{dx} - \frac{(r_o - r_i)}{2} \cdot \frac{dp}{dx} \tag{A4.7}$$

Dimensionless mass and momentum flux parameters are defined for the present geometry, respectively, as:

$$M_1 = \int_{\alpha}^{1} \frac{\rho}{\rho_e} \left(\frac{u}{u_b} \right) \frac{r}{r_o} d\left(\frac{r}{r_o} \right) \tag{A4.8}$$

and

$$M_2 = \int_{\alpha}^{1} \frac{\rho}{\rho_e} \left(\frac{u}{u_b} \right)^2 \frac{r}{r_o} d\left(\frac{r}{r_o} \right) \tag{A4.9}$$

With Eqs. (A4.7), (A4.8) and (A4.9), the friction factor, f, defined by Eq. (2.41) from section 2.5.3, then becomes:

$$f = \frac{2\rho_e r_o^2}{\rho(r_o + r_i)} \left(\frac{u_{\delta_i}}{u_b} \cdot \frac{dM_1}{dx} - \frac{dM_2}{dx} \right) - \frac{(r_o - r_i)}{\rho u_b^2} \cdot \frac{dp}{dx} \tag{A4.10}$$

If the momentum flux is negligible, Eqs. (A4.7) and (A4.10) are simplified as:

$$\bar{\tau} = -\frac{1}{2}(r_o - r_i) \cdot \frac{dp}{dx} \tag{A4.11}$$

and

$$f = -\frac{(r_o - r_i)}{\rho u_b^2} \cdot \frac{dp}{dx} \tag{A4.12}$$

Eqs. (A4.11) and (A4.12) are identical to those for the fully developed region.

In the Park's research [1971], the mass terms for M_1, M_2, and static pressure are plotted against the axial distance from the entrance, (x /De). The momentum flux values are approximately constant except very near the entrance, therefore, the static pressure term alone is sufficient to determine the wall shear stress or the friction factor except for the region very near the entrance.

For a Reynolds number of 44,000 and a radius ratio ($1/\alpha$) of 3.83, Eq. (A4.10) shows that the error introduced by neglecting the variation of momentum flux in the developing region of the flow was 0.018 % at (x/De) = 5.

From Eqs. (2.43) and (2.44):

$$\frac{dp}{dx}\cdot\left[\left(r_o^2 - R_o^2\right) + \left(R_i^2 - r_i^2\right)\right] = 2\,\bar{\tau}\left(r_i + r_o\right) \tag{2.43}$$

$$\frac{dp}{dx}\cdot\left(r_o^2 - R_o^2\right) = 2\,\tau_{w_o}\,r_o \tag{2.44}$$

divide Eq. (2.43) by Eq. (2.44) and simplify to obtain:

$$\frac{r_o\left(2r_o\delta_o - \delta_o^2 + 2r_i\delta_i + \delta_i^2\right)}{\left(2r_o\delta_o - \delta_o^2\right)\left(r_i + r_o\right)} = \frac{\bar{\tau}}{\tau_{w_o}} \tag{A4.13}$$

From Eqs. (A4.11) and (A4.12):

$$\frac{\bar{\tau}}{\tau_{w_o}} = \frac{-\frac{1}{2}\cdot\left(r_o - r_i\right)\cdot\frac{dp}{dx}}{\tau_{w_o}} = \frac{1}{2}\frac{u_b^2}{\left(\sqrt{\frac{\tau_{w_o}}{\rho}}\right)^2}\left[-\frac{\left(r_o - r_i\right)}{\rho u_b^2}\cdot\frac{dp}{dx}\right] = \frac{1}{f_{ax}}\cdot f_x \tag{A4.14}$$

substitute Eq. (A4.14) into Eq. (A4.13) to obtain:

$$f_x = \frac{r_o\left(2r_o\delta_o - \delta_o^2 + 2r_i\,\delta_i + \delta_i^2\right)}{\left(2r_o\delta_o - \delta_o^2\right)\left(r_i + r_o\right)} \cdot f_{ox} \tag{2.45}$$

The dimensionless form is:

$$f_x = \frac{r_o^+\left(2r_o^+\delta_o^+ - \delta_o^{+2} + 2r_i^{++}\,\delta_i^{++} + \delta_i^{++2}\right)}{\left(2r_o^+\delta_o^+ - \delta_o^{+2}\right)\left(r_i^{++} + r_o^+\right)} \cdot f_{ox} \tag{2.46}$$

A.4.3 Bulk Temperature

The bulk temperature of the fluid across the concentric annulus cross-section is defined as:

$$T_b = \frac{\int_{r_i}^{r_o} r\,u(r)\,T\,dr}{\int_{r_i}^{r_o} r\,u(r)\,dr} \tag{A4.15}$$

The dimensionless temperatures, T_j^+ and T_{bj}^+, are defined as:

$$T_j^+ = \frac{(T_{w_i} - T_j)\,c\,\tau_{w_j}}{q_{w_i}u_{\tau_j}} \tag{A4.16}$$

$$T_{bj}^+ = \frac{(T_{w_i} - T_b)\,c\,\tau_{w_j}}{q_{w_i}u_{\tau_j}} \tag{A4.17}$$

rearrange Eq. (A4.16) and integrate it as Eq. (A4.15) to obtain:

$$\frac{\int_{r_i}^{r_o} r\,u_j\,\frac{q_{w_i}u_{\tau_j}}{c\tau_{w_j}}T_j^+\,dr}{\int_{r_i}^{r_o} r\,u_j\,dr} = \frac{\int_{r_i}^{r_o} r\,u_j T_{w_i}\,dr}{\int_{r_i}^{r_o} r\,u_j\,dr} - \frac{\int_{r_i}^{r_o} r\,u_j T_j\,dr}{\int_{r_i}^{r_o} r\,u_j\,dr} = T_{w_i} - T_b \tag{A4.18}$$

multiply $\left(c\tau_{w_j}/q_{w_i}u_{\tau_j}\right)$ to both hand sides:

$$\frac{c\,\tau_{w_j}}{q_{w_i}u_{\tau_j}}\cdot\frac{\int_{r_i}^{r_o} r\,u_j\,\frac{q_{w_i}u_{\tau_j}}{c\tau_{w_j}}T_j^+\,dr}{\int_{r_i}^{r_o} r\,u_j\,dr} = \frac{c\,\tau_{w_j}}{q_{w_i}u_{\tau_j}}\cdot\left(T_{w_i}-T_b\right) = T_{bj}^+ \qquad \text{(A4.19)}$$

non-dimensionalize Eq. (A4.19):

$$T_{bj}^+ = \frac{\int_{r_i}^{r_o} r\,u_j T_j^+\,dr}{\int_{r_i}^{r_o} r\,u_j\,dr} = \frac{\int_{r_i^+}^{r_o^+} r^+u_j^+\,T_j^+\,dr^+}{\int_{r_i^+}^{r_o^+} r^+u_j^+\,dr^+} \qquad \text{(A4.20)}$$

Finally we obtain Eq. (2.66):

$$\left(T_b^+\right)_{x,j} = \left(\frac{\int_{r_i^+}^{r_o^+} r^+u^+\,T^+\,dr^+}{\int_{r_i^+}^{r_o^+} r^+u^+\,dr^+}\right)_{x,j} \qquad \text{(2.66)}$$

In the case of $\delta_i^+ = \delta_{ti}^+$ Eq. (2.66) can be rearranged to obtain the following:

$$\left(T_b^+\right)_{x,j} = \left(\frac{\int_{r_i^+}^{r_o^+} r^+u^+\,T^+\,dr^+}{\int_{r_i^+}^{r_o^+} r^+u^+\,dr^+}\right)_{x,j} = \frac{\left(\int_{r_i^+}^{r_o^+} r^+u^+\,T^+\,dr^+\right)_{x,j}}{\left(\int_{r_i^+}^{r_o^+} r^+u^+\,dr^+\right)_{x,j}} = \frac{A}{B} \qquad \text{(A4.21.a)}$$

$$A = \int_{r_i^+}^{R_i^+} T_i^+u_i^+r^+\,dr^+ + \frac{1}{2}T_{\delta_u}^+\,u_{\delta_i}^+\left(R_o^{++2}-R_i^{+2}\right) + T_{\delta_u}^+\int_{R_o^{++}}^{r_o^{++}} u_o^{++}r^{++}\,dr^{++}$$

$$= r_i^+\delta_i^+ \int_0^1 \left(1+\Delta_i\zeta_i\right) u_i^+ T_i^+ d\zeta_i \; + \; \frac{1}{2} T_{\delta_u}^+ u_{\delta_i}^+ \left(R_o^{++2} - R_i^{+2}\right)$$
$$+ \; r_o^{++}\delta_o^{++} T_{\delta_u}^+ \int_0^1 \left(1-\Delta_o\zeta_o\right) u_o^{++} d\zeta_o \qquad \text{(A4.21.b)}$$

$$\mathrm{B} = \left(\int_{r_i}^{r_o} r^+ u^+ dr^+ \right)_{x,i} = \; u_{bi}^+ \cdot \frac{1}{2} r_i^{+2} \left(\alpha^{-2} - 1 \right) \qquad \text{(A4.21.c)}$$

substitute Eqs. (A4.21.c) and (A4.21.b) into (A4.21.a) to obtain:

$$\left(T_b^+\right)_{x,i} = \frac{2}{r_i^{+2}(\alpha^{-2}-1)\,u_{bi}^+} \left[r_i^+\delta_i^+ \int_0^1 \left(1+\Delta_i\zeta_i\right) u_i^+ T_i^+ d\zeta_i \; + \; \frac{1}{2} T_{\delta_u}^+ u_{\delta_i}^+ \left(R_o^{++2} - R_i^{+2}\right) \right.$$
$$\left. + \; r_o^{++}\delta_o^{++} T_{\delta_u}^+ \int_0^1 \left(1-\Delta_o\zeta_o\right) u_o^{++} d\zeta_o \right] \qquad \textit{for} \quad \delta_i^+ = \delta_t^+ \qquad \text{(A4.22)}$$

In the same way for the cases of $\delta_i^+ < \delta_{ti}^+$ and $\delta_i^+ > \delta_{ti}^+$:

$$\left(T_b^+\right)_{x,i} = \frac{2}{r_i^{+2}(\alpha^{-2}-1)\,u_{bi}^+} \left\{ r_i^+\delta_i^+ \int_0^1 \left(1+\Delta_i\zeta_i\right) u_i^+ T_i^+ d\zeta_i \right.$$
$$+ \; u_{ti}^+ \left[r_i^+\delta_{ti}^+ \int_0^1 \left(1+\Delta_{ti}\zeta_{ti}\right) T_i^+ d\zeta_{ti} \; - \; r_i^+\delta_i^+ \int_0^1 \left(1+\Delta_i\zeta_i\right) T_i^+ d\zeta_i \right] \qquad \text{(A4.23)}$$
$$\left. + \; \frac{1}{2} T_{\delta_u}^+ u_{\delta_i}^+ \left(R_o^{++2} - r_{\delta_u}^{+2}\right) \; + \; r_o^{++}\delta_o^{++} T_{\delta_u}^+ \int_0^1 \left(1-\Delta_o\zeta_o\right) u_o^{++} d\zeta_o \right\}$$
$$\textit{for} \quad \delta_i^+ < \delta_t^+$$

$$\left(T_b^+\right)_{x,i} = \frac{2}{r_i^{+2}(\alpha^{-2}-1)\,u_{bi}^+} \left\{ r_i^+\delta_{ti}^+ \int_0^1 \left(1+\Delta_{ti}\zeta_{ti}\right) u_i^+ T_i^+ d\zeta_i \right.$$
$$+ \; T_{\delta_u}^+ \left[r_i^+\delta_i^+ \int_0^1 \left(1+\Delta_i\zeta_i\right) u_i^+ d\zeta_i \; - \; r_i^+\delta_{ti}^+ \int_0^1 \left(1+\Delta_{ti}\zeta_{ti}\right) u_i^+ d\zeta_{ti} \right] \qquad \text{(A4.24)}$$
$$\left. + \; \frac{1}{2} T_{\delta_u}^+ u_{\delta_i}^+ \left(R_o^{++2} - R_i^{+2}\right) \; + \; r_o^{++}\delta_o^{++} T_{\delta_u}^+ \int_0^1 \left(1-\Delta_o\zeta_o\right) u_o^{++} d\zeta_o \right\}$$
$$\textit{for} \quad \delta_i^+ > \delta_t^+$$

A.4.4 Nusselt number

The Nusselt number is defined as:

$$Nu = \frac{h \cdot 2(r_o - r_i)}{k} \tag{A4.25}$$

where h is defined as:

$$h = \frac{q_{w_i}}{(T_{w_i} - T_b)} \tag{A4.26}$$

from the definition of T_b^+, $(T_{w,i}-T_b)$ can be be obtained:

$$T_b^+ = \frac{(T_{w_i} - T_b)\, c\, \tau_{w_i}}{q_{w_i} u_{\tau_i}} \tag{A4.27}$$

substitution of Eqs. (A4.25) and (A4.26) in to Eq. (A4.24) yields:

$$\mathrm{Nu} = \frac{c\,\tau_{w_i}}{u_{\tau_i}} \frac{1}{T_b^+} \frac{2 \cdot (r_o - r_i)}{k} \tag{A4.28}$$

Eq. (A4.28) can be further reduced with $u_{\tau_i} = \sqrt{\frac{\tau_{w_i}}{\rho}}$ as:

$$\mathrm{Nu} = 2\left(\frac{1-\alpha}{\alpha}\right) \frac{1}{T_b^+} r_i^+ \nu \frac{\rho c}{k} \tag{A4.29}$$

Transform Eq. (A4.29) with Prandtl number, $\mathrm{Pr} = \frac{\nu}{k/\rho c}$, where (k / ρc)is thermal diffusivity to obtain Eq. (2.64):

$$\mathrm{Nu} = 2\left(\frac{1-\alpha}{\alpha}\right) \frac{r_i^+ \mathrm{Pr}}{T_b^+} \tag{A4.30}$$

APPENDIX 5
The Integration of Momentum Equation

The momentum integral equation in dimensionless form is derived as:

$$\left(\frac{x}{De}\right)_{M,J} = \int_{u_e^+}^{u_{\delta_j}^+} \frac{\delta_j^+(R_j^+ + r_j^+)}{2r_j^+(De^+)_j} u_{\delta_j}^+ \, du_{\delta_j}^+ - \int_0^{A^+} \frac{dA^+}{r_j^+(De^+)_j} + \int_0^{B^+} \frac{dB^+}{r_j^+(De^+)_j} \qquad (2.56)$$

where

$$A^+ = \int_0^{\delta_j^+} u_j^{+2} r^+ dy_j^+$$

$$B^+ = \int_0^{\delta_j^+} u_j^+ \, r^+ dy_j^+$$

$$\left(De^+\right)_j = 2\, r_i^+\left(\alpha^{-1} - 1\right) \text{ or } \quad = 2\, r_o^+(1-\alpha)$$

and $$\mathrm{Re} = \left(u_e^+\right)_j \cdot \left(De^+\right)_j \qquad (2.57)$$

Combine Eq. (2.57) and Eq. (2.56), to obtain:

$$\left(\frac{x}{De}\right)_{M,J} = \int_{\mathrm{Re}/2}^{E^+} \frac{\delta_j^+(R_j^+ + r_j^+)}{r_j^+(De^+)_j^2} u_{\delta_j}^+ \, dE^+ - \int_0^{A^+} \frac{dA^+}{r_j^+(De^+)_j} + \int_0^{B^+} \frac{dB^+}{r_j^+(De^+)_j} \qquad (A5.1)$$

where

$$E^+ = \frac{1}{2}\, u_{\delta_j}^+ \left(De^+\right)_j$$

From the differential of a product, we can write:

$$\left[\frac{1}{2}u_{\delta_j}^{+}\left(De^{+}\right)_j\right] d\left[\int_0^{\delta_j^{+}} u_j^{+}r_j^{+}dy_j^{+}\right] \equiv d\left\{\left[\frac{1}{2}u_{\delta_j}^{+}\left(De^{+}\right)_j\right]\cdot\int_0^{\delta_j^{+}} u_j^{+}r_j^{+}dy_j^{+}\right\} - d\left[\frac{1}{2}u_{\delta_j}^{+}\left(De^{+}\right)_j\right]\cdot\int_0^{\delta_j^{+}} u_j^{+}r_j^{+}dy_j^{+} \tag{A5.2}$$

Divide Eq. (A5.2) by $\left[r_j^{+}(De^{+})_j^2\right]$ and integrate both parts to obtain:

$$\int_0^{B^{+}} \frac{\left[u_{\delta_j}^{+}(De^{+})_j\right]dB^{+}}{r_j^{+}(De^{+})_j^2} = \int_0^{F^{+}} \frac{dF^{+}}{r_j^{+}(De^{+})_j^2} - 2\int_{Re/2}^{E^{+}} \frac{\left(\int_0^{\delta_j^{+}} u_j^{+}r^{+}dy_j^{+}\right)dE^{+}}{r_j^{+}(De^{+})_j^2} \tag{A5.3}$$

where

$$F^{+} = \left[u_{\delta_j}^{+}(De^{+})_j\right]\int_0^{\delta_j^{+}} u_j^{+}r^{+}dy_j^{+}$$

Rearrange Eq. (A5.3) to obtain:

$$\int_0^{B^{+}} \frac{u_{\delta_j}^{+}\,dB^{+}}{r_j^{+}(De^{+})_j} = \int_0^{G^{+}} \frac{dG^{+}}{r_j^{+}(De^{+})_j} - 2\int_{Re/2}^{E^{+}} \frac{\left(\int_0^{\delta_j^{+}} u_j^{+}r^{+}dy_j^{+}\right)dE^{+}}{r_j^{+}(De^{+})_j^2} \tag{A5.4}$$

where

$$G^{+} = u_{\delta_j}^{+}\int_0^{\delta_j^{+}} u_j^{+}r^{+}dy_j^{+}$$

Replace the last term of Eq. (A5.1) with Eq. (A5.4) to obtain:

$$\left(\frac{x}{De}\right)_{M,j} = \int_{Re/2}^{E^+} \left[\frac{\delta_j^+ (R_j^+ + r_j^+)}{r_j^+ (De^+)_j^2} u_{\delta_j}^+ \, dE^+ - \frac{2}{r_j^+ (De^+)_j^2} \int_0^{\delta_j^+} u_j^+ r^+ dy_j^+ \right] dE^+ + \int_0^{D^+} \frac{dD^+}{r_j^+ (De^+)_j} \tag{A5.5}$$

where

$$D^+ = \int_0^{\delta_j^+} \left(u_{\delta_j}^+ - u_j^+ \right) u_j^+ \, r^+ dy_j^+$$

Eq. (A5.5) is Eq. (2.58) in section 2.5.4.

REFERENCES

Abberch, P.H. and Churchill, S.W., "The Thermal Entrance Region in Fully Developed Turbulent Flow," *A. I. Ch. E. Jour.*, vol. 6, pp. 150-255, 1964.

Barrow, H., "Heat Transfer in the Entry Region of a Pipe," *The Engineer*, vol. 220, pp. 139-143, 1968.

Barrow, H., Lee, Y., and Roberts, A., "The Similarity Hypothesis Applied to Turbulent Flow in an Annulus," Int. Jour. Heat Mass Transfer, vol. 8, p. 1499, 1965.

Brighton, J.A. and Jones, J.B., "Fully Developed Turbulent Flow in Annuli," J. of Basic Eng., Trans. ASME, Sec. D., vol. 86, pp. 835-844, 1964.

Chapra, S.C. and Canale, R.P., *Numerical Methods for Engineers*, 2th ed., McGraw-Hill, New York, 1990.

Chen, J.C. and Yu,W.S. "Entrance Region and Variable Heat Flux Effects in Turbulent Heat Transfer to Liquid Metals Flowing In Concentric Annuli," *Int. J. Heat Mass Transfer*, vol.13, pp. 667-680, 1970.

Coles, D., "The Law of the Wake in the Turbulent Boundary Layer," *J. of Fluid Mechanics*, vol. 1, pp. 191-226, 1956.

Deissler, R.G., "Turbulent Heat Transfer and Friction in The Entrance Regions of Smooth Passages," *Trans. ASME*, vol. 88, pp. 1221-1223, 1955.

Dwyer, O.E., "Recent Development Liquid-Metal Heat Transfer," *Atomic Energy Review*, vol. 4, pp. 3-92, 1966.

Farman, R.F. and Beckmann, R.B., "Entrance Region Heat Transfer in an Annulus," *American Inst. Chemical Eng. Heat Transfer with Phase Change. Chem. Eng. Progress Symposium Ser.*, vol. 63, 1967.

Hanratty, "Developing of Temperature Profile for Turbulent Heat Exchange in a Pipe," Tech. Report No. 10, University of Illinois, 1961.

Heaton, H.S., Reynolds, W.C., and Kays, W.M., "Heat Transfer in Annular Passages ; Simultaneous Development of Velocity and Temperature Fields in Laminar Flow," *Int. J. Heat Mass Trans.*, vol. 7, pp. 763-781, 1964.

Hinze, J., *Turbulence*, 2th ed., McGraw-Hill, New York, 1975.

Holman, J.P., *Heat Transfer*, 8th ed., McGraw-Hill, New York, 1997.

Jerkins, R., "Variation of the Eddy Conductivity with Prandtl Modules and it's Use in Prediction of Turbulent Heat Transfer Coefficients," Heat Transfer and Fluid Mechanics Inst., 147, Stanford Univ. Press, Stanford, California, 1951.

Johnson, D.S., "Velocity and Temperature Fluctuation Measurements in a Turbulent Boundary Layer Downstream for Stepwise Discontinuity in Wall Temperature," Trans. ASME. 61, pp. 705-710, 1939.

Kays, W.M., "Numerical Solutions for Laminar-Flow Heat Transfer in Circular Tubes," *Trans. ASME*, vol. 77, pp. 1265-1274, 1955.

Kays, W.M. and Crawford, M.E., *Convective Heat and Mass Transfer*, 3rd ed, McGraw-Hill, New York, 1993.

Kays, W.M. and Leung, E.Y., "Heat Transfer in Annular Passage Hydrodynamically Developed Turbulent Flow with Arbitrarily Prescribed Heat Flux," *Int Jour. of Heat & Mass Transfer*, vol. 6, pp. 537-557, 1963.

Kim, M.W., "Effect of Transverse Convex Curvature on Turbulent Flow and Heat Transfer," *Ph.D. Thesis*, University of Ottawa, 1996.

Kim, M.W. Kim, K.C. Lee, Y., "Effect of Transverse Convex Surface Curvature on Fluid Flow and Heat Transfer for Turbulent Boundary Layer Flow Longitudinal to a Circular Cylinder : Analysis and Experiment," *Conference of Heat Transfer in Turbulent Flows ASME.*, HTD., San Francisco, vol. 318, pp. 137-144, 1995.

Kim, K.C., Lee, Y. and Ma, E, "Effect of Transverse Convex Curvature on Turbulent Flow and Heat Transfer," *First International Symposium on Experimental and Computational Aerothermodynamics of Internal Flows*, Beijing, pp. 202-207, 1990.

Kjellström, B. and Hedberg, S., "On Shear Stress Distributions for Flow in Smooth or Partially Rough Annuli," AE-243, Aktiebolaget, Atomenergi, Stockholm, Sweden, 1966.

Knudsen, J.G. and Katz, D.L., *Fluid Dynamics and Heat Transfer*, McGraw-Hill, 1958.

Lana, I.G.D. and Christiansen, S.E., "Air Flow in a Tube with a Diverging Inlet: Development of The Turbulent Velocity Profile", *The Canadian J. of Chem. Eng.*, vol. 45, 1967.

Langhaar, H.L., "Steady Flow in the Transition Length of a Straight Tube," *J. appl. Mech.*, vol. 9, pp. A55-58, 1942.

Lee, Y. "Turbulent Heat Transfer from the Core Tube in Thermal Entrance Regions of Concentric Annuli," *Int. J. of Heat and Mass Transfer*, vol. 11, pp. 509-522, 1968.

Lee, Y., "Turbulent Flow and Heat Transfer in Concentric and Eccentric Annuli," *Ph.D. Thesis*, University of Liverpool, 1964.

Lee, Y. and Barrow, H., "Turbulent Flow and Heat Transfer in Concentric and Eccentric Annuli," *Proceedings, I. Mech. E.*, vol. 178, pp. 1-16, 1964.

Lee, Y. and Kim, K.C., "An Analysis on Effect of Transverse Convex Curvature on Turbulent Flow and Heat Transfer," *Wärme-und Stoffübertragung*, vol. 28, pp. 89-95, 1993.

Leung, E.Y., Kays, W.M. and Reynolds, W.C., "Heat Transfer with Turbulent Flow in Concentric and Eccentric Annuli with Constant and Variable Heat Flux," Report AHT4, Stanford University, 1962.

Levy, S., "Turbulent Flow in an Annulus," *J. Heat Transfer*, ASME, vol. 89, pp. 25-31, Feb., 1967.

Ludwieg, H., "Bestinmmung des Verhältnisses der Austauschkoeffizienten für Wärme und Impuls bei turbulenten Grenzschichten," ZFW 4, pp. 73-81, 1956.

Mizushina, T., Ito, R. and Ogino, F., "Eddy Diffusivity Distribution Near the Wall," *4th Int. Heat Transfer Conference*, vol. 2, FC 218, 1970.

Okiishi, T.H. and Serovy, G.K., "An Experimental Study of the Turbulent Flow Boundary-Layer Development in Smooth Annuli," *J. of Basic. Eng. Trans. ASME,* vol. 89, pp. 823-836, 1967.

Olson, R.M. and Sparrow, E.M., "Measurements of Turbulent Flow Development in Tubes and Annuli with Square or Round Entrances," *A. I. CH. E. Jour.*, vol. 9, pp. 766-770, Nov, 1963.

Page, F., Schlinger, W.G., Breaux, D.K. and Sage, B.H., "Point Values of Eddy Conductivity and Viscosity in Uniform Flow Between Parallel Plates," *Ind. Eng. Chem.*, vol. 44, pp. 424-430, 1952.

Park, S.D. and Lee, Y., "Diabatic Turbulent Flow in the Entrance Region of Concentric Annuli", *84th Annual Meeting*, The Eng. Inst. Canada, Paper No. 70-CSME-9, 1970.

Park, S.D., "Developing Turbulent Flow and Heat Transfer in Concentric Annuli; An Analytical and Experimental Study," *Ph.D. Thesis*, University of Ottawa, 1971.

Prandtl, L., "Über Flüssig keitsvewegung bei sehr kleiner Reibung," *Proc. 3rd. Int. Math. Cong. Heidelberg*, 1904, Reprinted in NACA TM 452, 1928.

Quarmby, A., "Some Measurement of Turbulent Heat Transfer in the Thermal Entrance region of Concentric Annuli," *Int. J. Heat Mass Transfer*, vol. 10, pp. 267-276, 1967.

Quarmby A. and Anand, R.K., "Turbulent Heat Transfer in the Thermal Entrance Region of Concentric Annuli with Uniform Wall Heat Flux," *Int. J. Heat Mass Transfer*, vol.13, pp. 395-411, 1970.

Quarmby A. and Anand, R.K., "Turbulent Heat Transfer in the Thermal Entrance Region of Concentric Annuli with Constant Wall Temperatures," *J. of Heat Transfer, Trans. ASME*, pp. 33-45, Feb., 1970.

Rao, G.N.V., "The Law of The Wall in a Thick Axisymmetric Turbulent Boundary Layer," *J. Appl. Mech.*, vol. 34, pp. 237-238, 1967.

Rao, G.N.V. and Keshavan, N.R., "Axisymmetric Turbulent Boundary Layers in Zero Pressure Gradient Flows," *J. Appl. Mech.*, vol. 39, pp. 25-32, 1972.

Reichardt, H., "Die Wärmeübertragung in Turbulent Reibungschichten," *Z. Angew. Math. Mech.*, vol. 20, p. 297, 1940, Available in English translation as NACA TM1047, 1943.

Roberts, A., "A Comment on the Turbulent Flow Velocity Profile in a Concentric Annulus," *Int. J. Heat and Mass Transfer*, vol. 10, pp. 709-712, 1967.

Roberts, A. and Barrow, H., "Turbulent Heat Transfer to Air in the Vicinity of the Entry of an Internally Heated Annulus," *Proceedings, Thermodynamics and Fluid Mechanics Conv., Bristol*, 1968.

Rothfus, R.R., Monrad, C.C., Sikchi, K.G., and Keideger, W.J., "Isothermal Skin Friction in Flow through Annular Sections," *Indus. and Eng. Chem.*, vol. 47, p. 913, 1955.

Schlichting, H., *Boundary Layer Theory*, 7th ed., McGraw-Hill, New York, 1979.

Sleicher, C. and Tribus, M., "Heat Transfer to a Pipe with Turbulent Flow and Arbitrary Wall Temperature Distribution," *Trans. ASME*, vol 79, p.789, 1957.

Sparrow, E.M., "Analysis of Laminar Forced-Convection Heat Transfer in Entrance Region of Flat Rectangular Ducts," NACA TN 3331, 1955.

Sridhar, K., Nicol, A.A. and Padmanabha, A.V.A., "Settling Length for Turbulent Flow of Air in Smooth Annuli with Square-Edged or Bellmouth Entrances," *J. of Applied Mech., Trans. ASME*, vol. 25-28, Mar., 1970.

Van Driest, E.R., "On Turbulent Flow Near a Wall," *J. Aero. Sci.*, vol. 23, pp. 1007-1012, 1956.

White, F.M., *Fluid Mechanics*, 2nd ed., McGraw-Hill, Singapore, pp. 330-332, 1968.

Willmarth, W.W. and Yang, C.S., "Wall Pressure Fluctuations beneath Turbulent Boundary Layers on a Flat plate and a Cylinder," *J. Fluid Mech.*, vol 41, pp. 47-80, 1970.

Wilson, N.W. and Medwell, J.O., "An Analysis of The Developing Turbulent Hydrodynamic and Thermal Boundary Layers in an Internally Heated Annulus," *Trans. ASME*, Paper No. 70-HT-9, pp.1-7, 1970.

Yu, Y.S., "Effect of Transverse Curvature on Turbulent Boundary Layer Characteristics," *J. Ship Research*, vol. 2, pp. 33-51, 1958.

Table 2.1 Variable von Kármán Constant, κ_i

r_i (in)	κ_i
0.01′	0.958
0.02′	0.921
0.063′	0.768
0.125′	0.606
0.25″	0.548
0.5″	0.52
1.0″	0.443

′ : Deduced from experimental data [Willmarth, 1970]

″ : Deduced from experimental data [Kim and Lee, 1990, 1993]

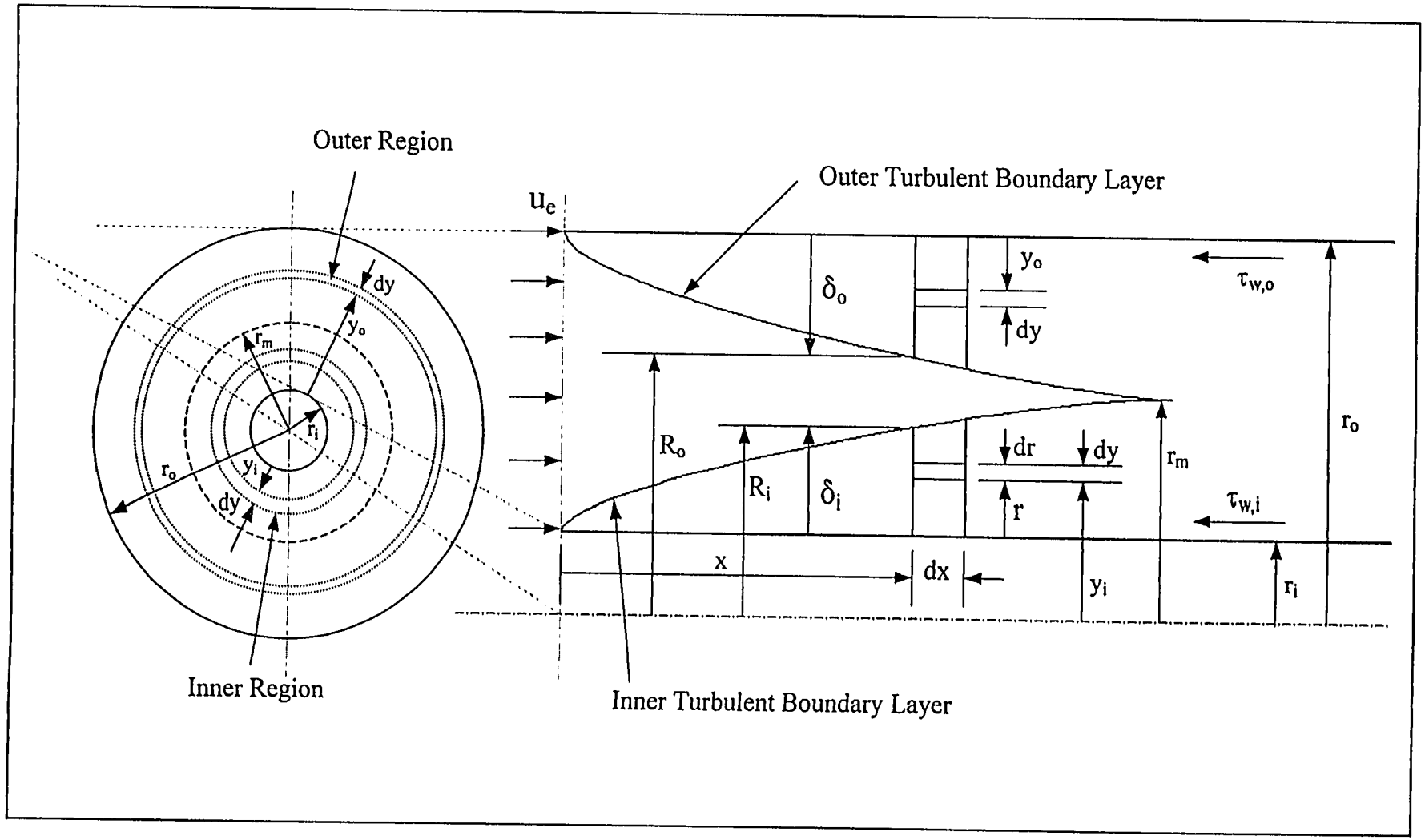

Figure 2.1 Idealized Model: Hydrodynamic Turbulent Boundary Layer

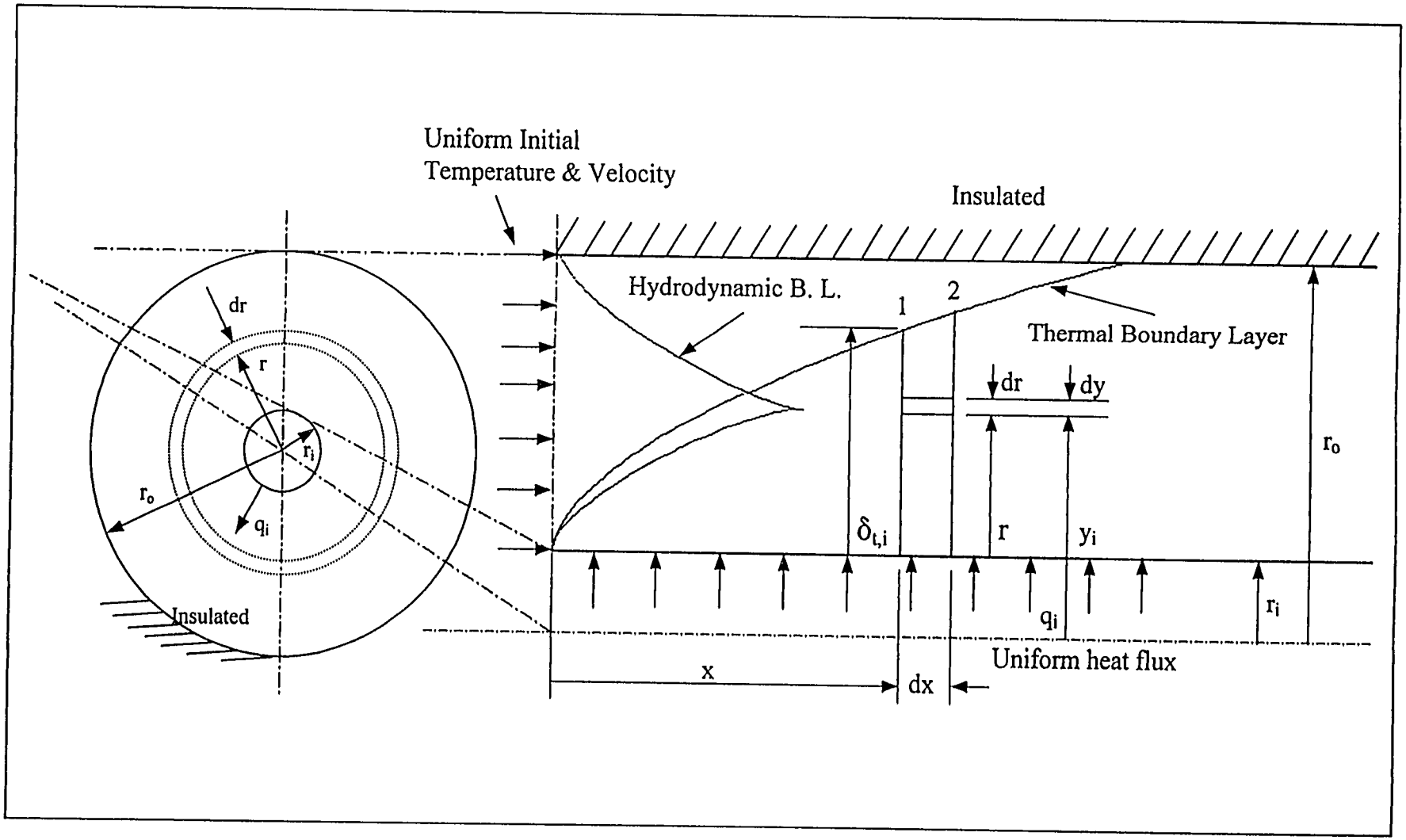

Figure 2.2 Idealized Model: Thermal Boundary Layer

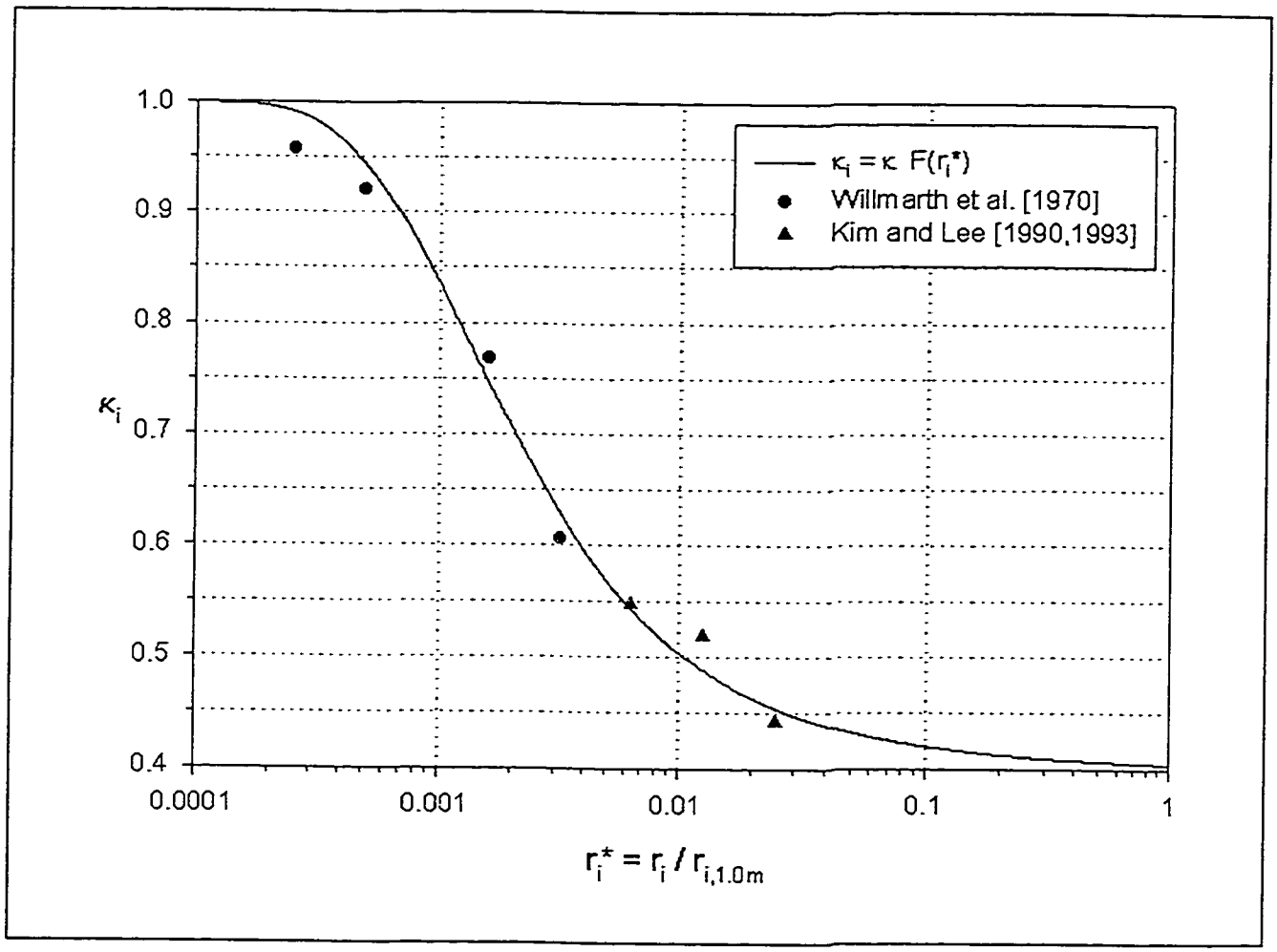

Figure 2.3 Effect of Transverse Convex Surface Curvature on von Kármán's Constant, κ_i

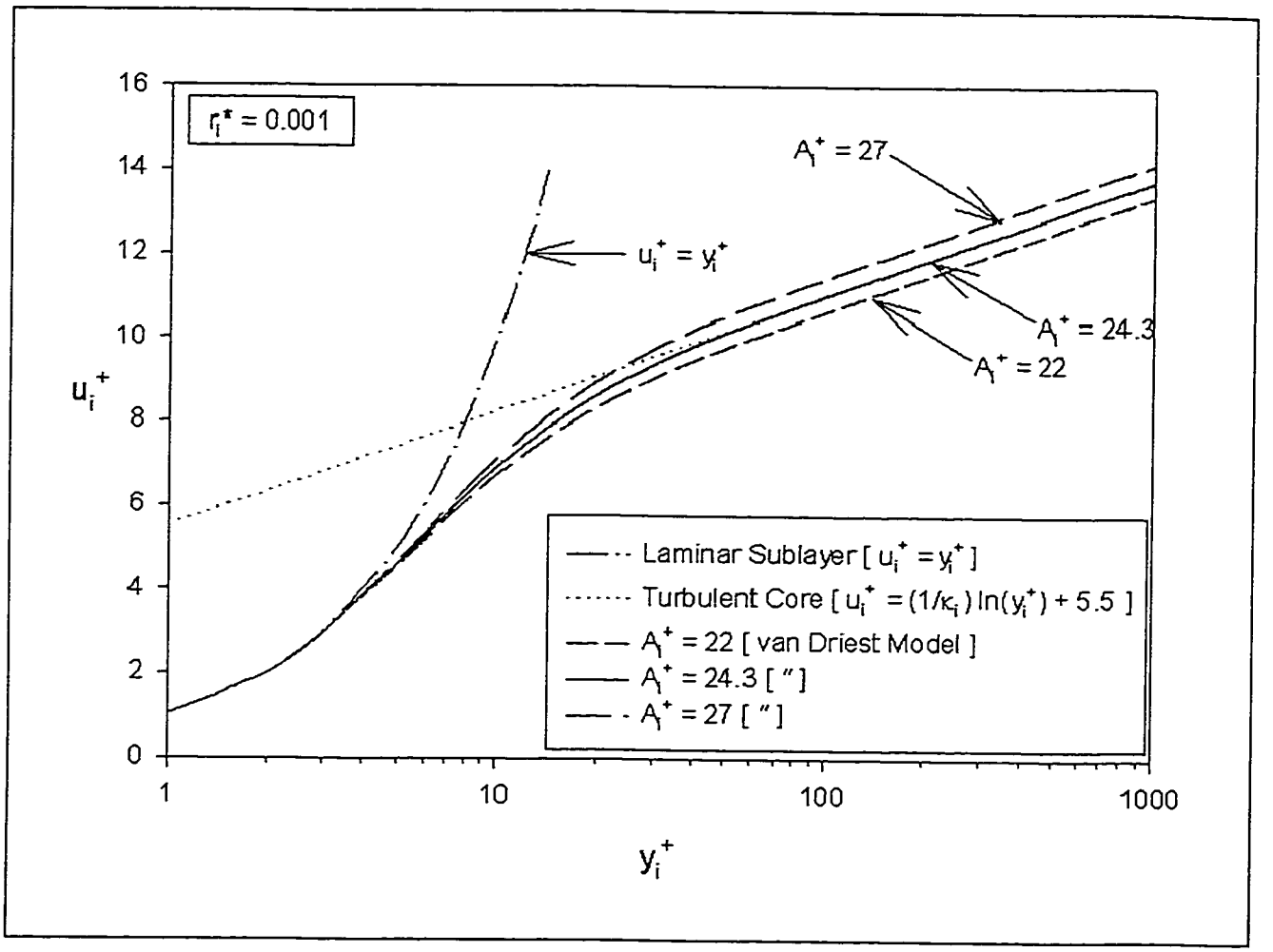

Figure 2.4 Effect of Transverse Convex Curvature on the van Driest Damping Parameter, A_i^+, for the Inner Region; $r_i^* = 0.001$

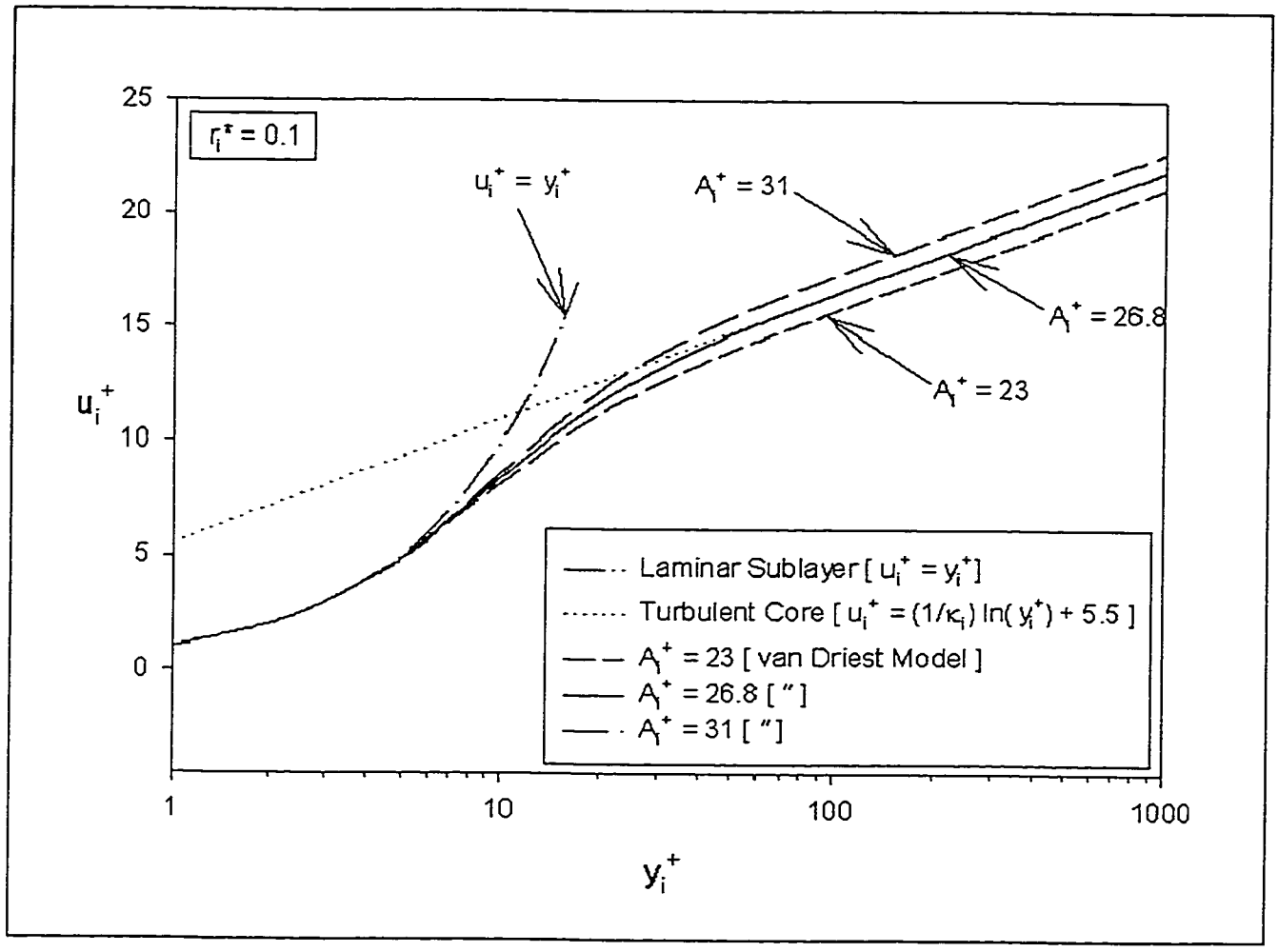

Figure 2.5 Effect of Transverse Convex Curvature on the van Driest Damping Parameter, A_i^+, for the Inner Region; $r_i^* = 0.1$

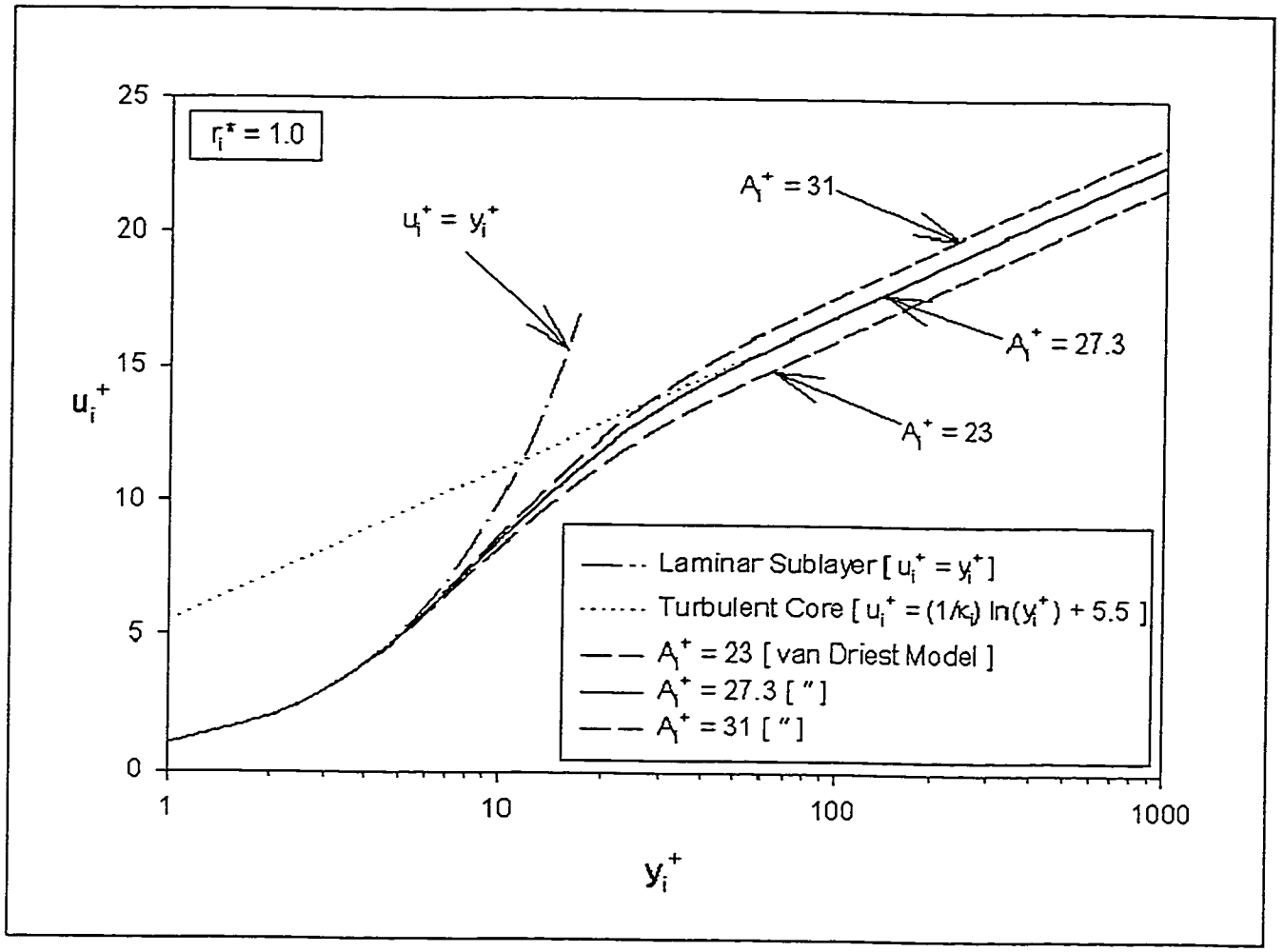

Figure 2.6 Effect of Transverse Convex Curvature on the van Driest Damping Parameter, A_i^+, for the Inner Region; $r_i^* = 1.0$

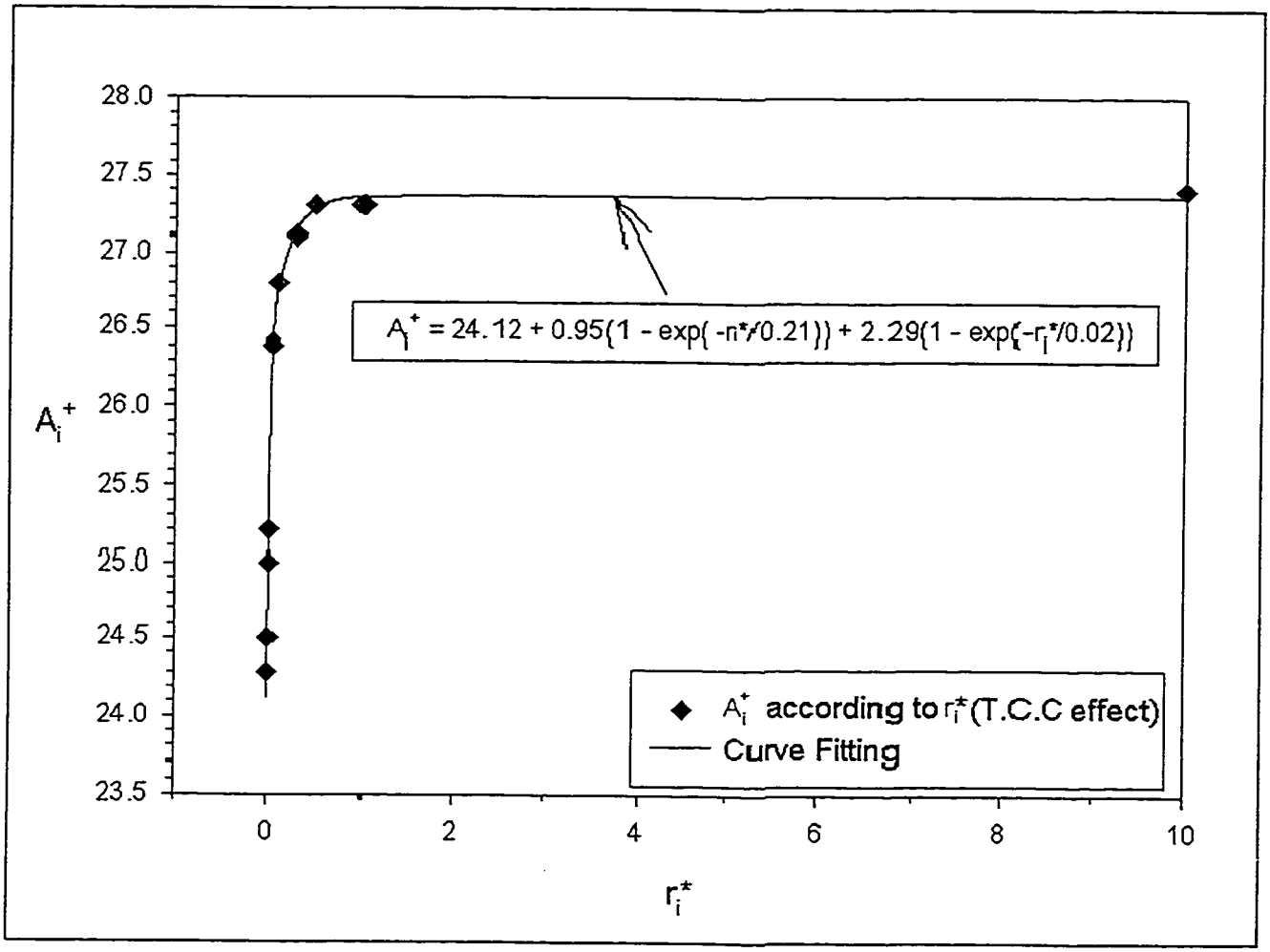

Figure 2.7 Variation of van Driest Damping Parameter for Inner Region, A_i^+, with Inner Core Radius, r_i^*; Effect of Transverse Convex Curvature

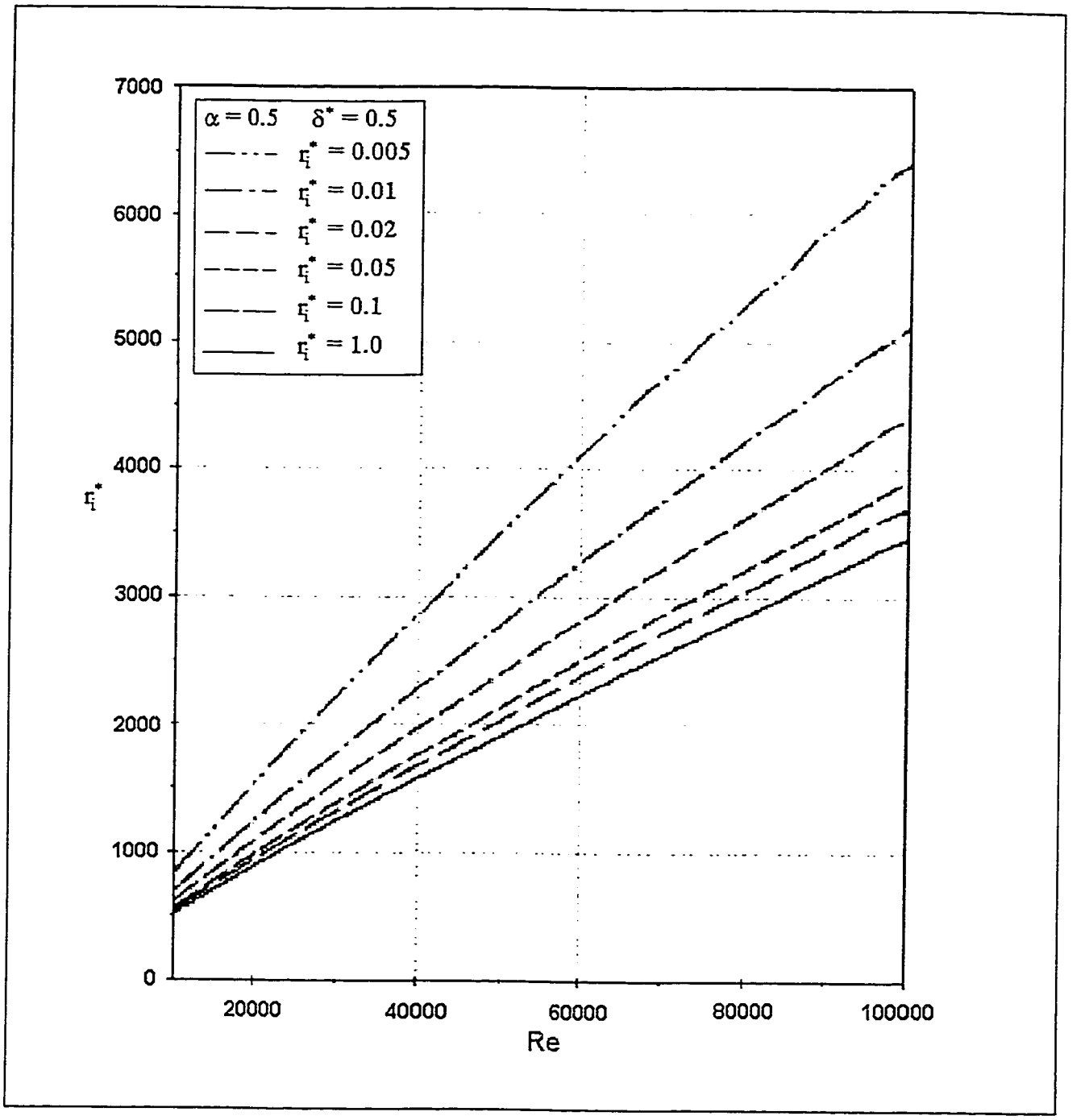

Figure 2.8 Relationship between r_i^+ and Reynolds Number, $Re = u_b \cdot 2(r_o - r_i)/\nu$

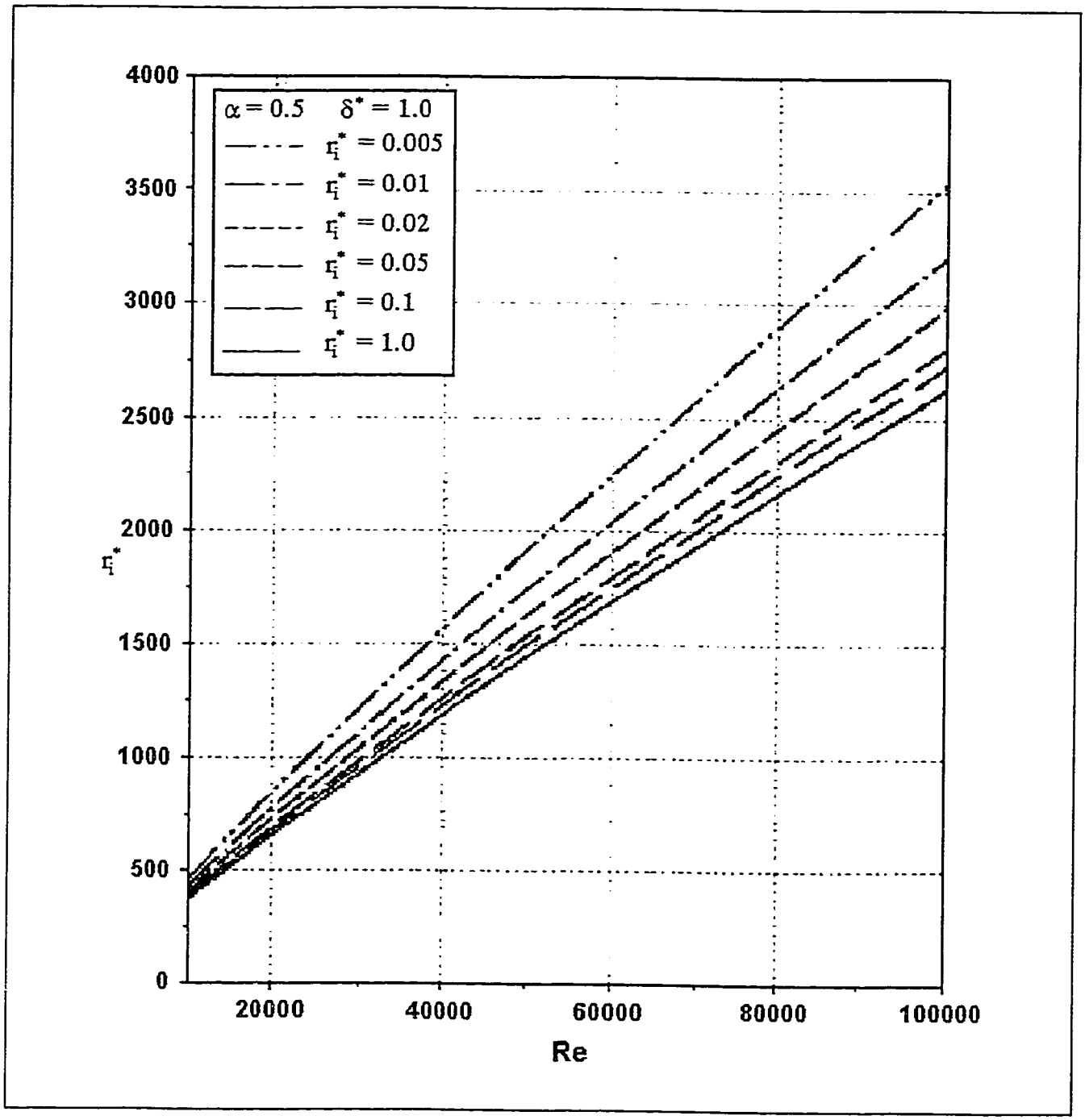

Figure 2.9 Relationship between r_i^+ and Reynolds Number, $Re = u_b \cdot 2(r_o - r_i)/\nu$

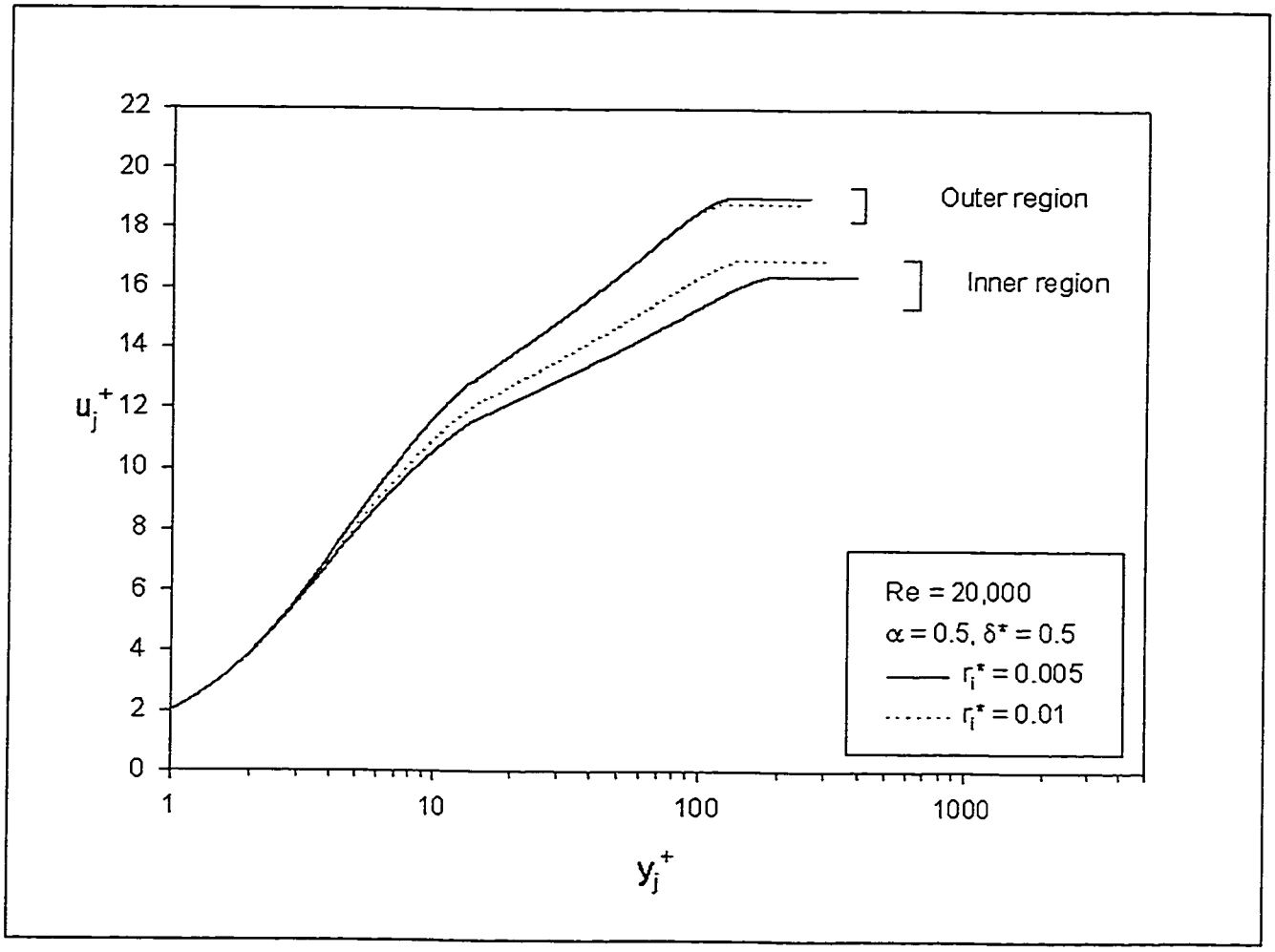

Figure 2.10 Effect of Transverse Convex Curvature on Velocity Distribution in Developing Turbulent Flow in a Concentric Annulus; Theory

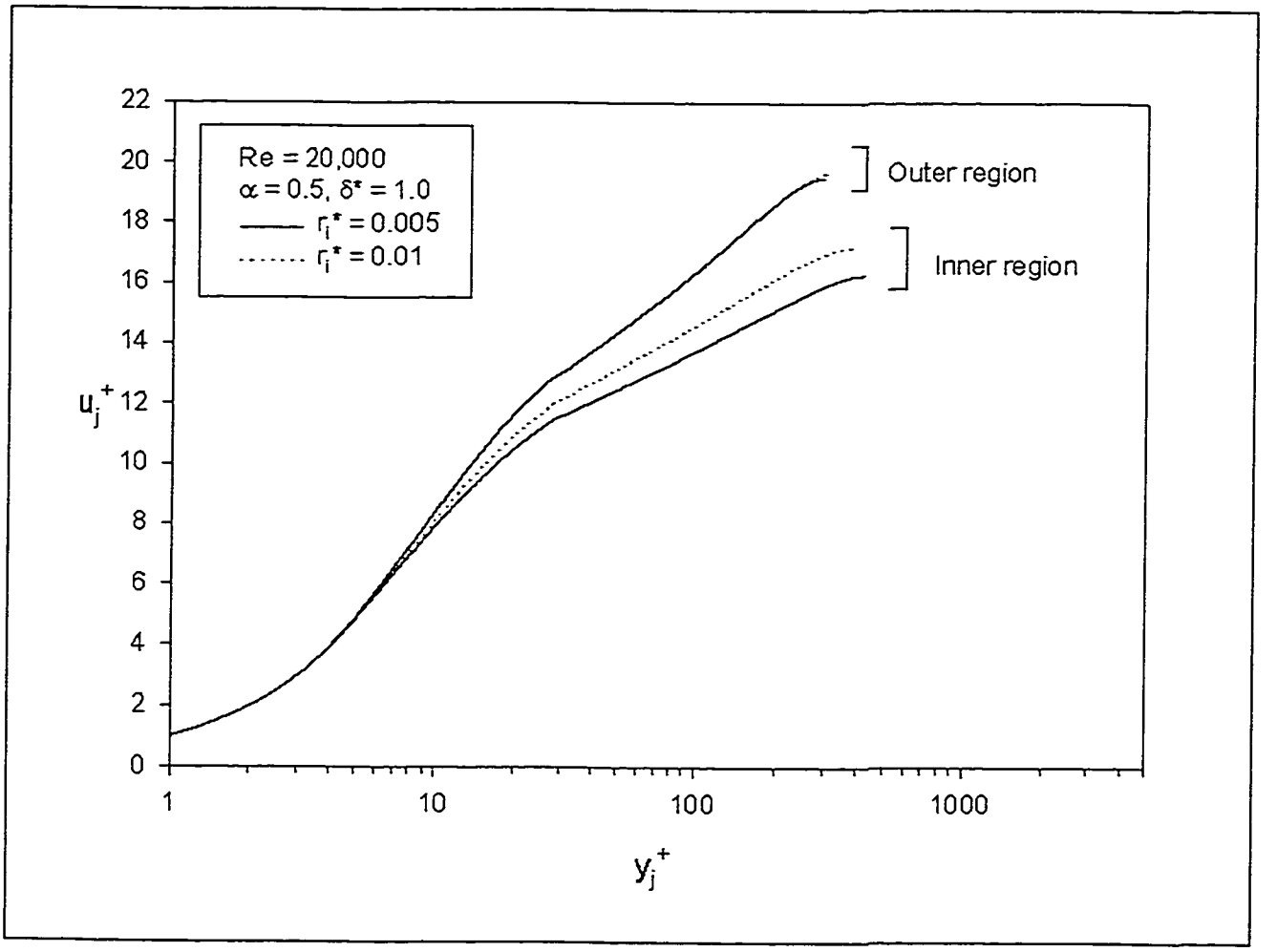

Figure 2.11 Effect of Transverse Convex Curvature on Velocity Distribution in Developing Turbulent Flow in a Concentric Annulus; Theory

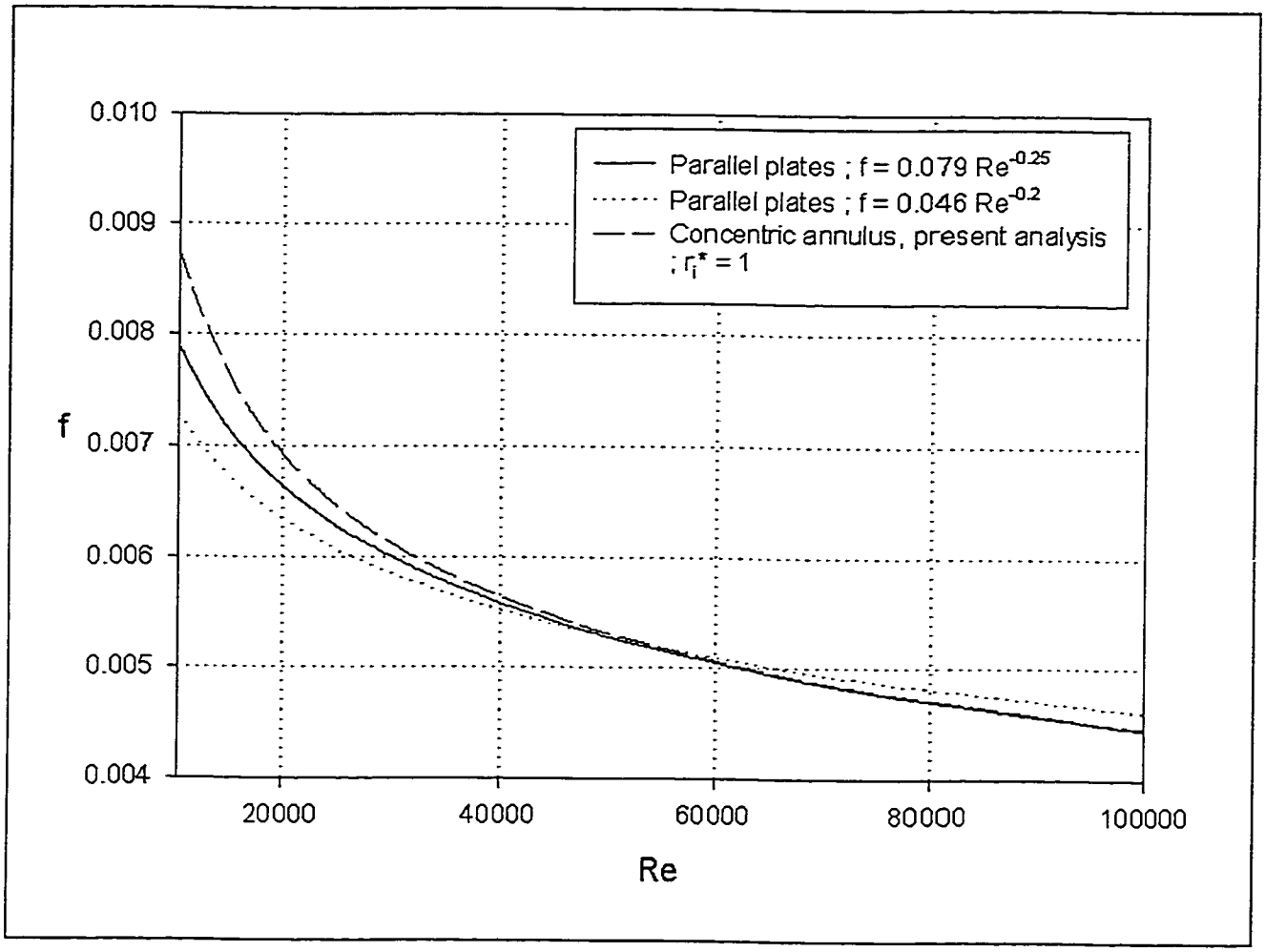

Figure 2.12 Friction Factors for Fully Developed Turbulent Flow between Parallel Plates and in a Concentric Annulus, $r_i^* = 1.0$, and $\alpha = 0.999$; $Re = u_b \cdot 2(r_o - r_i)/\nu$

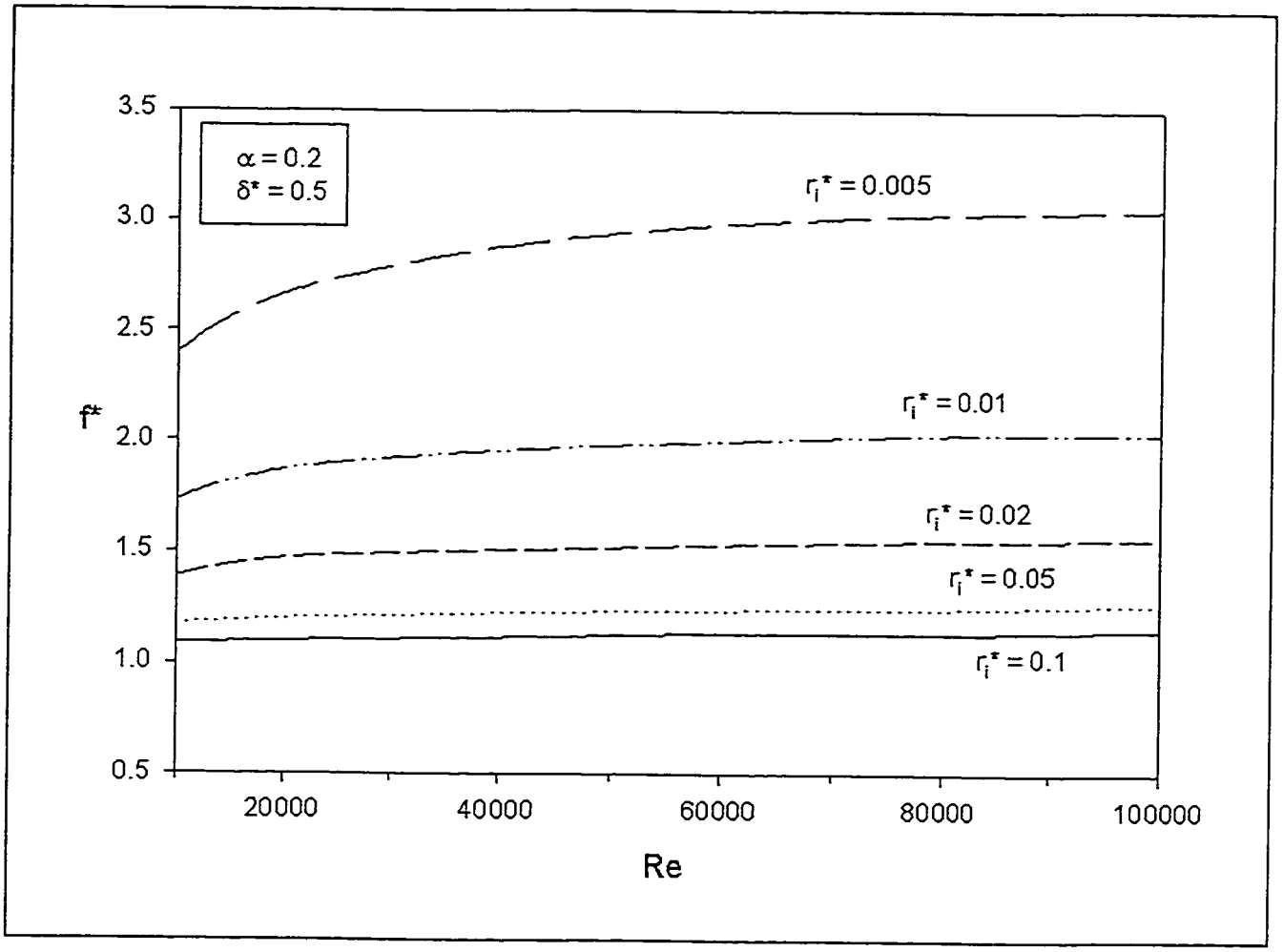

Figure 2.13 Effect of Transverse Convex Curvature on Friction Factors ($f^* = f / f_{1.0m}$), Developing Turbulent Flow; $\alpha = 0.2$, $\delta^* = 0.5$; $Re = u_b \cdot 2(r_o - r_i)/\nu$

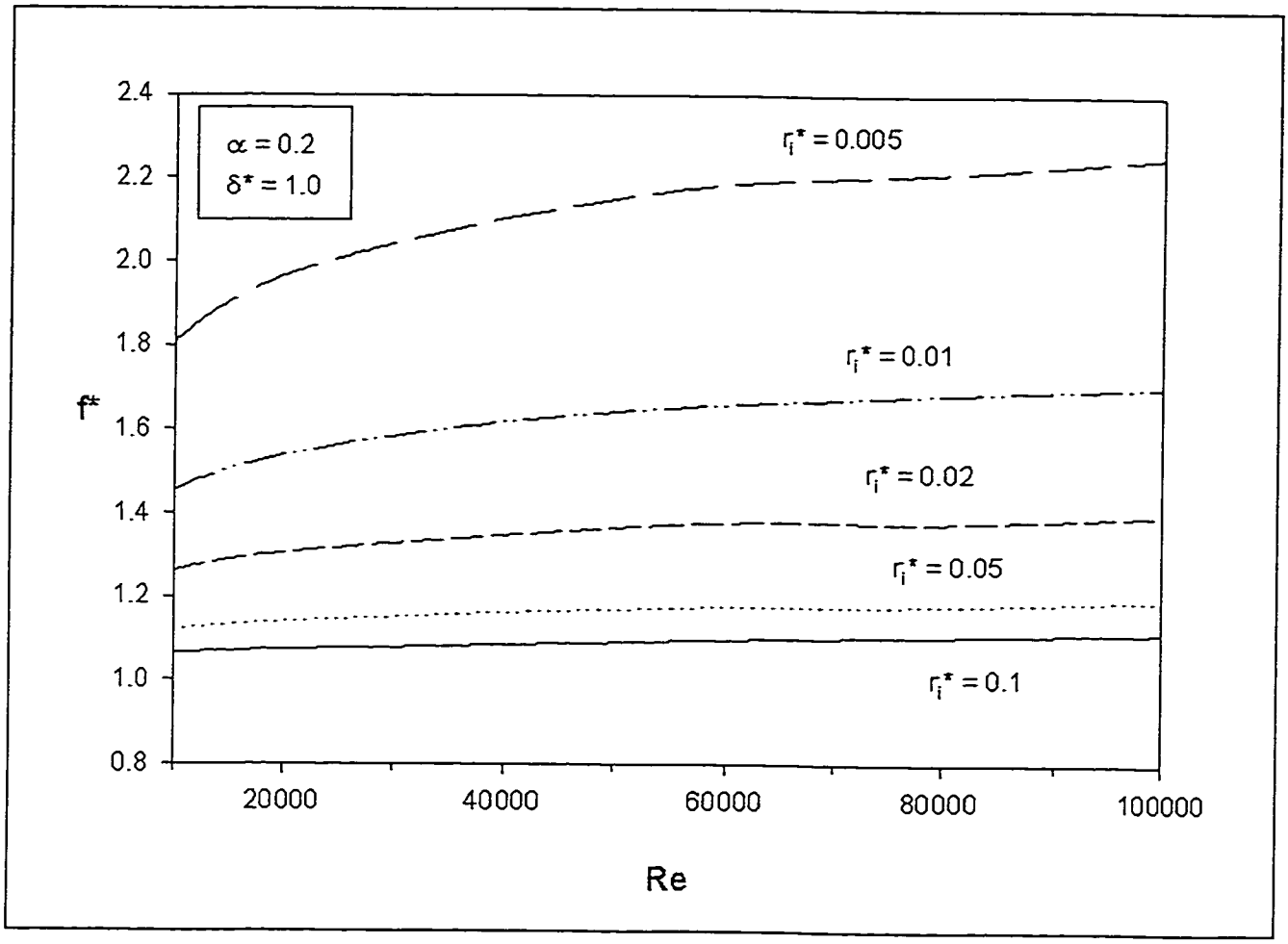

Figure 2.14 Effect of Transverse Convex Curvature on Friction Factors ($f^* = f / f_{1.0m}$), Developing Turbulent Flow; $\alpha = 0.2$, $\delta^* = 1.0$; $Re = u_b \cdot 2(r_o - r_i)/\nu$

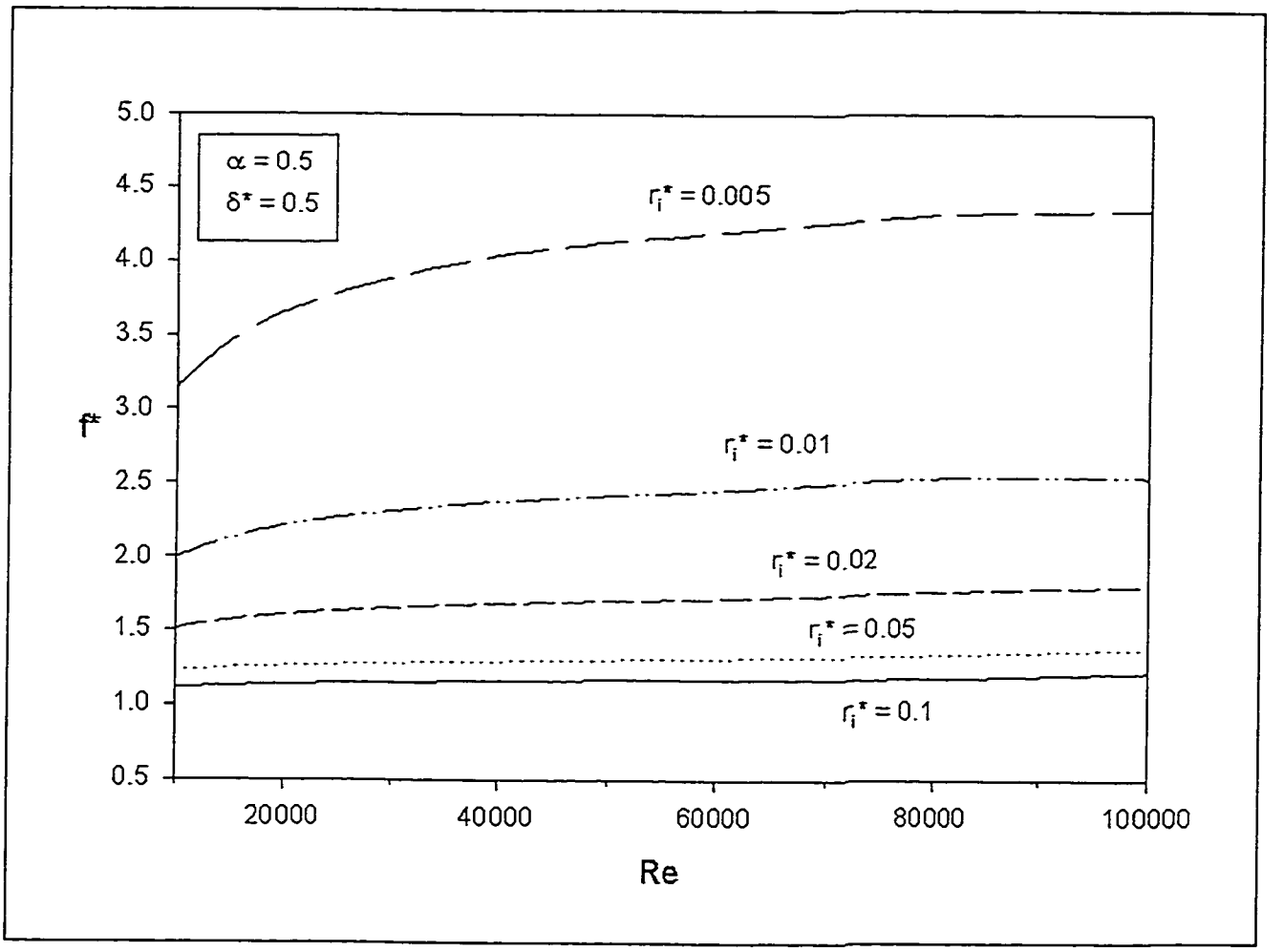

Figure 2.15 Effect of Transverse Convex Curvature on Friction Factors ($f^* = f / f_{1.0m}$), Developing Turbulent Flow; $\alpha = 0.5$, $\delta^* = 0.5$; $Re = u_b \cdot 2(r_o - r_i)/\nu$

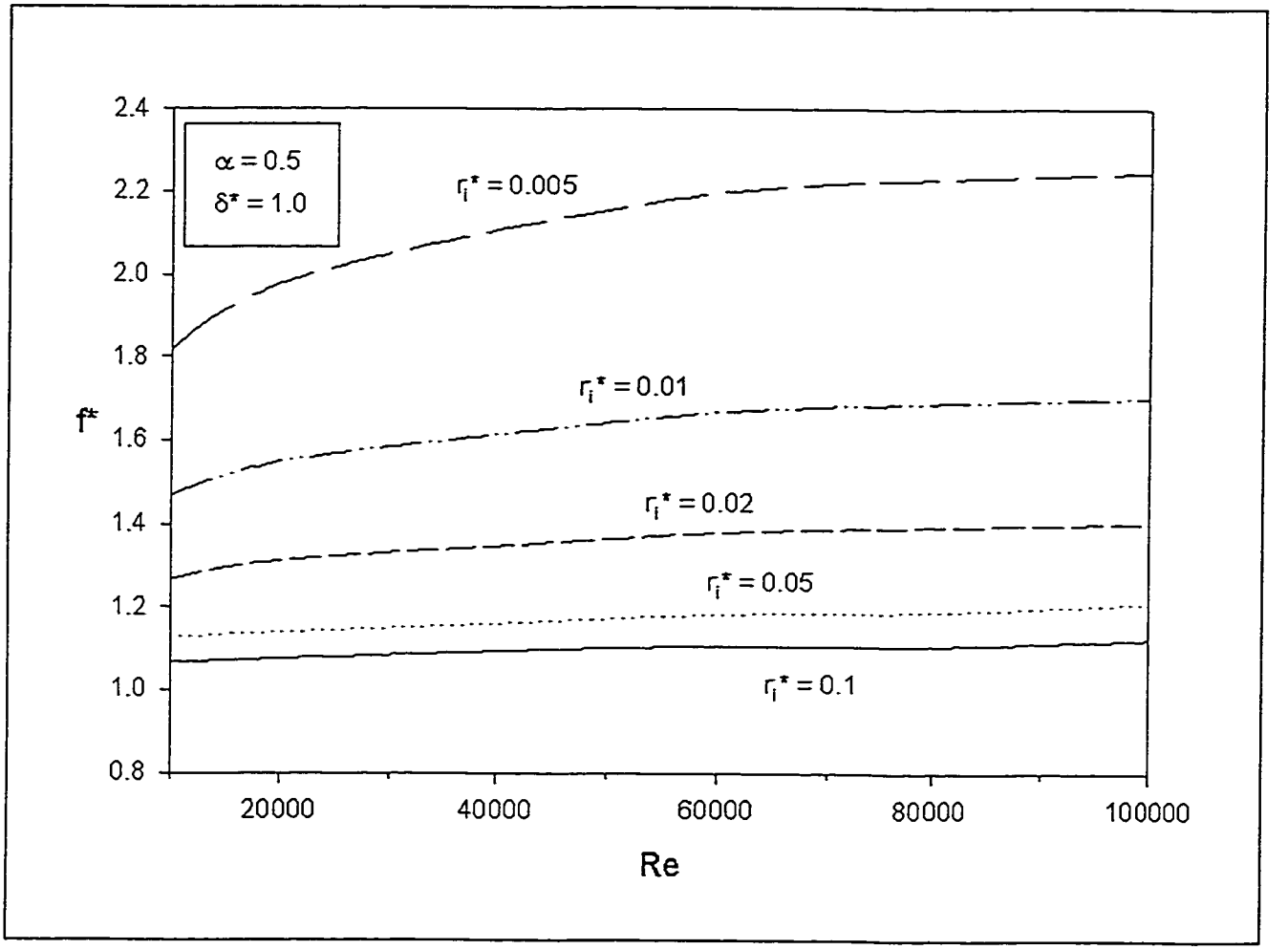

Figure 2.16 Effect of Transverse Convex Curvature on Friction Factors ($f^* = f / f_{1.0m}$), Developing Turbulent Flow; $\alpha = 0.5$, $\delta^* = 1.0$; $Re = u_b \cdot 2(r_o - r_i)/\nu$

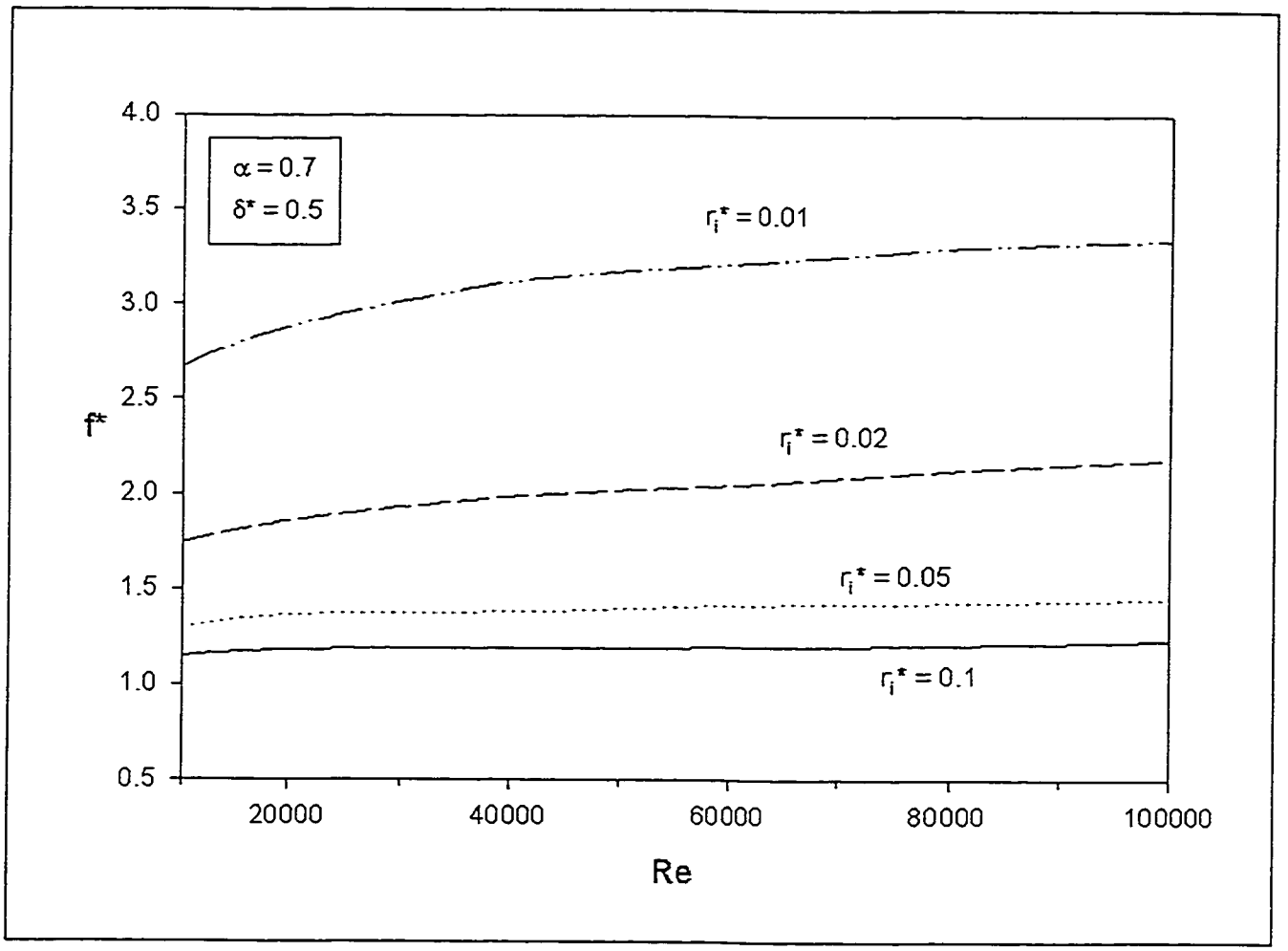

Figure 2.17 Effect of Transverse Convex Curvature on Friction Factors ($f^* = f / f_{1.0m}$), Developing Turbulent Flow; $\alpha = 0.7$, $\delta^* = 0.5$; $Re = u_b \cdot 2(r_o - r_i)/\nu$

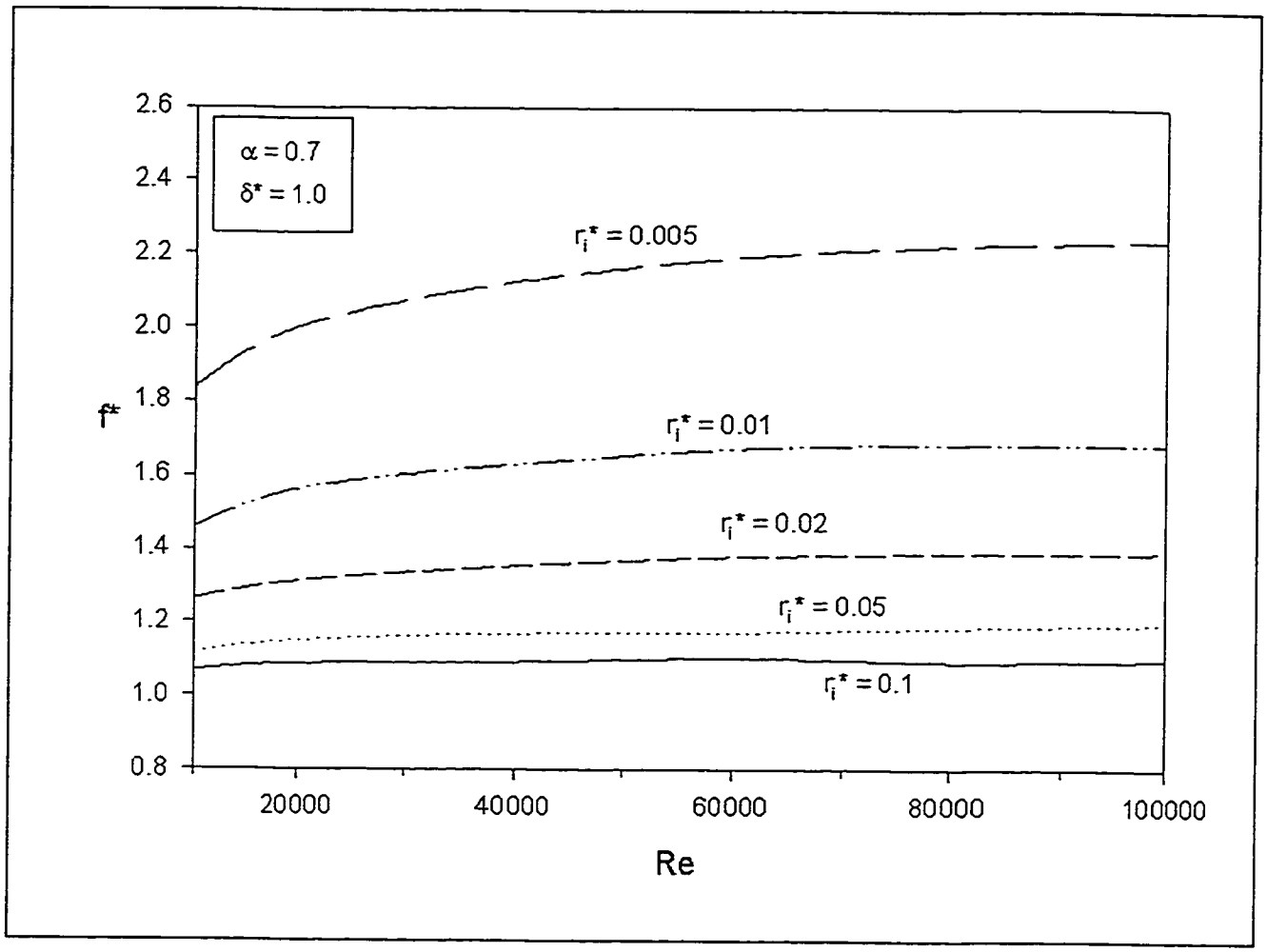

Figure 2.18 Effect of Transverse Convex Curvature on Friction Factors ($f^* = f / f_{1.0m}$), Developing Turbulent Flow; $\alpha = 0.7$, $\delta^* = 1.0$; $Re = u_b \cdot 2(r_o - r_i)/\nu$

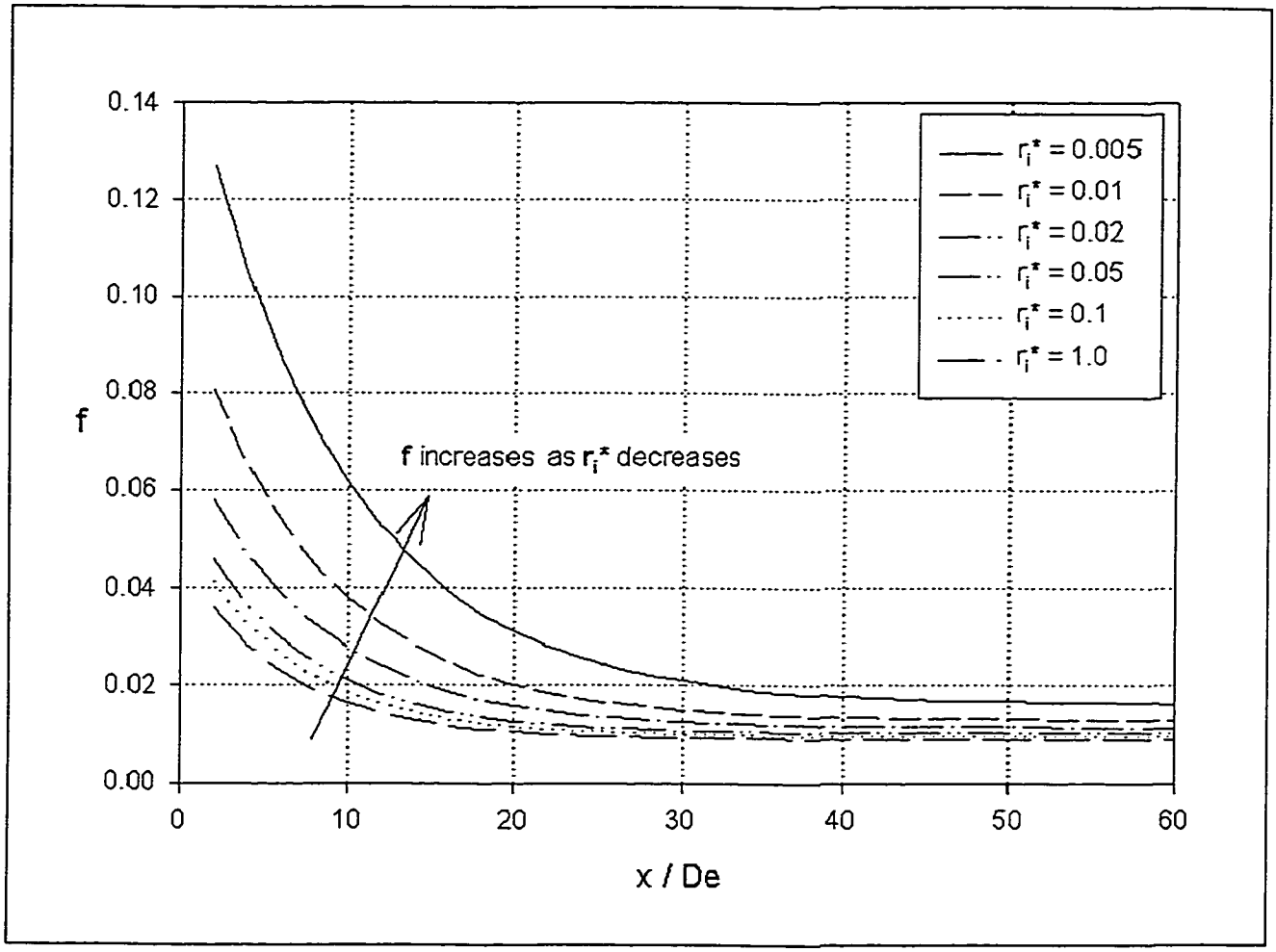

Figure 2.19 Predicted Friction Factor on Entrance Region in a Concentric Annulus with Transverse Convex Curvature Effect

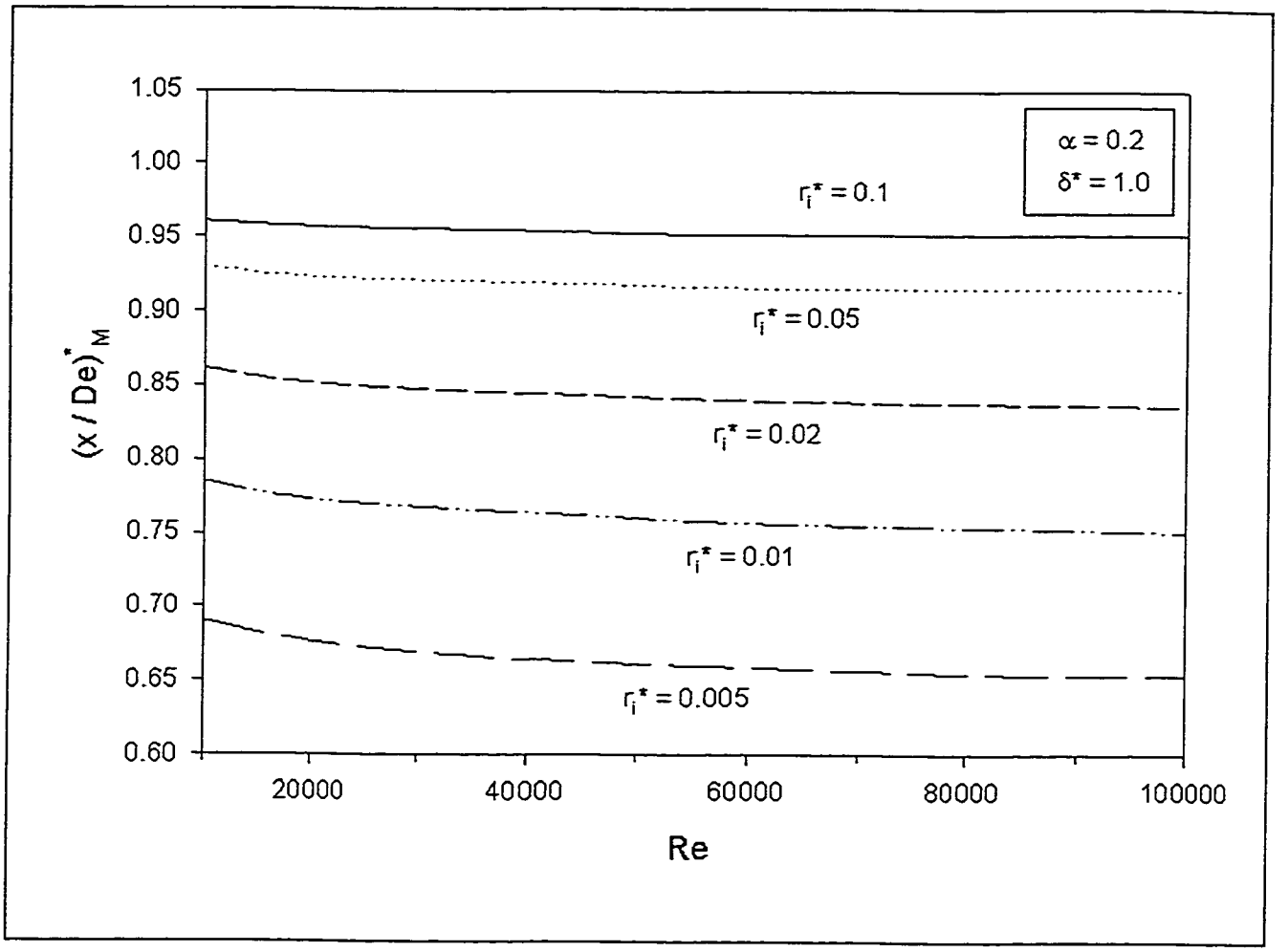

Figure 2.20 Effect of Transverse Convex Curvature on Entrance Length $(x / De)^*_M$, Developing Turbulent Flow; $\alpha = 0.2$, $\delta^* = 1.0$; $Re = u_b \cdot 2(r_o - r_i)/\nu$

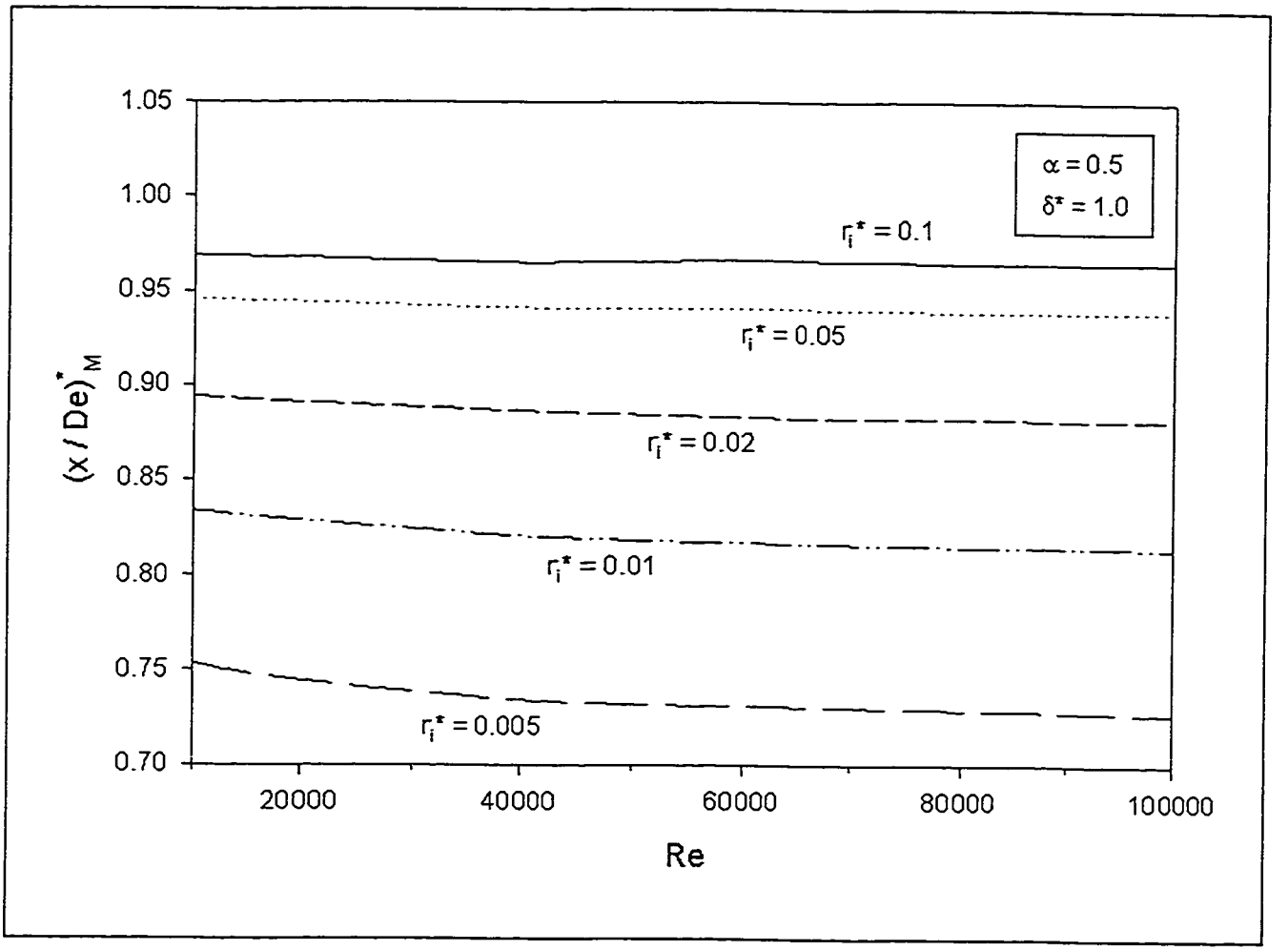

Figure 2.21 Effect of Transverse Convex Curvature on Entrance Length $(x / De)^*_M$, Developing Turbulent Flow; $\alpha = 0.5$, $\delta^* = 1.0$; $Re = u_b \cdot 2(r_o - r_i)/\nu$

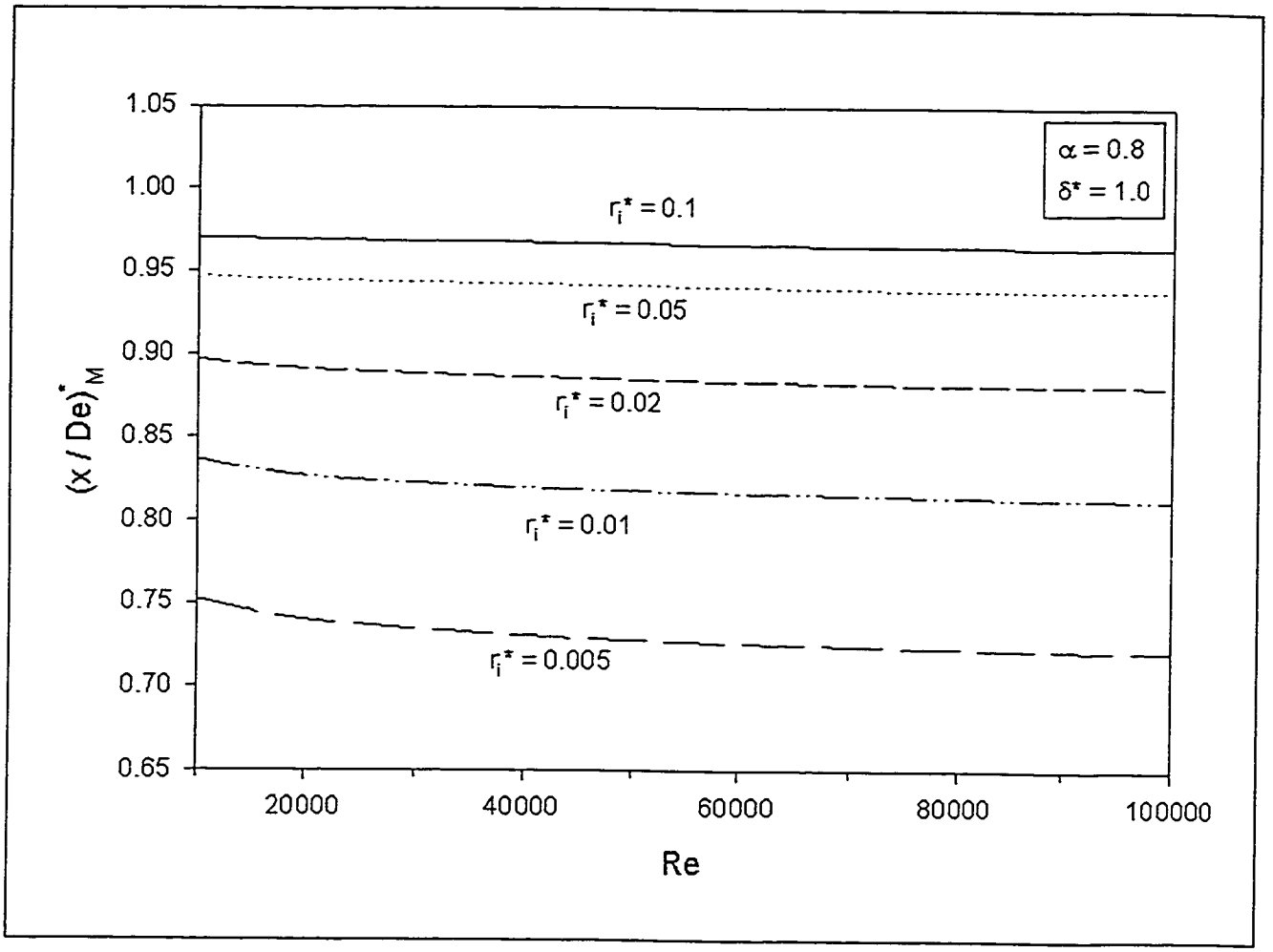

Figure 2.22 Effect of Transverse Convex Curvature on Entrance Length $(x / De)^*_M$, Developing Turbulent Flow; $\alpha = 0.8$, $\delta^* = 1.0$; $Re = u_b \cdot 2(r_o - r_i)/\nu$

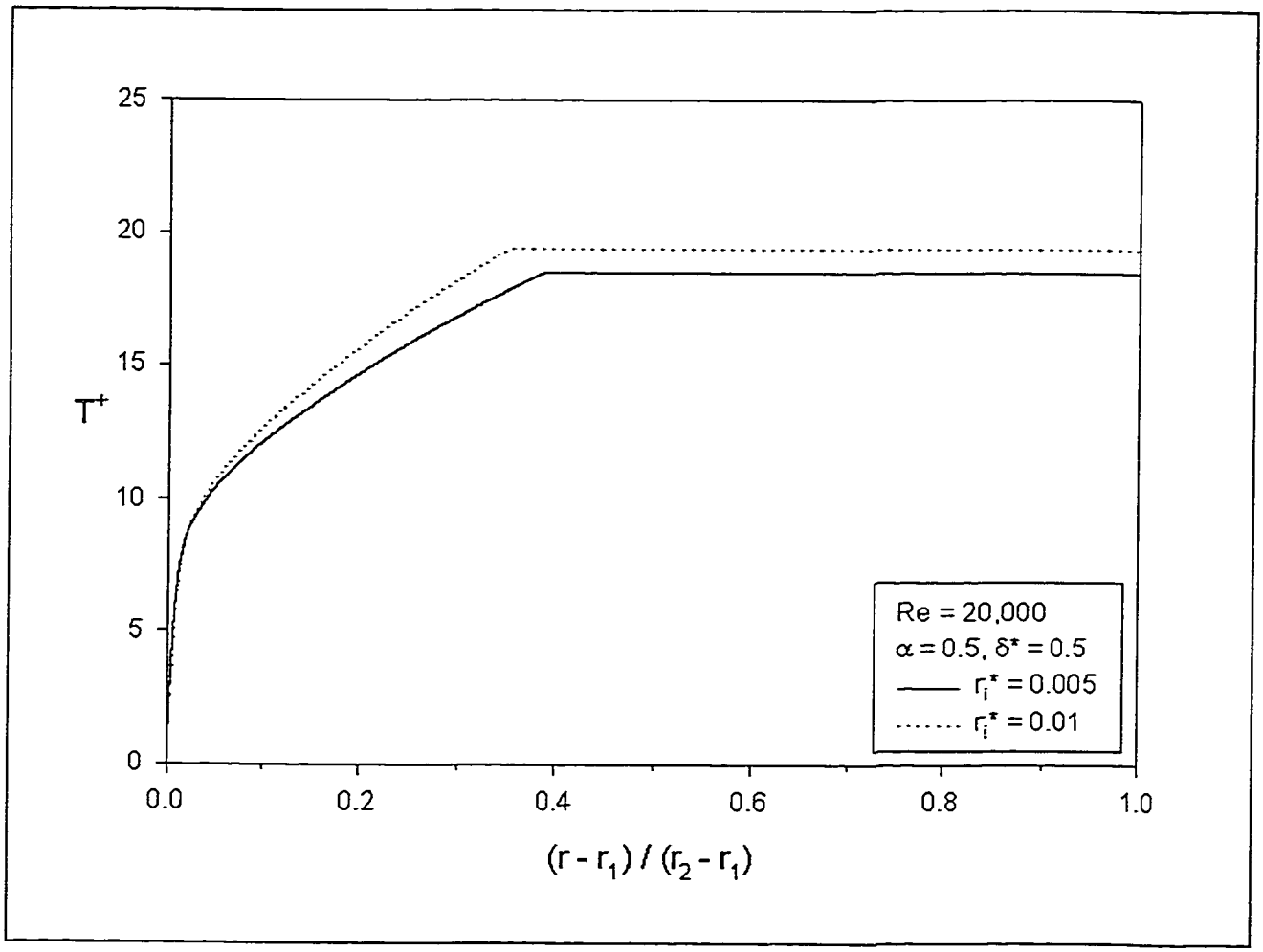

Figure 2.23 Effect of Transverse Convex Curvature on Temperature Distribution for Developing Turbulent Flow in a Concentric Annulus, $r_i^* = 0.005$ & 0.01 and $\alpha = 0.5$; Constant Heat Flux; Inner Core Heated and Outer Insulated; Pr = 0.7, Re = 20,000

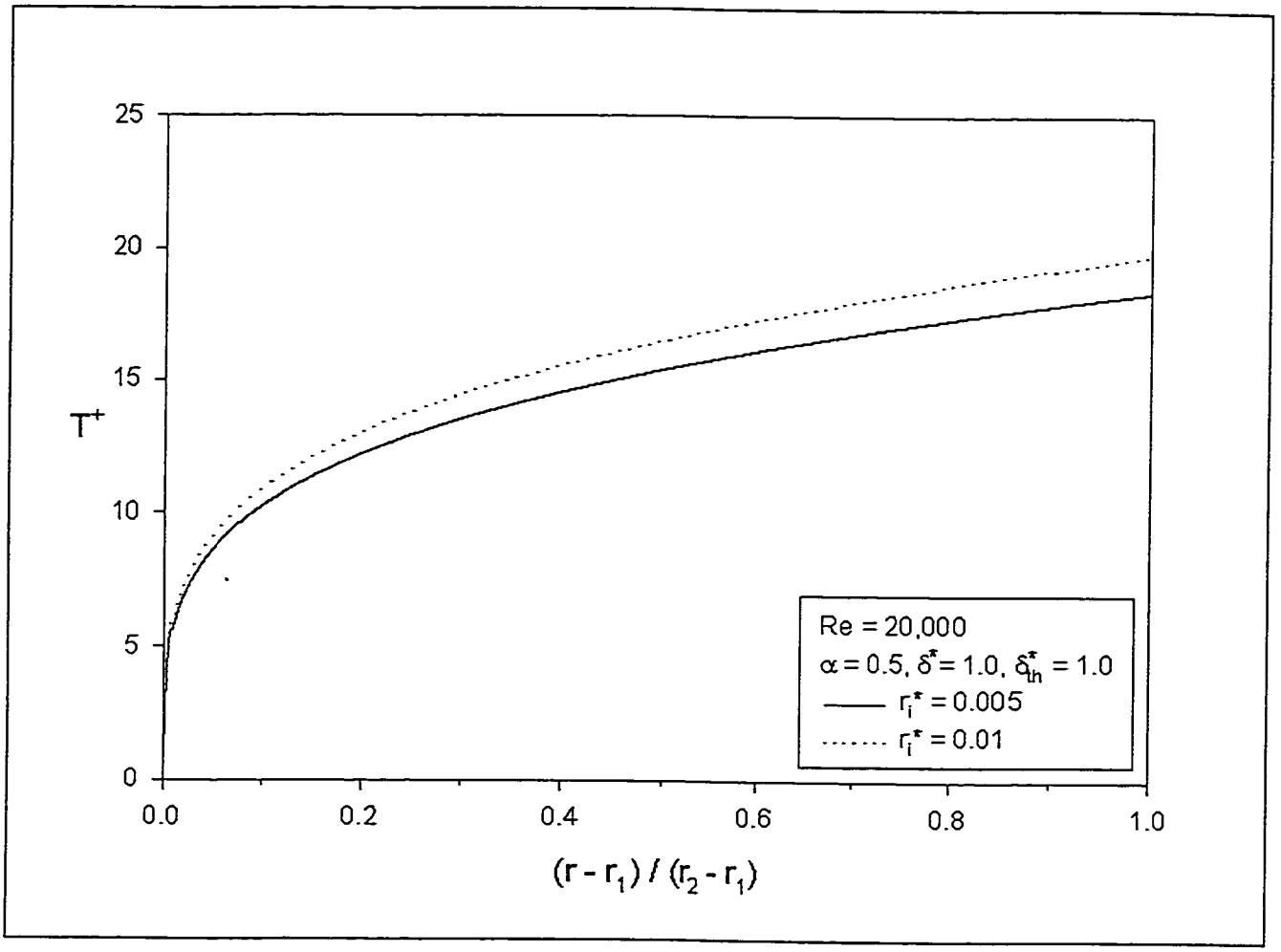

Figure 2.24 Effect of Transverse Convex Curvature on Temperature Distribution for Fully Developed Turbulent Flow in a Concentric Annulus, $r_i^* = 0.005$ & 0.01 and $\alpha = 0.5$; Constant Heat Flux; Inner Core Heated and Outer Insulated; Pr = 0.7, Re = 20,000

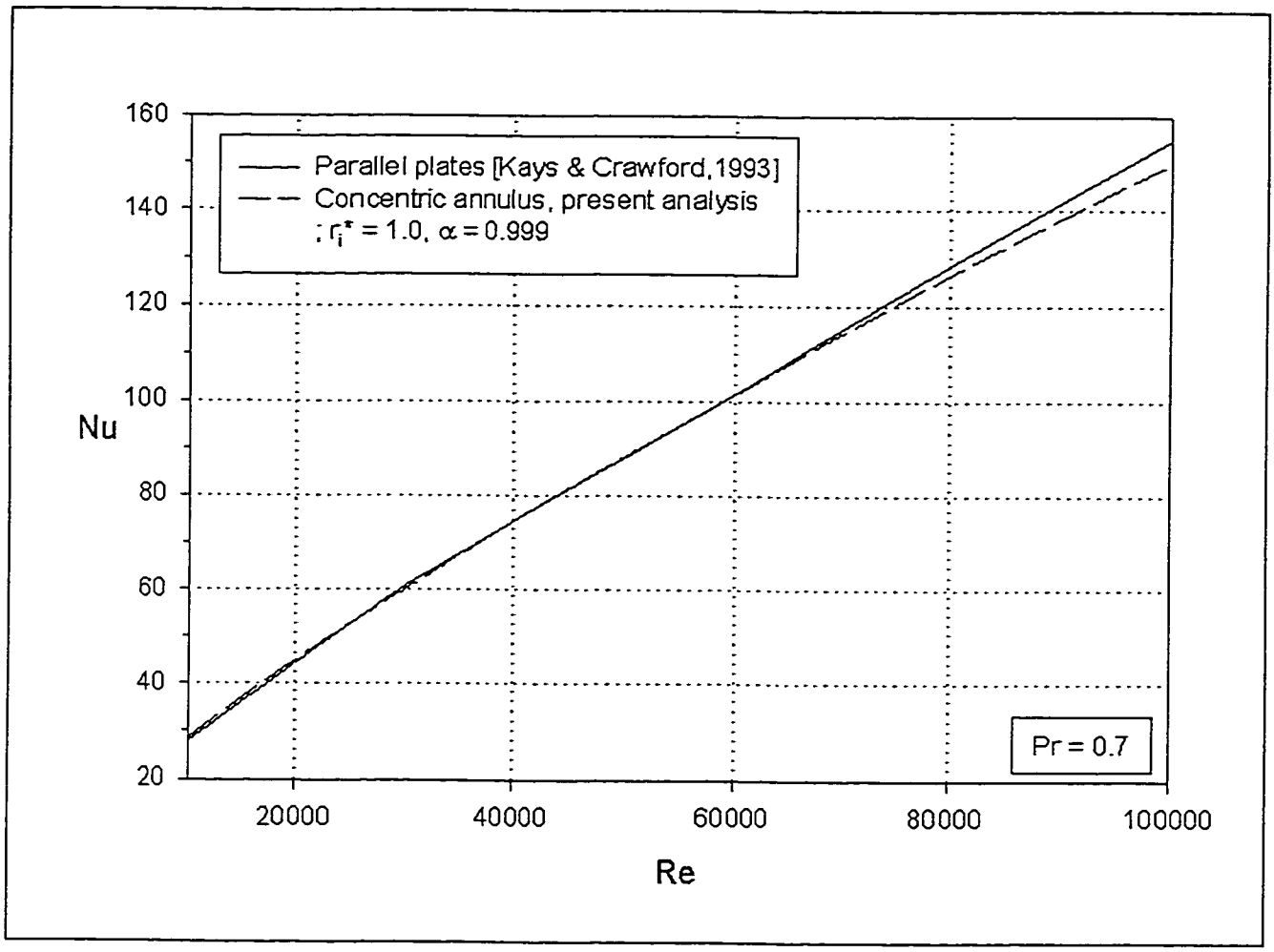

Figure 2.25 Nusselt Numbers for Fully Developed Turbulent Flow between Parallel Plates and in a Concentric Annulus, $r_i^* = 1.0$, and $\alpha = 0.999$; Constant Heat Flux; Inner Core Heated and Outer Insulated; Pr = 0.7; $Re = u_b \cdot 2(r_o - r_i)/\nu$

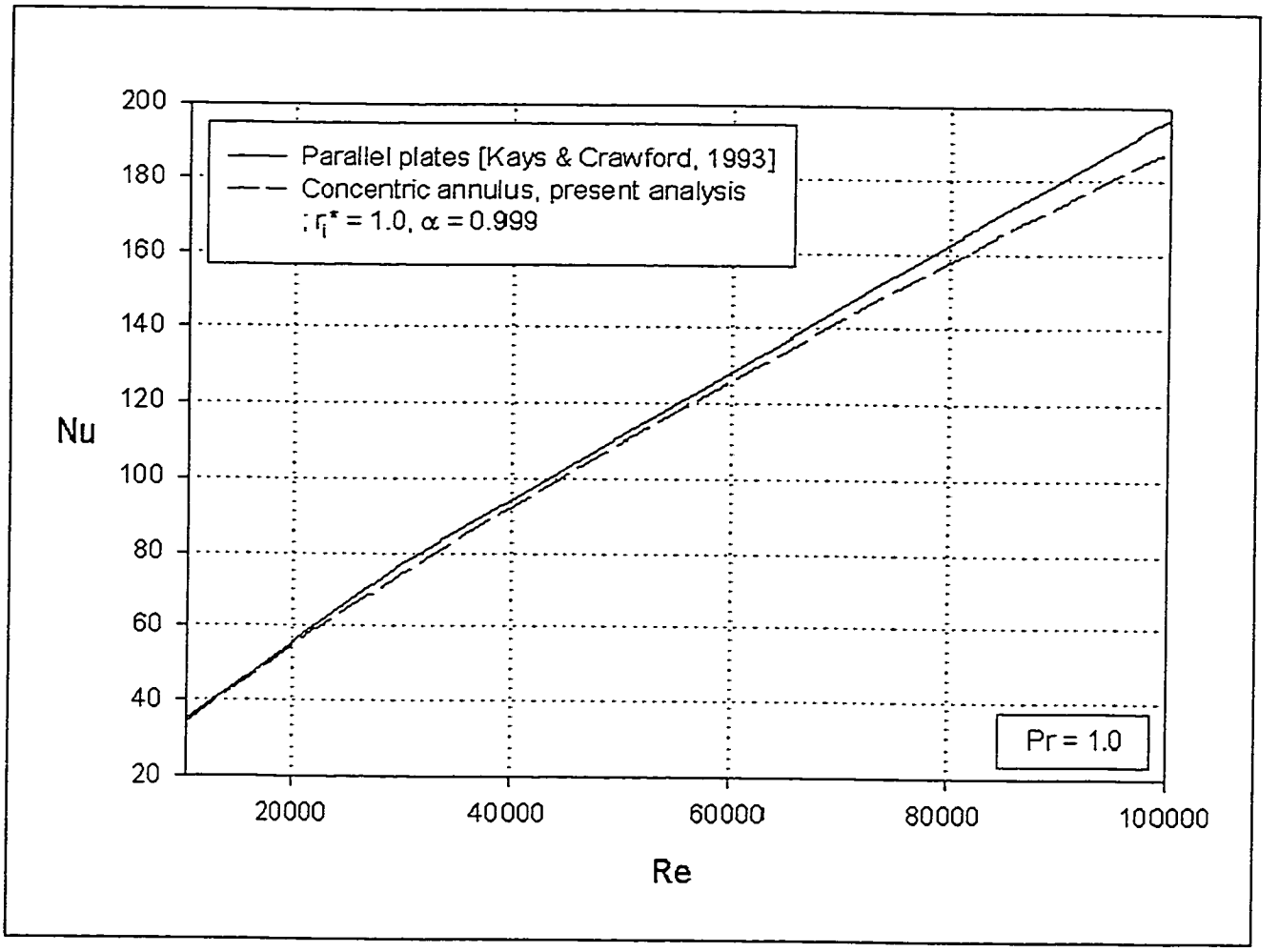

Figure 2.26 Nusselt Numbers for Fully Developed Turbulent Flow between Parallel Plates and in a Concentric Annulus, $r_i^* = 1.0$, and $\alpha = 0.999$; Constant Heat Flux; Inner Core Heated and Outer Insulated; Pr = 1.0; $Re = u_b \cdot 2(r_o - r_i)/\nu$

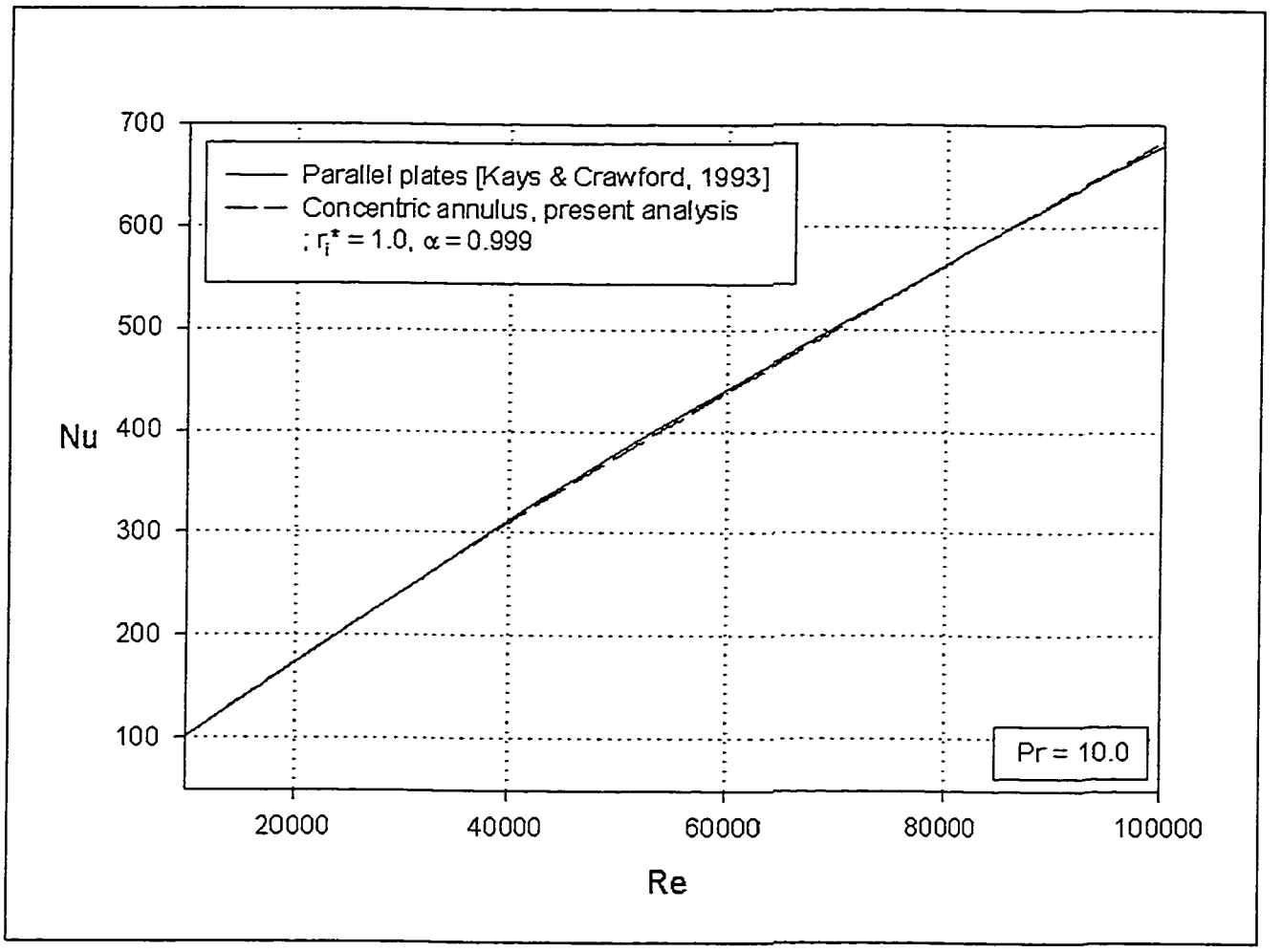

Figure 2.27 Nusselt Numbers for Fully Developed Turbulent Flow between Parallel Plates and in a Concentric Annulus, $r_i^* = 1.0$, and $\alpha = 0.999$; Constant Heat Flux; Inner Core Heated and Outer Insulated; Pr = 10.0; $Re = u_b \cdot 2(r_o - r_i)/\nu$

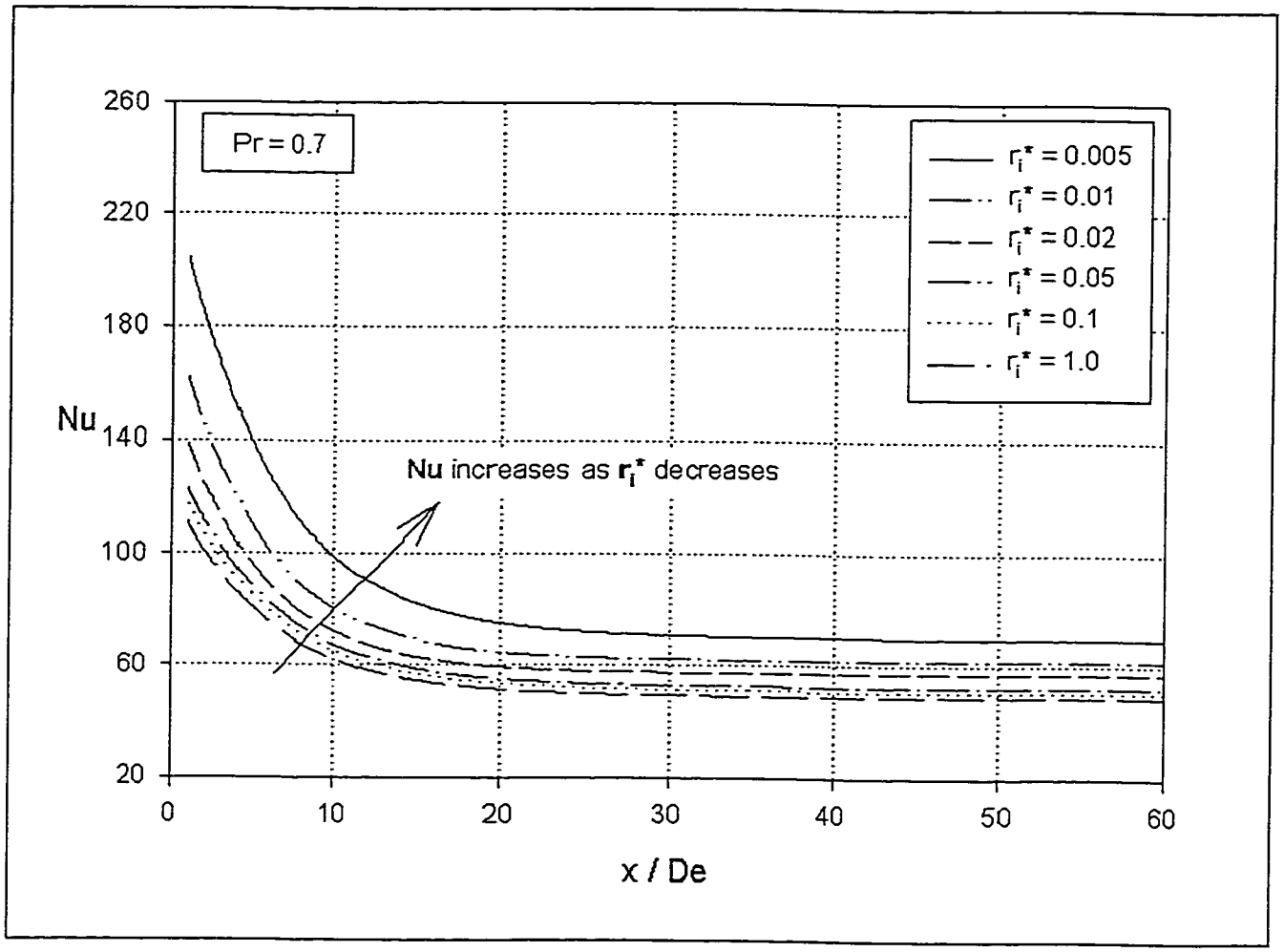

Figure 2.28 Predicted Nusselt Numbers for the Entrance Region in a Concentric Annulus with Transverse Convex Curvature Effect; Constant Heat Flux; Inner Core Heated and Outer Insulated; Pr = 0.7, Re = 20,000, $\alpha = 0.5$

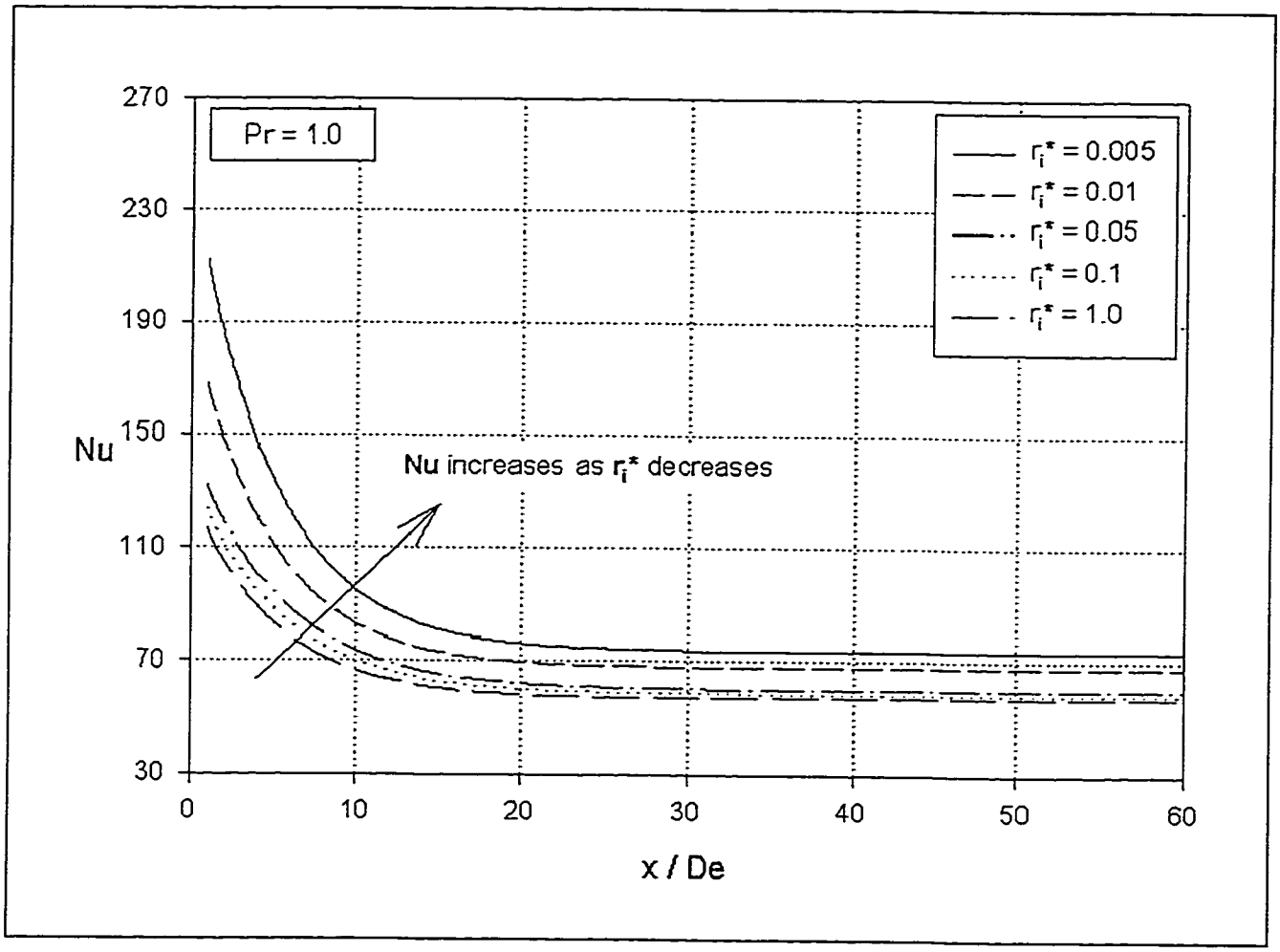

Figure 2.29 Predicted Nusselt Numbers for the Entrance Region in a Concentric Annulus with Transverse Convex Curvature Effect; Constant Heat Flux; Inner Core Heated and Outer Insulated; Pr = 1.0, Re = 20,000, $\alpha = 0.5$

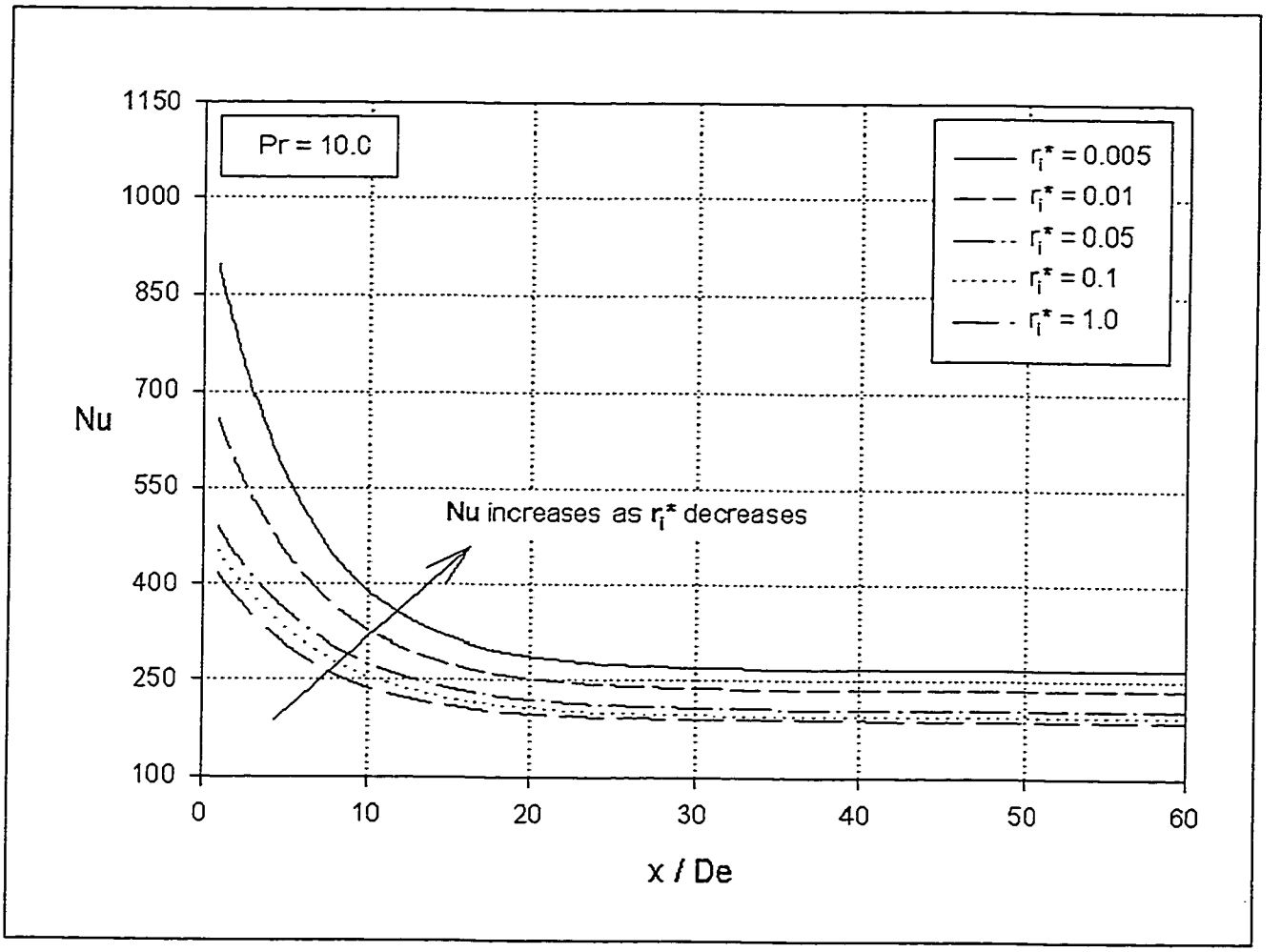

Figure 2.30 Predicted Nusselt Numbers for the Entrance Region in a Concentric Annulus with Transverse Convex Curvature Effect; Constant Heat Flux; Inner Core Heated and Outer Insulated; Pr = 10.0, Re = 20,000, $\alpha = 0.5$

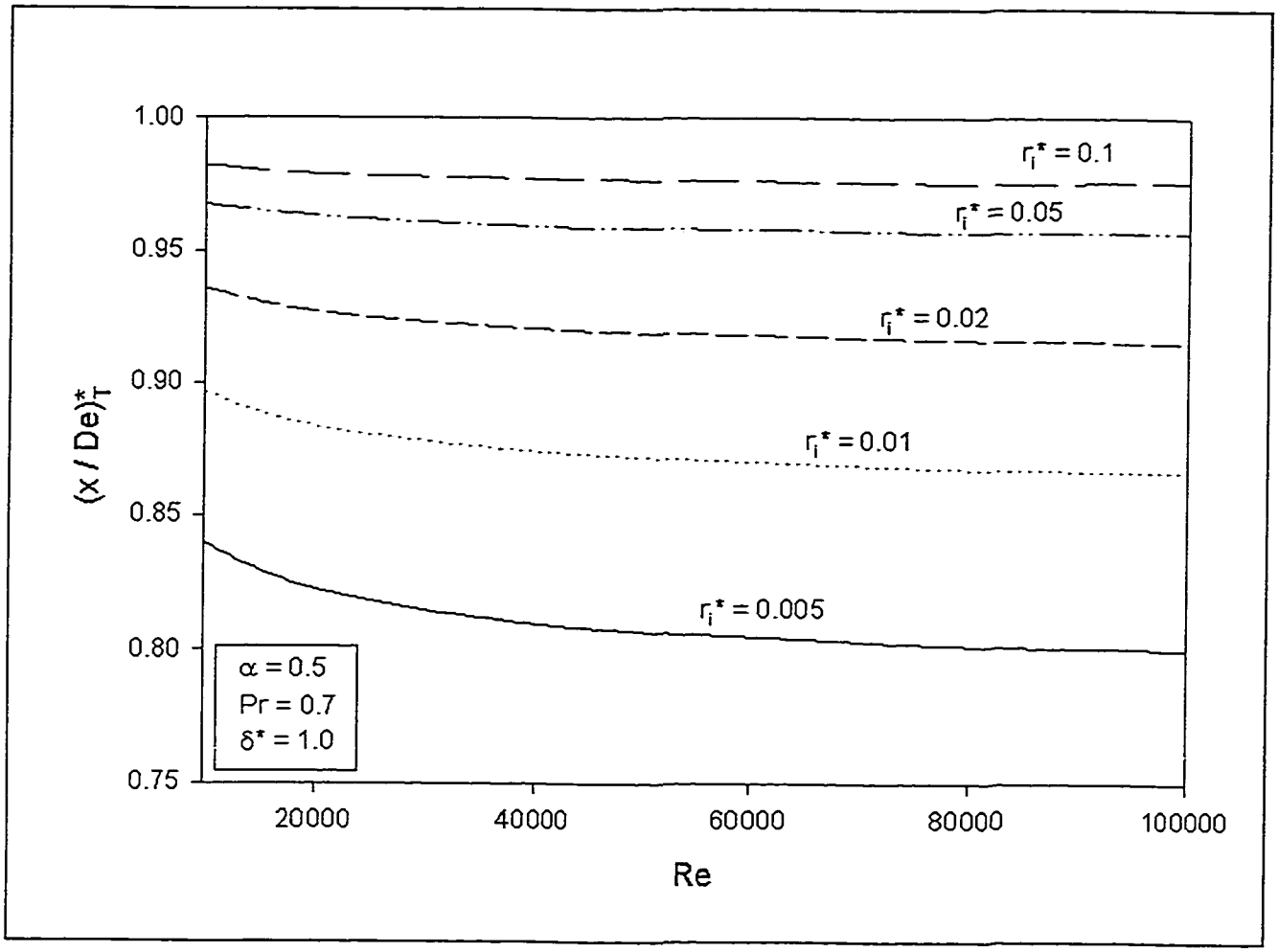

Figure 2.31 Effect of Transverse Convex Curvature on Entrance Length $(x / De)^*_T$, Developing Turbulent Flow; $\alpha = 0.5$, $Pr = 0.7$, & $\delta^* = 1.0$; $Re = u_b \cdot 2(r_o - r_i)/\nu$

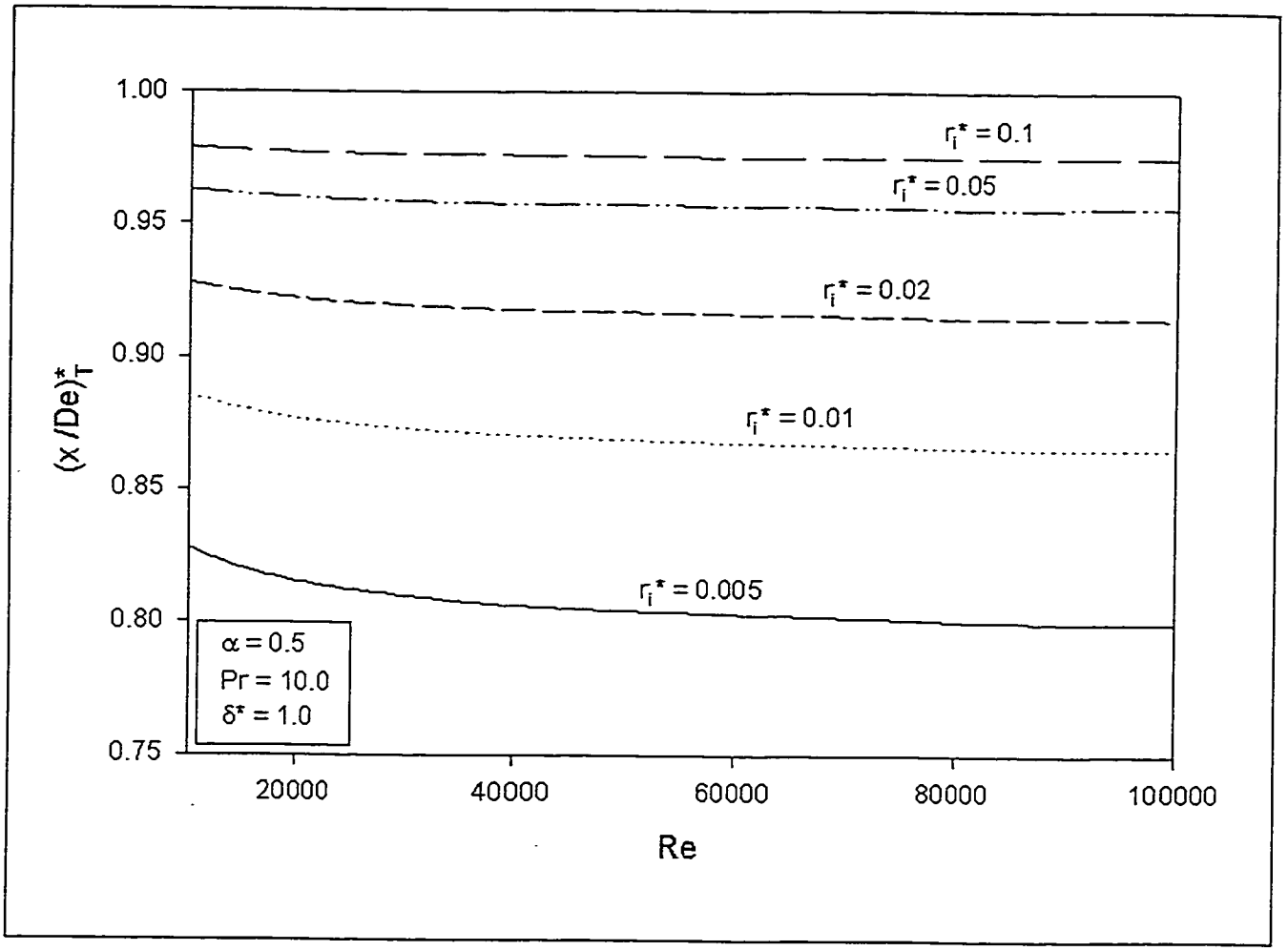

Figure 2.32 Effect of Transverse Convex Curvature on Entrance Length $(x / De)^*_T$, Developing Turbulent Flow; $\alpha = 0.5$, $Pr = 10.0$, & $\delta^* = 1.0$; $Re = u_b \cdot 2(r_o - r_i)/\nu$

IMAGE EVALUATION TEST TARGET (QA-3)

150mm

6″

APPLIED IMAGE . Inc
1653 East Main Street
Rochester, NY 14609 USA
Phone: 716/482-0300
Fax: 716/288-5989